Université Ferhat ABBAS Sétif 1

UNIVERSITÉ FERHAT ABBAS - SETIF1

FACULTÉ DE TECHNOLOGIE

THESE

Présentée au Département d'Electrotechnique

Pour l'obtention du diplôme de

DOCTORAT EN SCIENCES
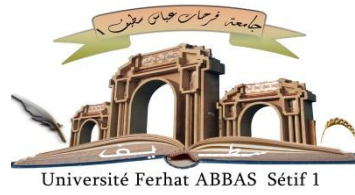
Option: Automatique

Par

AYAT Rahma

THÈME

Contribution à la Commande Synergétique d'une Installation de Production d'Energie Photovoltaïque Autonome

Soutenue le ……./……./…… devant le Jury:

M. CHAOUI Abdelmadjid	Professeur	Univ. Ferhat Abbas Sétif 1	Président
M. BOUAFIA Abdelouahab	Professeur	Univ. Ferhat Abbas Sétif 1	Directeur de thèse
M. GAUBERT Jean-Paul	Professeur	Univ. de Poitiers France	Co-Directeur
M. RAHMANI Lazhar	Professeur	Univ. Ferhat Abbas Sétif 1	Examinateur
M. CHOUDER Aissa	Professeur	Univ. M. Boudiaf de M'sila	Examinateur
M. KESSAL Abdelhalim	Professeur	Univ. M. B. El Ibrahimi BBA	Examinateur

الجمهورية الجزائرية الديمقراطية الشعبية

People's Democratic Republic of Algeria

Ministry of Higher Education and Scientific Research

Université Ferhat ABBAS Sétif 1

UNIVERSITY FERHAT ABBAS - SETIF1

FACULTY OF TECHNOLOGY

THESIS

Presented to the Department of Electrical Engineering

A thesis submitted in accordance with the requirements for the degree of

PhD

Option: Automatic

By

M. AYAT Rahma

THEME

Contribution to the Synergetic Control of Stand-Alone Photovoltaic Energy Production Installation

July 2021

Dedication

I dedicate this thesis

To my dear parents

To my dear sisters

To my husband and my children

RAFA and IDRIS

To the memory of my father in law

To all my family, colleagues and friends

Without whom none of my success would be possible

AYAT Rahma

01/06/2021

Acknowledgement

<div dir="rtl">

وَفَوْقَ كُلِّ ذِي عِلْمٍ عَلِيمٌ

</div>

Over all endued with knowledge is the All-Knowing (ALLAH).

Keywords

- ✓ Stand alone PV system
- ✓ DC-DC boost converter
- ✓ Maximum Power Point Tracking
- ✓ Synergetic control
- ✓ Fast Terminal Synergetic control
- ✓ Finite Time convergence
- ✓ Robustness and Stability

Abstract

Among the different renewable energy resources, photovoltaic energy has found increased attention and wide attraction from researchers in many applications, for its capabilities of direct electric energy conversion without any environmental damage, ease of implementation, flexibility in size and low operation cost. The performance of the PV system is mainly depended to temperature, irradiation, dirt and shadows during its operation. Thus, we should extract the maximum power available by the photovoltaic generator (PVG) and transfer it to the load to enhance the PV system's efficiency at any moment although PV units are exposed to non-uniform climate changes. Competent maximum power point tracking (MPPT) technique is needed to track the MPP and maintain the operating point of the PV system at the MPP under any cases. The main purpose of this thesis work is to develop and implement new nonlinear MPPT strategies based on Synergetic Control (SC) and Fast Terminal Synergetic Control (FTSC) able to track the MPP for stand-alone PV system under different conditions and therefore increase the PV system efficiency. The obtained results under different conditions have validated the developed strategies and highlighted their good performance and high robustness compared to other MPPT controllers.

Table of contents

List of abbreviations

ABC   Artificial Bee Colony.

ACO   Ant Colony Optimization.

AC   Alternative current.

ANN   Artificial neural network.

DC/AC   Conversion direct/alternative.

DC/DC   Conversion direct/direct.

FF   Fill factor.

FLC   Fuzzy Logic Controller.

FTS   Fast Terminal Synergetic.

FTSC   Fast Terminal Synergetic Control.

GA   Genetic Algorithm.

HC   Hill Climbing.

IncCond   Incrémental Conductance.

MPP   Maximum Power Point.

MPPT   Maximum Power Point Tracking.

PSO   Particle Swarm Optimization.

PV   Photovoltaic.

PVG   Photovoltaic Generator.

P&O   Perturbation and   Observation.

SC   Synergetic Control.

SMC   Sliding Mode Control.

STC   Standard Test Conditions.

List of symbols

A   Diode ideality factor.

C_{in} Input capacity.

C_o output capacity,

D   Duty cycle.

D_d Discrete control.

D_{eq} Equivalent control.

D_{FTSC} Fast Terminal Synergetic Control law

f_s Frequency.

G_{STC} Reference irradiance at standard test conditions (1000 [W/m²]).

K_i Short-circuit current coefficient.

K_b Boltzmann's constant ($1,3854*10^{-23}$ [J/K]).

K_v Open circuit voltage coefficient.

I_{ph} Photogenerated current [A].

I_{pv} PV output current [A].

$I_{ph\text{-}STC}$ Photo-current generated at standard test conditions [A].

I_{sc} Short circuit current [A].

I_0 Saturation current of the diode[A].

L   Inductance.

M   Conversion ratio.

N_s Identical cells in series.

N_p Identical cells in parallel.

P_{in} Incident light power.

P_{max} Theoretical maximum power.

P_{out} Output power extracted from the PV array.

q   Electron charge ($1.6*10^{-19}$ [C]).

R   resistive load

R_s Series resistance.

R_{sh} Shunt resistance.

S   Sliding surface.

T	PV cell temperature [°K].
T_s	Switching time.
T_{STC}	Reference temperature at standard test conditions (298 [°K]).
$V_{OC\text{-}STC}$	Open circuit voltage at standard test conditions [V].
V_{pv}	PV output voltage.
V_{oc}	Open circuit voltage.
V_i	Input voltage.
V_o	Output voltage.
V_{ref}	reference voltage

List of figures

List of tables

General introduction

Due to the ever-increasing energy demand in all areas and the inability to cover all needs, scientists over the world have resorted to searching for alternative energies that would relieve the pressure on fossil fuels and reduce the environmental problems caused by the latter. Renewable energy is one of the most prominent solutions in the past few decades to produce sustainable and inexhaustible energy that helps in human development and without any environmental damage. Among the various renewable energy sources, solar energy or more known as photovoltaic energy has found great attention and wide attraction from researchers in different applications. This energy is produced from the conversion of solar radiation by capturing sun rays and directly converting them into electricity through photovoltaic solar panels.

Many people probably wonder: if solar energy is so beneficial as an alternative or complement to the conventional energies, why don't we consume it more? The answer to this question is the unbalance between the high installation cost and the low energy conversion of PV array, where many photovoltaic units must be gathered in series and/or in parallel to cover the problem of low electric energy conversion which is mainly undergo to cell temperature, irradiation level, dirt and shadows during its operation. Thus, because of these limitations, we should extract the maximum power available by the photovoltaic generator (PVG) and transfer it to the load to enhance the PV system's efficiency at any moment although PV units are exposed to non-uniform climate changes. The most usual technique consists in using an adaptation stage between the PVG and the load. This stage acts as an interface between the two elements by ensuring, through a control strategy, the transfer of the power delivered by the PV generator to the load so that it is as close as possible to the maximum power available. This challenge can be accomplished by the wise choice of Maximum Power Point Tracker (MPPT) which determines the best functioning of the PV systems.

A large number of MPPT control algorithms have been developed for years, which drive the PV array to operate at the peak of the power against environment changes. Each MPPT technique has its own advantages and disadvantages. These control techniques could be classified into two categories namely the conventional methods and intelligent methods.

Among the various conventional MPPT control algorithms mentioned in literature, perturbation and observation (P&O), hill climbing (HC) and incremental conductance (IC) are the most used for their simplicity and ease of implementation. The P&O algorithm consists of disturbing the PV output voltage and observing the PV output power to determine the peak power direction. The IC method compares between the instantaneous conductance (I/V) of PV array and the incremental conductance (dI/dV) to track MPP. The HC technique locates the MPP by relating changes in the power output to changes in duty ratio of the converter. However, the main drawbacks of these MPPT are the power oscillation around the MPP and the confusion in the tracking direction that occur because of the rapid change in atmospheric conditions. Moreover, these algorithms differ in speed of convergence, cost and efficiency.

In order to overcome the above-mentioned drawbacks, a large number of intelligent and advanced control techniques have attracted a lot of interest over the past few years such as fuzzy logic controller, artificial neural-network, sliding mode control and meta-heuristic techniques like Genetic Algorithm (GA), Particle Swarm Optimization (PSO), Artificial Bee Colony (ABC) and Ant Colony Optimization (ACO). Despite of their effectiveness, right tracking and fast response compared to the conventional techniques, these MPPT techniques are more complex and require large knowledge in the design of the control system otherwise they will lead the system to instability.

Recently, sliding mode control (SMC) is considered to be a powerful technique because of its fast convergence and high robustness. On the other hand, its major flaw is a chattering phenomenon caused by the switching in the control law which induces many undesirable oscillations in control signal and that may lead the system into instability.

From all difficulties inspired from the above study in particular, oscillation behavior, robustness and speed of the MPPT in tracking the optimal power, have guided to improve the performance of the PV system. To achieve this objective, two of the most robust control strategies named Synergetic Control (SC) and Fast Terminal Synergetic Control (FTSC) are adopted.

In this context, the main purpose of this thesis work is to develop and implement new nonlinear MPPT strategies based on Synergetic Control (SC) and Fast Terminal Synergetic Control (FTSC) able to track the maximum power point (MPP) for stand-alone PV system under different atmospheric conditions and therefore increase the PV system efficiency. Both algorithms were simulated via Matlab/Simulink^{MT}, obtained results have confirmed the

excellent performances compared to other techniques. The Synergetic based MPPT technique was also validated experimentally using dSPACE RTI 1104 real-time platform.

The thesis is presented in four chapters.

In the first chapter, the principle of converting solar energy into electrical energy is presented without forgetting to present its equivalent electrical circuit and the main parameters that are used to characterize her performance. The effect of temperature and solar radiation on the I-V and P-V characteristics of a PV array is also discussed in this chapter to show the importance of using an adaptation stage to ensuring, through a control strategy, the transfer of the power delivered by the PV generator to the load so that it is as close as possible to the maximum power available. As the PV system proposed in this work is a stand-alone system, the focus was on the DC-DC boost converter by presenting the electrical circuit and explaining its operating concept.

In the second chapter, the maximum power point tracking (MPPT) issue is presented and explained in order to extract the maximum power from the PV array and thus increase the efficiency of the PV system. Besides that, this chapter reviewed the operating principle of the most commonly MPPT techniques (conventional or intelligent) that are discussed in the literature along with their advantages and disadvantages through a substantial bibliographic investigation.

In the third chapter, a nonlinear Maximum Power Point Tracking (MPPT) controller based on Synergetic Control theory applied to a stand-alone PV system is presented. The developed controller was tested both in simulation using Matlab/Simulink^{MT} tool and experimentally using dSPACE RTI 1104 real-time platform. Furthermore, the EN 50530 standard test with different ramp gradients values is used to calculate the MPPT efficiency under irradiance changes from the slow to the very fast.

Chapter four presents, a new controller to track the MPP based on Fast Terminal Synergetic theory for a standalone PV system which includes PV generator, DC–DC boost converter and a resistive load. The effectiveness and the robustness of the proposed MPPT controller were confirmed by simulation using Matlab/Simulink^{MT} tools not only under atmospheric conditions change but also under load resistance change.

Finally, thesis general conclusion, the author's contribution and suggestions for future researches are presented.

Chapter 1:

Introduction to Photovoltaic Systems

Table of Contents

1.1. Introduction

The huge restriction of fossil fuels on human development and the ever-increasing energy demand in every sphere have resulted to her depletion without forget the serious problems at the environment. To break these drawbacks, research and development of new energy has sparked wide interest in the worldwide.

Over the past few decades, renewable energy sources are considered to be a perfect choice to generating sustainable, abundant, inexhaustible energy and even more of that environmentally friendly. Among the various types of renewable energy sources, solar energy or more popularly known as photovoltaic energy (PV energy) has attracted a lot of interest with many important applications expanding continuously from lighting systems to pumping systems.

1.2. Renewable energies

The development of renewable energies not only responds to an environmental issue, but also corresponds to the need to diversify our energy sources. Renewable energies are an alternative solution to be explored to replace and/or complement other traditional energy sources that provide electrical energy. In the following, the 5 types of renewable energy available are mentioned.

1.2.1. Geothermal energy

Geothermal means in Greek "heat of the earth". Geothermal energy is therefore the energy that is produced by the heat stored below the earth's surface. The advantage of this energy is that it does not depend on climatic conditions or seasons. Geothermal energy comes in two forms:

- ✓ Low temperature to heat private homes.
- ✓ High temperature, in this case, it is a means of producing electricity.

1.2.2. Biomass energy

Biomass energy is the oldest form of energy used by man since the discovery of fire in prehistoric times. The energy from biomass is a renewable energy source which depends on the cycle of living plant and animal matter, this energy is used to produce electricity from the heat released by the combustion of these materials (wood, plants, agricultural waste, organic household waste) or biogas from the fermentation of these materials in biomass power plants.

1.2.3. Hydraulic energy

Water is also a renewable source since it regenerates through the cycle of evaporation and precipitation. Its strength has been known and exploited for thousands of years through dams, water mills and irrigation systems. Hydraulic energy makes it possible to generate electricity, in hydroelectric power stations, using the force of water. This force depends either on the height of the waterfall or on the flow of rivers.

1.2.4. Wind energy

Wind energy is a source of energy that depends on the wind. The sun heats the earth unevenly, which creates zones of different temperatures and atmospheric pressure all around the globe. From these pressure differences arise movements of air, called the wind. This energy is used to produce electricity in wind turbines, also called wind generators, using the force of the wind. It is an energy that does not emit any greenhouse gases and its raw material, wind, is available all over the world and is completely free.

1.2.5. Solar energy

Solar energy is one of the most important renewable resources on earth, widely distributed and increasingly used. This energy is produced from the conversion of solar radiation and exploited using two techniques:

✓ Photovoltaic solar energy: Capturing sun rays and directly converting them into electricity through photovoltaic solar panels.

✓ Solar thermal energy: Capturing, collecting and turning the sunlight into heat that warms up water or air.

In this thesis, photovoltaic solar energy is explained in more detail in the next paragraphs.

1.3. Photovoltaic cells

1.3.1. PV cell history

The history of the PV system goes back to 1839, when a French experimental physicist, Edmund Becquerel discovered the photovoltaic effect. This process occurs when light is absorbed by a material and creates electrical voltage [1]. In 1873, English electrical engineer, Willoughby Smith identified the photoconductive ability of selenium [2]. Three

years later, in 1876 William Grylls Adams and Richard Evans Day conducted an experiment on the photoconductivity of selenium that successfully demonstrated the possibility of generating current with the effect of light in solid selenium [3]. This experiment was the starting point for the current PV cell.

In 1883, American inventor Charles Fritts developed the first PV cell by coating the semiconductor material selenium with a thin layer of gold at an efficiency of less than 2% [2]. The first usable PV cell, using crystalline silicon with efficiency of 6%, was invented by Chapin, Fuller and Pearson in 1954 at the Bell laboratories [4]. The first practical application of PV solar technology took place in 1959, the invention was adopted by the aerospace industry for use in the Vanguard 1 Satellite [5]. Despite the exorbitant cost at that time, PV technology was widely adopted and is now the main source of power for many satellites [6]. Moreover, the telecommunication technology would never have developed if not for PV powered satellites.

Improving solar PV efficiency over the last years, have more encouraged researchers and investors to use this technology as an alternative to generating electricity from fossil fuel, as well as being a good environmental option because it is free from any harmful emissions, polluting gases or any noise.

1.3.2. PV cell technologies

In general, the semiconductor material used in the PV cell is silicon. The latter comes in different forms and offers many advantages, it is present in abundance in the earth's crust and it is a non-toxic material. In addition to its semiconductor properties, it is easy to modify the electrical properties of silicon by introducing doping atoms such as Boron (inducing P-type doping) or Phosphorus (inducing N-type doping) [7].

There are different types of PV cells. However, the most commonly and commercially available types are: monocrystalline, polycrystalline, and amorphous [8, 9, 10, 11]. The advantages and disadvantages vary from one type to another depending on efficient, cost and the intended application.

1.3.2.1. Monocrystalline solar cells

First generation cells, Monocrystalline solar cells are manufactured from near pure silicon in which the structure of the crystal is homogeneous throughout the material. This type of solar cell has higher efficiency (24% in research laboratories and over 17% in industrial

production [9]). The manufacturing process required to produce monocrystalline silicon is complicated, resulting in slightly higher costs than other technologies.

1.3.2.2. Polycrystalline solar cells

Also sometimes known as multicrystalline cells, unlike the monocrystalline solar cells, polycrystalline silicon cells are constructed from an ingot of melted and recrystallised silicon. The ingots are then saw-cut into very thin wafers and assembled into complete cells. Therefore, their production is generally cheaper than monocrystalline cells due to the simpler manufacturing process, but they tend to be slightly less efficient with average efficiencies of 12% to 15% [10, 11].

1.3.2.3. Amorphous solar cells

As second generation solar cells technology, amorphous silicon cells are manufactured by depositing a thin layer of silicon on a base material such as glass or metal. As amorphous silicon absorbs light more effectively than crystalline silicon [11], the cells can be thinner, hence its alternative name of 'thin film cells'. This technology is, however, less efficient than crystalline silicon, with typical efficiencies of around 5% to 7% [10, 11, 12], but it tends to be easier and cheaper to produce. Amorphous solar cells are commonly used for low power applications such as calculators, watches and garden lights.

1.3.3. PV cell structure

The solar cell, which is the basic building block of the PV system, made of various semiconductor materials, most commonly silicon. A typical PV cell is formed with two layers; positive charge is located on one layer (P-type silicon) and negative charge on the other layer (N-type silicon). The P-type silicon layer is produced by adding atoms such as boron that have one less electron in their outer energy level than does silicon. While the N-type silicon layer is made by including atoms that have one more electron in their outer level than does silicon, such as phosphorus. In between the two layers, a P-N junction is created, and so the free electrons in the N-layer diffuse into P-layer causing a depletion zone to be created [7].

When the PV cell is exposed to light, some photons are reflected or pass through the cell without being absorbed. The others are absorbed and hole-electron pairs are then generated. The holes and electrons are then separated by the electric field produced by the P-

N junction [8]. This results in a potential difference and a current flow if the PV cell is connected to a load. Figure 1.1 shows the principle of converting solar energy into electrical energy by photovoltaic cells.
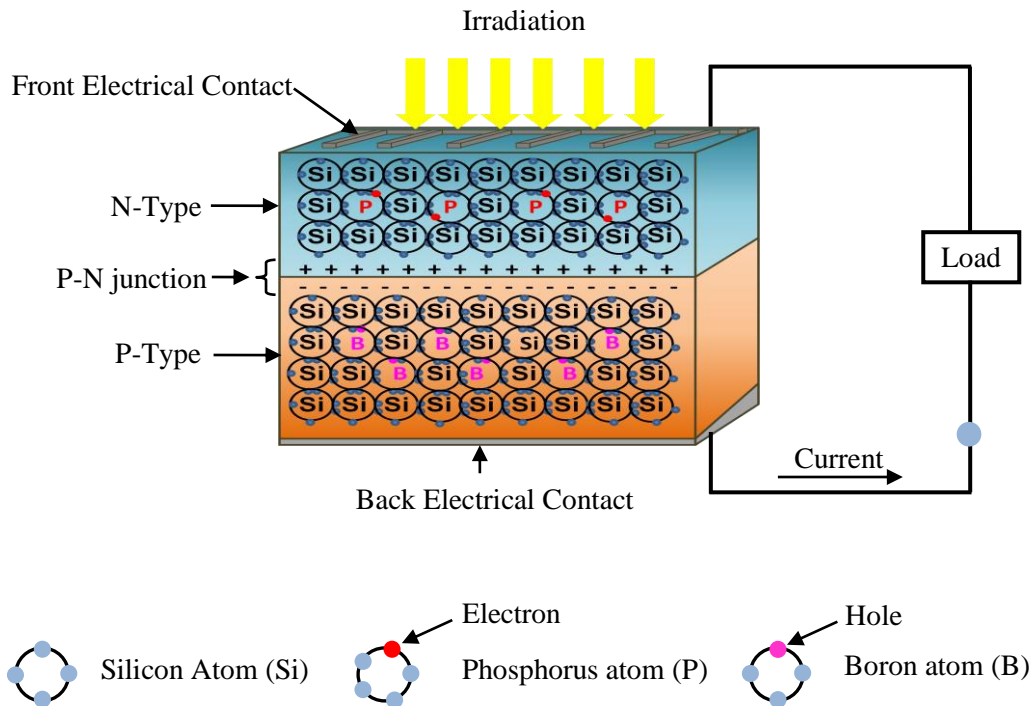
Fig. 1.1 Structure and working mechanism of a PV cell.

1.3.4. PV cell modeling

Many mathematical models of PV cells have been developed to represent their very strongly non-linear behavior due to the semiconductor junction. These models differ from each other by mathematical procedures and the number of parameters involved in calculating the voltage and the current of the photovoltaic module. In the literature two equivalent circuit models of PV cell have been discussed and analyzed [9, 13, 14]: single diode model and double diode model, both are based on the well known Shockley diode equation.

For simplicity, the PV single diode model, shown in Figure 1.2, is studied and used in this work. This model offers a good compromise between simplicity and accuracy. The equivalent circuit consists of a photocurrent source in parallel with one diode. The solar cell losses are represented by two resistances, the series resistance R_s to represents the ohmic resistance losses (such as the resistance of the semiconductor, metal contacts, and contacts between them) and the shunt resistance R_{sh}, to describe the leakage currents through the edges of the solar cell as well as the P-N junction (due to material defects).

10
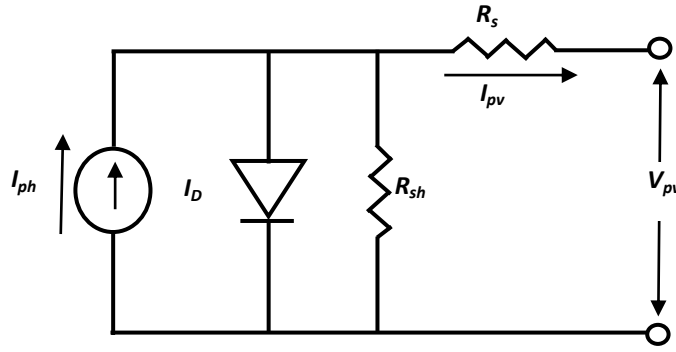
Fig. 1.2. Single diode based-equivalent circuit of solar cell.

According to this scheme, the mathematical model of the generated current in a PV system is represented by:

$$I_{pv} = I_{ph} - \underbrace{I_0 \left[\exp\left(\frac{q(V_{pv} + I_{pv} R_S)}{A T K_b}\right) - 1\right]}_{I_d} - \frac{V_{pv} + I_{pv} R_S}{R_{Sh}}$$
(1.1)

Where:

I_{pv} is the PV output current.

V_{pv} is the PV output voltage.

A is the diode ideality factor.

k_b is Boltzmann's constant ($1,3854*10^{-23}$ [J/K]).

q is the electron charge ($1.6*10^{-19}$ [C]).

T is the PV cell temperature [°K].

I_{ph} is the photogenerated current, depends on temperature and solar irradiance G [W/m²], often given by:

$$I_{ph} = \frac{G}{G_{STC}} \left[I_{ph\_STC} + K_i(T - T_{STC})\right]$$
(1.2)

Where:

T_{STC} is the reference temperature at standard test conditions (298 [°K]).

G_{STC} is the reference irradiance at standard test conditions (1000 [W/m²]).

I_{ph_STC} is the photo-current generated at standard test conditions [A].

K_i is the is the short-circuit current coefficient, normally supplied by the manufacturer.

I_0 is the saturation current of the diode given as follows:

$$I_0 = \frac{I_{ph\_STC} + K_i(T - T_{STC})}{\exp(q[V_{oc-STC} + K_v(T - T_{STC})]/ATK_b) - 1} \tag{1.3}$$

Where:

V_{oc_STC} is the is the open circuit voltage at standard test conditions [V].

K_v is the is the open circuit voltage coefficient, supplied by the manufacturer.

1.3.5. PV cell characteristic

Equation (1.1) shows that a PV cell has a non-linear I-V characteristics curve as shown in Figure 1.3. This curve depends on the internal characteristics of the solar cell (R_s, R_{sh}) and on the external influences, such as the cell temperature level and the sun irradiance. The PV cell I-V curve is divided into three important parts, as follows:

✓ In the region left of the MPP, the PV current is almost constant and the PV cell can be approximated as a constant current source.

✓ In the region right of the MPP, the PV current begins a sharp decline and the PV cell can be approximated as a constant voltage source.

✓ In the region around of the MPP, at which the current is I_{mpp} and the voltage is V_{mpp}. The resulting power $P_{mpp} = I_{mpp} * V_{mpp}$, is the maximum PV power that can be delivered for the given environmental conditions.

For each point of the previous PV cell I-V curve, we can calculate the power and draw the PV cell P-V curve, as shown in Figure 1.4.
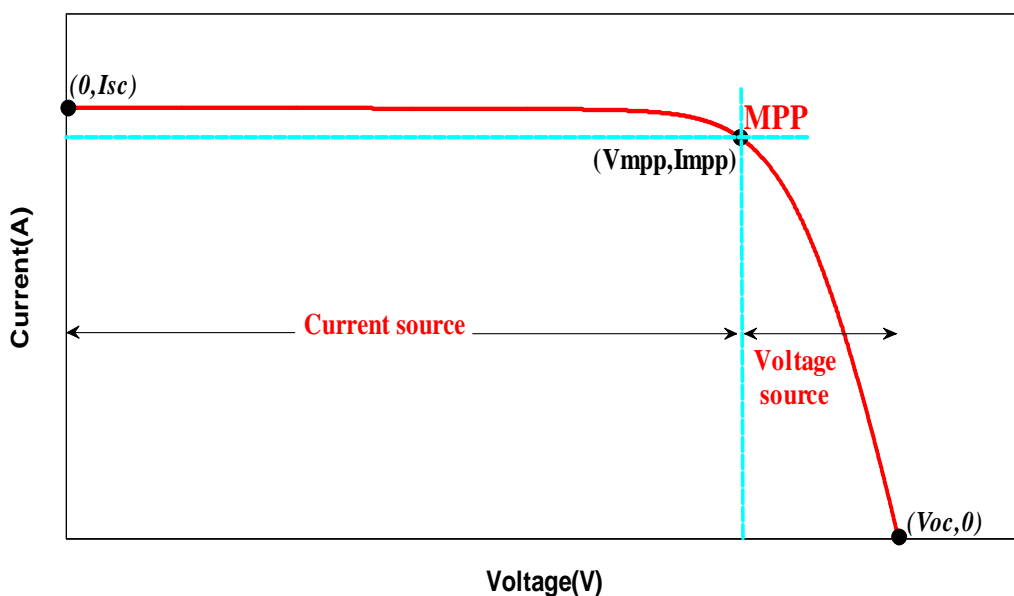
Fig. 1.3. PV cell I-V characteristic curve.
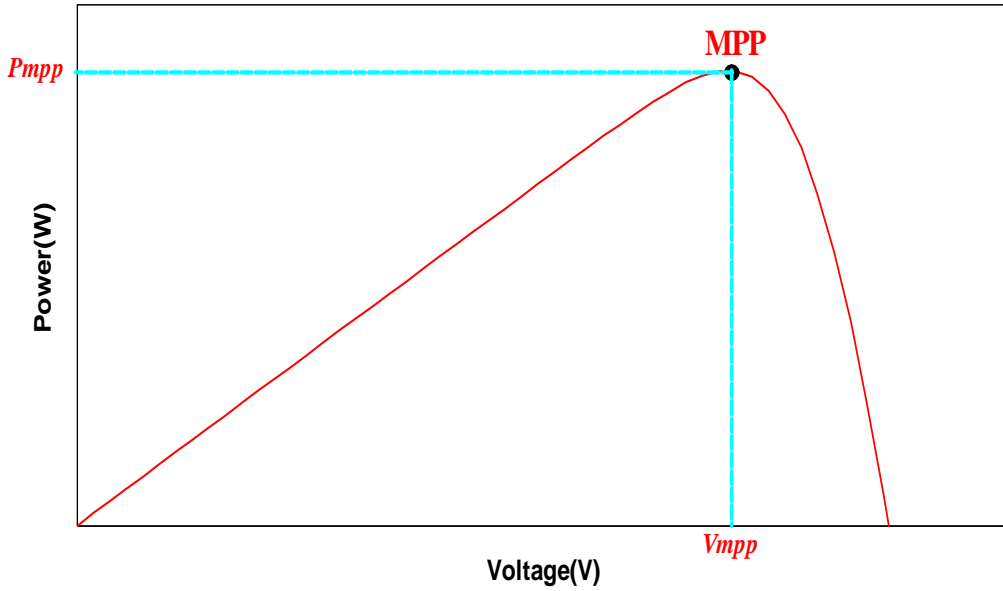
Fig. 1.4. P-V characteristic curve of PV cell.

1.3.6. PV cell parameters

The main parameters that are used to characterise the performance of solar cells can be determined from the I-V and P-V curves, or from the characteristic equation. The most common parameters are the following [10, 11, 12, 15]:

✓ **Short-circuit current I_{sc}:** It is the value of the current which imposes a zero voltage across the terminals of the PV solar cell. It can be obtained by canceling the voltage V in equation (1.1), we obtain:

$$I_{sc} = I_{ph} - I_0 \left[\exp\left(\frac{q I_{sc} R_S}{AT K_b} \right) - 1 \right] - \frac{I_{sc} R_S}{R_{Sh}} \qquad (1.4)$$

For most PV cells, whose series resistance is low, the term below is negligible compared to I_{ph}.

$$I_0 \left[\exp\left(\frac{q I_{sc} R_S}{ATK_b} \right) - 1 \right]$$

The approximate expression of the short circuit current is then:

$$I_{sc} = \frac{I_{ph}}{\left(1 + \frac{R_S}{R_{Sh}} \right)} \qquad (1.5)$$

✓ **Open circuit voltage V_{oc}:** It is the voltage for which the current delivered by the cell is zero. It represents the maximum voltage of a photovoltaic cell under given climatic conditions; it decreases with temperature and varies little with light intensity. Its expression is deduced as follows:

$$0 = I_{ph} - I_0 \left[\exp\left(\frac{qV_{oc}}{ATK_b}\right) - 1 \right] - \frac{V_{oc}}{R_{Sh}} \tag{1.6}$$

So:

$$V_{oc} = \left(\frac{ATK_b}{q}\right) \ln\left(\frac{I_{ph}}{I_0} - \frac{V_{oc}}{R_{Sh}I_0} + 1\right) \tag{1.7}$$

In the ideal case, $R_{sh} \to \infty$, which simplifies this expression:

$$V_{oc} = \left(\frac{ATK_b}{q}\right) \ln\left(\frac{I_{ph}}{I_0} + 1\right) \tag{1.8}$$

✓ **Maximum power point P_{mpp}:** It is the operating point P_{mpp} (V_{mpp}, I_{mpp}) in Figure 1.3, for which the power generated by the solar cell is maximum under given climatic conditions. The power is zero in short circuit, it increases until P_{mpp} at the maximum power point (MPP) then decreases to zero again in open circuit. Professionals characterize a PV module by its maximal power at Standard Test Conditions STC (generally: irradiance of 1000 W/m² and temperature of 298 K).

✓ **Fill factor FF:** It is an important parameter to qualify the quality of a photovoltaic cell compared to an ideal cell (FF = 1). It is the ratio between the maximum power delivered by the PV cell on the product of the short circuit current (I_{sc}) and the open circuit voltage (V_{oc}).

$$FF = \frac{P_{mpp}}{I_{sc} * V_{oc}} = \frac{I_{mpp} * V_{mpp}}{I_{sc} * V_{oc}} \tag{1.9}$$

✓ **Efficiency η:** It is the ratio of conversion of light energy into electrical energy, which is defined as the ratio between the maximum power delivered by the PV cell P_{mpp} and the incident light power P_{in}. The value of P_{in} is equal to the product of the illumination E (W/m²) by the surface of the module S (m²).

$$\eta = \frac{P_{mpp}}{P_{in}} = \frac{FF * I_{sc} * V_{oc}}{S * G} \tag{1.10}$$

14

1.4. Photovoltaic configuration

A photovoltaic system consists of a solar array which is a group of series/parallel connected modules, where the basic component within the module is the solar cells [8, 16]. Arrays are a way to increase the potential of a solar electricity system, to provide a greater output of electricity. Figure 1.5 represents a photovoltaic system configuration.

PV array

PV module

PV cell

From a PV cell to a PV array
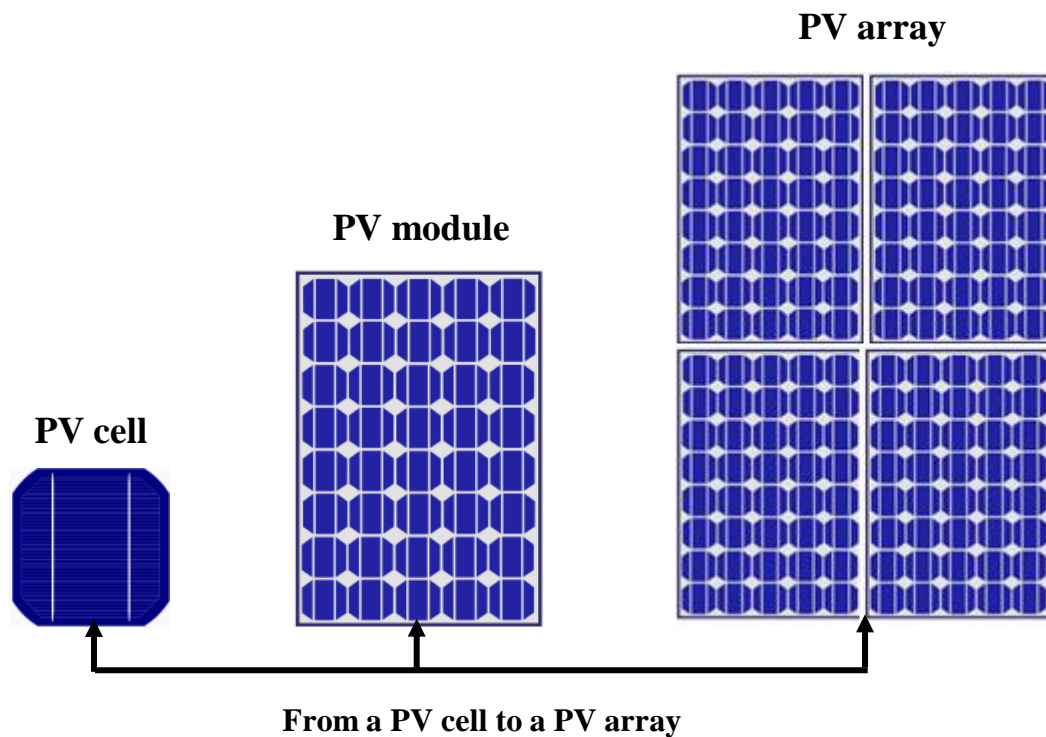
Fig. 1.5. Photovoltaic system configuration.

1.4.1. Photovoltaic modules

The photovoltaic module is a set of solar cells assembled to generate an exploitable electric power during its exposure to solar irradiation. Indeed, a PV solar cell produces only a very low electrical power, typically from 1 to 3 W with a voltage of 0.5 to 1.5 Volts depending on their technology [15, 17]. To generate more power, solar cells are generally grouped in series and / or in parallel to form a PV module. In addition, the fragility of cells makes them vulnerable to breakage and corrosion, which requires protection from their environment, so they are usually encapsulated under glass [10, 15].

The I-V characteristic of any group of cells will be compatible with the I-V curve of a basic cell. Consequently, everything that has been said for an individual cell will remain valid for a grouping of cells.

1.4.1.1. Serial association

In a grouping of N_s identical cells in series (figure 1.6), the current of the branch remains the same but the voltage increases in proportion to the number of cells connected in series. The characteristic of the grouping is obtained by multiplying point by point and for the same current the individual voltage by N_s [18]. The optimal impedance of the grouping will be N_s greater than that of the basic cell.
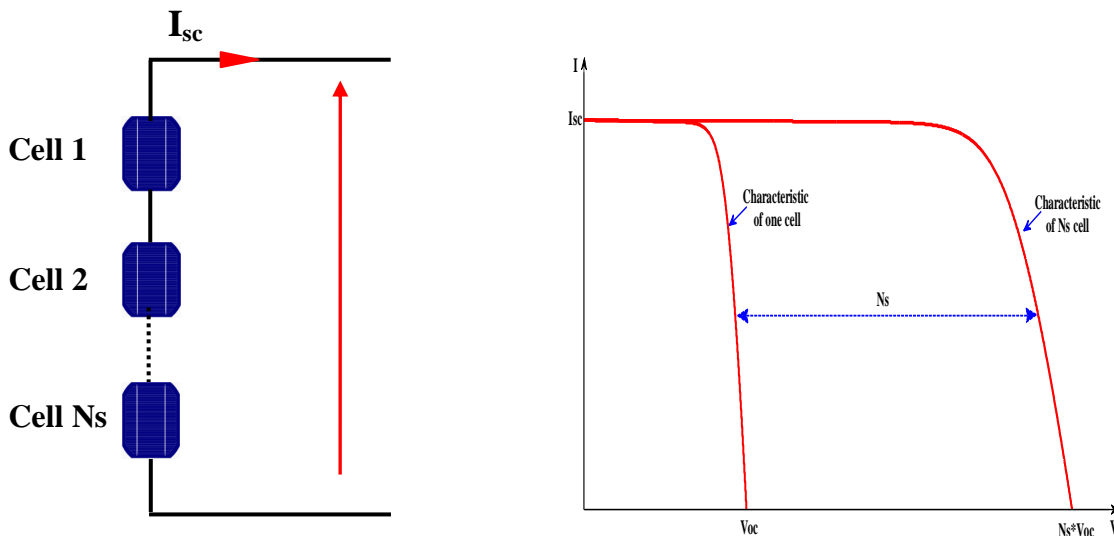
Fig. 1.6. Serial association of N_s identical cells.

1.4.1.2. Parallel association
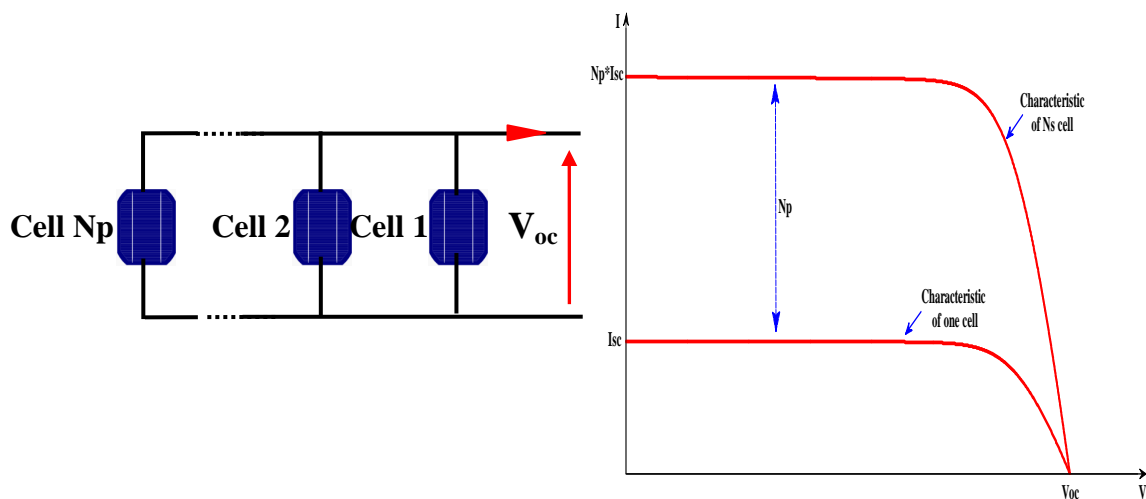
Fig. 1.7. Parallel association of N_p identical cells.

A parallel association of N_p cells is possible and makes it possible to increase the output current. In a group of identical cells connected in parallel, the cells have the same voltage and the new curve is obtained by multiplying point by point and for each voltage value, the current of the elementary cell by N_p [18]. The optimal impedance of the grouping will be N_p lower than that of the basic cell. Figure 1.7 shows the resulting characteristic obtained from a parallel association of Np cells.

1.4.1.3. Serial/Parallel association

A hybrid association of N_s cells in series and N_p cells in parallel has a general curve comparable to that of an elementary cell, provided that there is no imbalance between the characteristics of each cell (uniform irradiation and temperature). Figure 1-8 shows the resulting characteristic obtained by associating, N_s in series and N_p in parallel, identical cells.
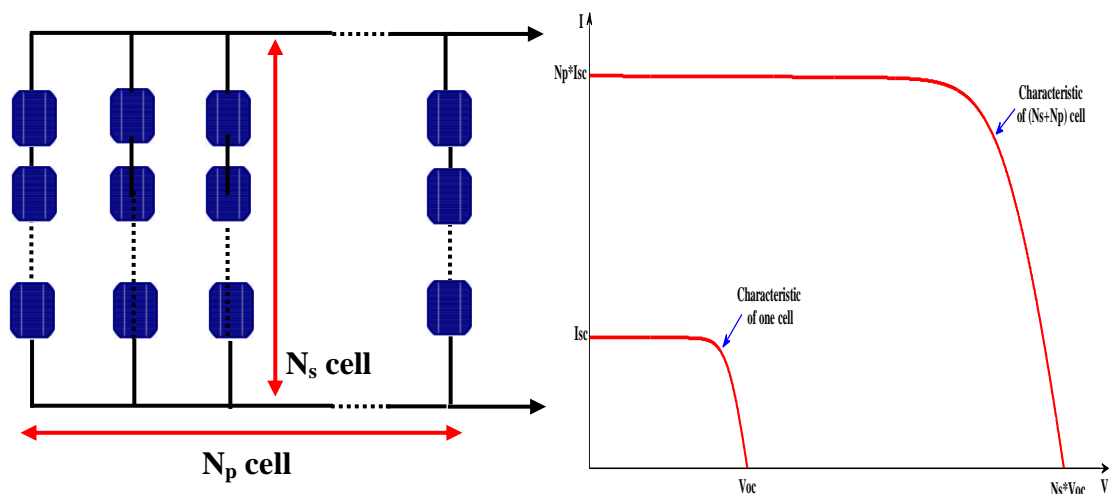
Fig. 1.8. Hybrid association of identical cells.

1.4.2. Photovoltaic array

A PV array consists of a group of series-parallel connected PV modules as shown in Figure 1.5, to generate the required voltage and current values for the system. The size of the PV array varies from a single PV module to any number of modules, where the number of PV modules in each string should the same to get equal parallel voltages [8, 19]. Depending on equation1.1, the nonlinear current-voltage characteristic of the PV array is modeled by the following equation where all cells are identical [16, 20]:

17

$$I_{pv} = N_p I_{ph} - N_p I_0 \left[\exp\left(\frac{q\left(N_s V_{pv} + (N_s/N_p)I_{pv} R_S\right)}{AT K_b N_s} \right) - 1 \right] - \frac{N_s V_{pv} + (N_s/N_p)I_{pv} R_S}{(N_s/N_p)R_{Sh}} \qquad (1.11)$$

Where N_s is the number of series PV modules in one PV string and N_p is the number of the parallel strings in the PV array.

The PV panel considered for this thesis is Kyocera KC85T consists of 36 solar cells connected in series to give a maximum output power of 87 W. Its electrical characteristics at standard test conditions (1000 W/m² and T=25°C) are given in Table 1.1 and its characteristic curves are plotted for different environmental conditions.

Table 1.1. Electrical characteristics of Kyocera KC85T PV module.

Description	Kyocera KC85T
Maximum power (Pmax)	87 W
Open-circuit voltage (Voc)	21.7 V
Short-circuit current (Isc)	5.34 A
Optimum operating voltage (Vmpp)	17.4 V
Optimum operating current (Impp)	5.02 A
Temperature coefficient of I_{sc}	2.12e-3 A/°C
Temperature coefficient of V_{oc}	-8.21e-2 V/°C

1.4.2.1. Influence of external parameters on the PV array characteristics

In order to highlight the strong dependence of PV array performance and efficiency on temperature and irradiance level, the Kyocera KC85T PV module characteristics curves are plotted for different atmospheric conditions. There is a single MPP for a certain irradiance level and cell temperature. As the PV module characteristics curves shift with changing irradiance or cell temperature, this MPP moves.

The figure 1.9 shows the I-V and P-V curves of the PV module under different solar irradiance level at fixed temperature T=25 C°. It is obvious that the irradiance has a significant effect on the short circuit current value (I_{sc}). On the contrary, the irradiance level has a slight effect on the open circuit voltage value (V_{oc}). The increase of the solar irradiance also results in an increase of the available maximum power.

(a)   (b)
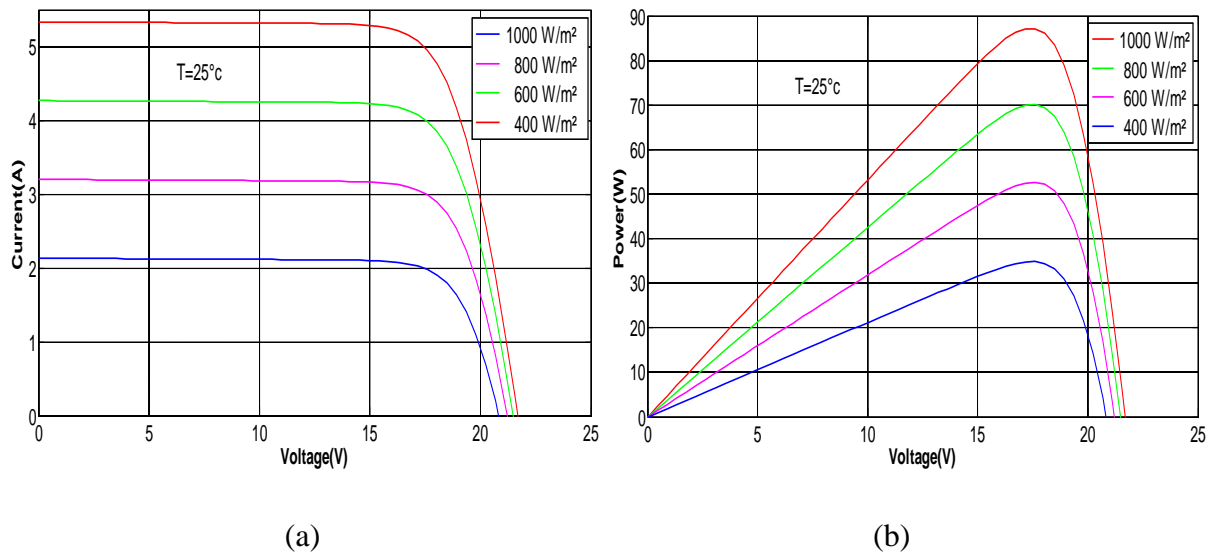
Fig. 1.9. I–V characteristics (a) and P–V characteristics (b) under different solar irradiation levels at 25°C.

On the other hand, the figure 1.10 shows the I-V and P-V curves of the PV module under different cell temperature at fixed irradiance G=1000 W/m². The cell temperature has a negligible effect on the short circuit current value (I_{sc}), whereas it has an important effect on the open circuit voltage value (V_{oc}). The increase of the temperature also results in a decrease of the available maximum power as shown in figure 1.11(b). It is worth noting that once thermal stability occurs, the cell temperature usually changes quite slowly and almost fixed with respect to the variation in the irradiation level during the day [8, 21].

(a)   (b)
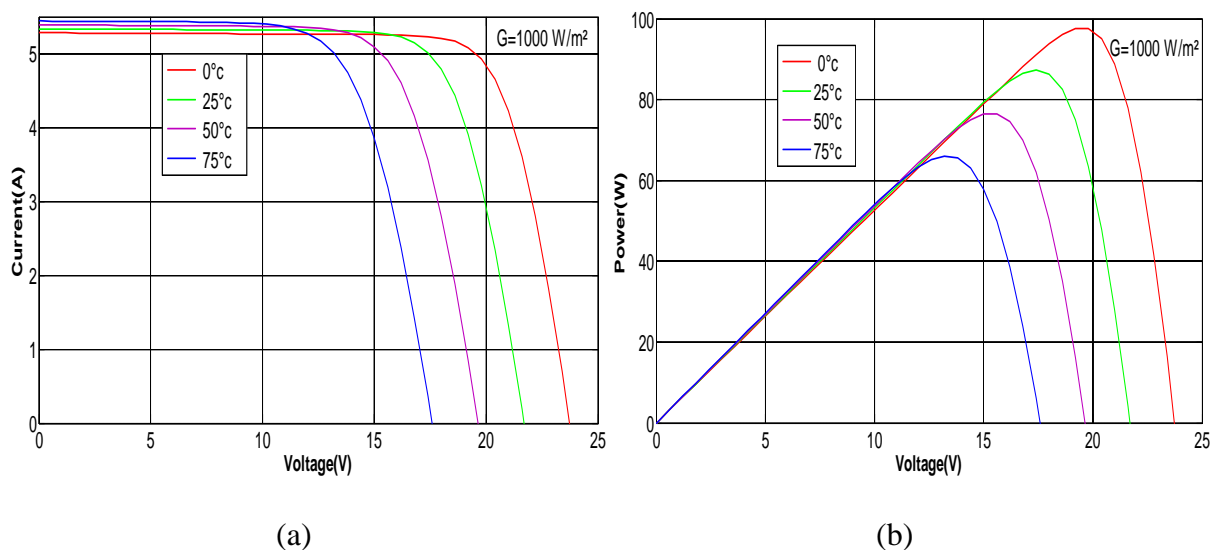
Fig. 1.10. I–V characteristics (a) and P–V characteristics (b) under different cell temperature at 1000 W/m².

19

1.4.2.2. Partial shading impacts

Fig. 1.11. Effects of partial shading on PV array.

Since PV systems generate electricity based on the amount of sunlight they receive, it stands to reason that when a shadow is cast on a panel for example by a dust, bird dung or nearby trees (Figure 1.11), its power output decreases. However, the decrease in power could be a lot worse than it initially seems.

Intuition indicates that power output of the PV array will be reduced proportionally to the area that is shaded. But, this is not the case in actually. In his book *Renewable Energy and Efficient Electric Power Systems*, Stanford University, Gil Masters demonstrates how shading just one out of 36 cells in a small solar module can reduce power output by over 75% [22].

Because of the serial connection of the photovoltaic cells or module, shading of one cell in the string leads to the cell acting as a load rather than a generator, which causes a significant increase in the cell temperature. If the temperature reaches too high values and if the system is not appropriately protected, hot spot problem can arise [12, 19, 23, 24]. The hot spots phenomenon can be also occur when the photovoltaic modules are connected in parallel with different open circuit voltages. For example, if one of the parallel PV modules has lowest voltage due to the shadow effect, the PV array can behave as a load and consume the power generated by the other modules. In severe cases, the cell or module can be irreversibly damaged and affects the whole PV array.

Fortunately, there are a number of different approaches that can be applied in PV system design to reduce shading losses. These include the use of bypass diodes and blocking diodes.

1.4.2.3. PV array protection

To reduce the PV power losses that caused by partial shading and prevent hot-spots occurring in underperforming PV cells, the reverse voltage is usually limited through the use of so-called "bypass" and "blocking" diodes. These diodes are easy to implement since they can be encapsulated in the PV module during manufacturing.

✓   **Bypass diodes:** have the role of protecting the cells which become passive. These diodes have been connected in parallel but with opposite polarity to a solar cell .When bypass diode starts to work, short-circuits part of the panel as shown in figure 1.12, thus avoiding the circulation of reverse currents within the defective cells. So the degradation of a single cell condemns the group of cells associated with the defective cell and protected by the bypass diode not to produce power. The ideal is to place one bypass diode for each solar cell [25] but for reason of cost, usually just one bypass diode for each group of cells should be applied. Several configurations are presented but the most adopted is to place 2 to 5 diodes depending on the number of cell [12, 26].
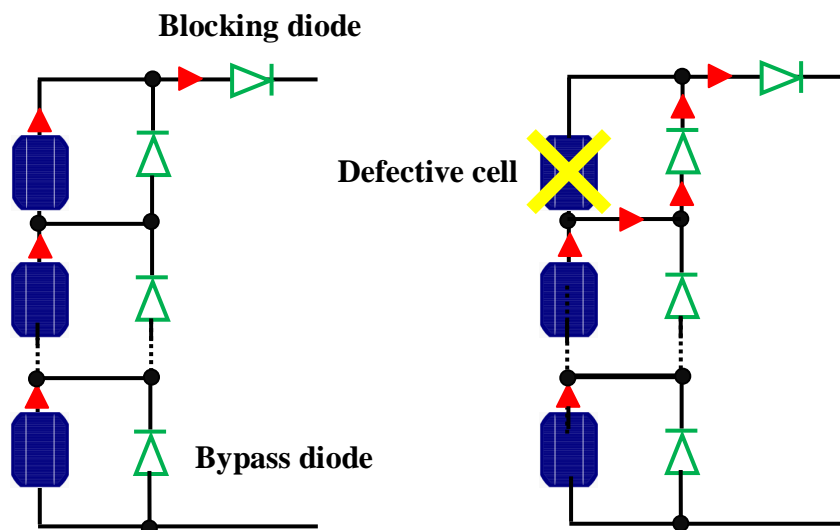
Fig. 1.12. Protection diodes for PV array.

✓   **Blocking diodes:** When strings of modules are wired in parallel, the hot spots phenomenon can be also occur when one of the strings is not performing well. Instead of supplying current to the PV array, a malfunctioning or shaded string can withdraw current from the rest of the array. To avoid this phenomenon and prevent the reverse current drawn by a shaded string, blocking diodes or what also called by isolation diodes are connected in series at the top of each string as shown in figure. 1.12.

1.5. Types of photovoltaic systems

Photovoltaic systems are generally classified according to their operational requirements and how the equipment is connected to other power sources and electrical loads. The two principal classifications are stand-alone systems and grid-connected systems, the former supplies power directly to electrical equipment while the latter feeds energy into the public electricity grid.

1.5.1. Stand-alone PV systems

The stand-alone PV systems are generally used in isolated locations and operated independently of the utility grid. They are particularly suitable for applications as a pump in the garden, lighting in isolated areas, Lighthouses at sea, etc.

Stand-alone PV systems are designed to supply either DC or AC electrical loads [8, 22]. For DC load application, PV systems utilize single-stage DC/DC power converters (boost, buck or buck-boost). As for AC load application, a two-stage topology is used. In the first stage, the DC/DC converter is utilized. In the second stage, the DC/AC inverter is used to convert the DC power to AC power.

In some PV applications, battery banks are essential for stand-alone PV systems [26, 27] as electricity generation is neither constant nor controllable, it depends on atmospheric conditions (solar irradiance and temperature). With batteries banks, the electricity generated by PV panels can be stored and used to supply the required load power when the sunshine is insufficient (at night or on cloudy days). Figure 1.13 shows the stand-alone PV system with battery bank.
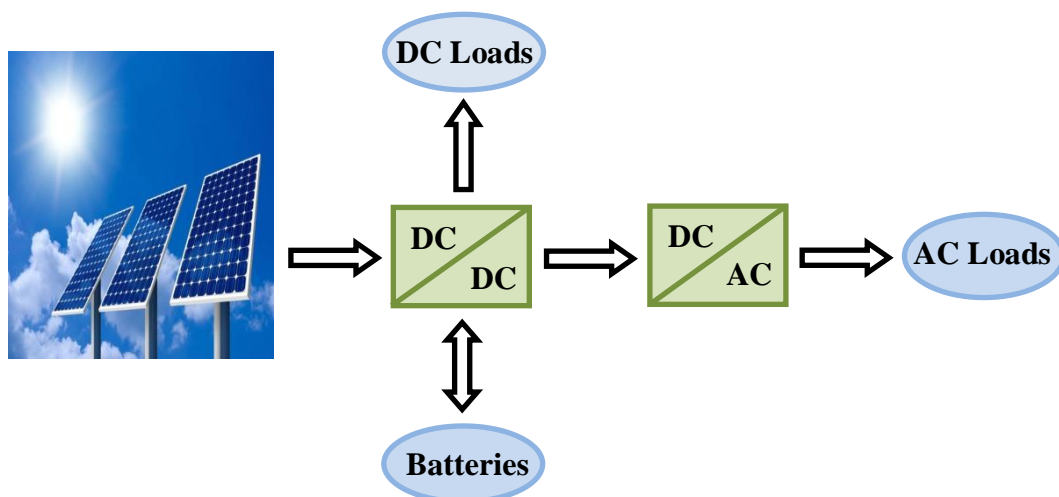
Fig. 1.13. Stand-alone PV system with battery bank.

1.5.2. Grid-connected PV systems

In these systems, the PV installations are connected to the public electricity network into which they inject the electricity they produce for best utilization without the need of battery back-up. This type of systems offers a lot of ease for the producer / consumer since it is the network that takes care of the balance between the production and consumption of electricity.

The PV panels generate DC power. Therefore, to inject the PV power into the grid, the photovoltaic DC power must be converted to AC power. In order to convert electricity from direct current (DC) as produced by the PV panels to alternating current (AC), a power electronics inverter is employed (DC/AC) as shown in Figure 1.14. The typical efficiency of an inverter is about 95%, there are different power inverters and are designed specifically for photovoltaic applications [20].
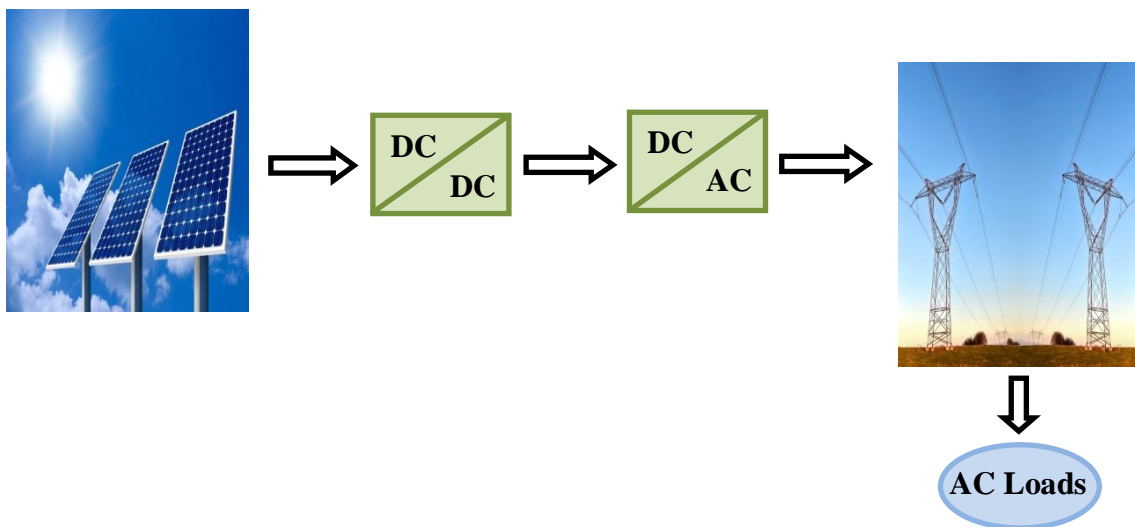
Fig. 1.14. Grid-connected PV system.

1.6. Interfacing PV generator to load

1.6.1. Direct connection (PV generator-load)

When connecting directly a load with a PV generator (PVG) without passing through another electrical device, it is the case of direct connection. This choice is mainly related to the simplicity and the cheap of the operation. Figure 1.15 shows the principle of a direct connection between a PVG and a load.
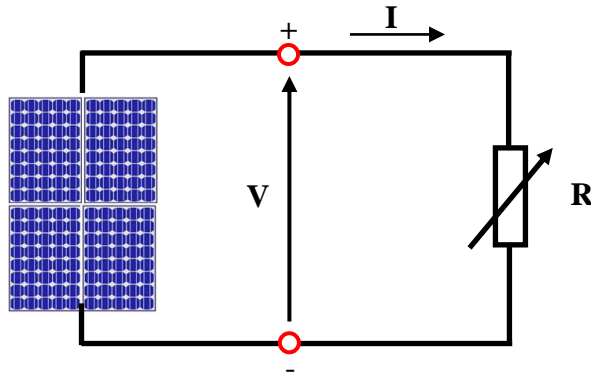
Fig. 1.15. Direct connection between a PVG and a load.

In this case, the operating point of the PVG depends on the impedance of the load to which it is connected and it is determined by the intersection of the I-V characteristic of the PVG and the load curve. For a resistive load, the I-V characteristic is a straight line with a slope of 1/R as shows in figure 1.16.

Therefore, if the resistance R is small, the operating point is located in the AB region of the curve and so the PVG behaves like a current source. On the other hand, if R is large, the PVG operates in the CD region of the curve. In this zone, the PVG behaves like a voltage source. In the BC region on the curve, the PVG can be characterized neither by a current source nor by a voltage source. It is in this area that the Maximum Power Point (MPP) is located for fixed atmospheric conditions. The value of the resistance corresponding to this point is noted R_{opt} [28, 30].
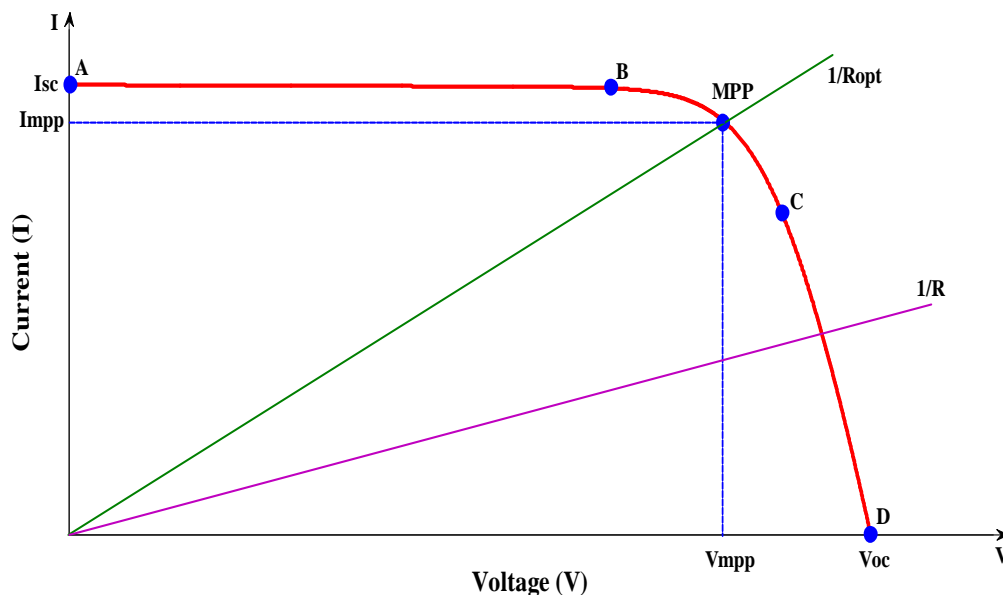
Fig. 1.16. Operating points of a PVG in direct connection depending on the load.

The disadvantage of this configuration is that the PVG is badly exploited, the power extracted from PVG is often very far from the maximum power that the PVG can delivered [29]. On the other hand, certain types of loads need alternative currents. Direct connection is therefore not possible because the PVG provides direct current. Through these examples, we can show the limits of the direct connection. To remedy this problem, an adaptation stage between the load and PVG must be added.

1.6.2. Indirect connection (PV generator-load) through an adaptation stage

As we saw earlier, a PVG has non-linear I(V) characteristics with maximum power points (MPP). These characteristics depend on irradiance level and cell temperature. In addition, depending on the characteristics of the load, we can find a very large difference between the output power of the PVG and that actually transferred to the load in the direct connection mode.

In order to extract every moment the maximum power available by the PVG and transfer it to the load, the most usual technique consists in using an adaptation stage between the PVG and the load as shown in figure 1.17 [10, 31]. This stage acts as an interface between the two elements by ensuring, through a control strategy, the transfer of the power delivered by the PV generator to the load so that it is as close as possible to the maximum power available [32].
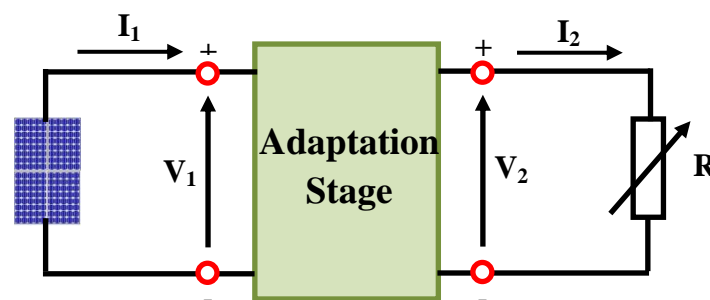
Fig. 1.17. Adaptation stage between PVG and load.

The adaptation stage usually consists of a static power converter, which is located between the PVG and the load. Depending on the application and the degree of production optimization desired, the adaptation stage can consist of one or more static converters.

A static converter is composed of a set of electrical components building a meshed network of electrical components that acts as a linking, adapting or transforming stage between two sources aims at improving the efficiency. The principle of the converter is based

on the automatic variation of the duty cycle of the converter to approach t the optimum value so as to maximize the power at the output of the PV generator [33].

Today, two distinct types of adaptation stages which are more present on the market. The first type is DC-DC converter (chopper), used to connect the PVG to a continuous load. This type is mostly used for isolated site operation (off-grid). In some cases, there is no choice because the characteristics of the load are not compatible with the form of electricity produced by the PVG. This is the case for all loads requiring AC voltages. In this case, a DC-AC converter (inverter) is used which makes it possible to perform a DC-AC conversion.

In the content of this thesis we are just interested in DC-DC converter topology as an interface between the PVG and the load because it is best appropriate to our work.

1.7. DC-DC converter topology

The DC-DC converter plays a major part in the PV system configuration. The use of DC-DC converter makes it possible to convert the voltage of a DC source from one level to another with very great flexibility and a high efficiency which in our case will allow us to track the optimum operating point and ensuring at the same time a good performance coping with power changes introduced by the change in the environmental conditions [35]. Depending on the relationship between the input and the output voltages, a DC-DC converter can be designed to step the voltage up or down by controlling the converter duty ratio (D) with maximum power point tracking algorithms (MPPT) [37]. In addition, this control can be conducted at a normal or high frequency (generally in the range of 1 kHz to 1 MHz, depending on the switching speed of semiconductor devices) [6, 15].

A DC-DC converter consists of capacitors, inductors, and switches [34]. All these devices in the ideal case consume no energy; this is the reason why this type of converters is characterized by a high efficiency. The switch is realized with a semiconductor device in switched mode, generally a MOSFET or IGBT transistor [36, 38]. If the semiconductor device is in the open state, its current is zero and therefore there is no power dissipation. If it is in the closed state (saturated), the voltage drop is almost zero and therefore the power dissipated will be very low.

During the operation of the converter, the transistor will be switched at a constant frequency (f_s) with a closing time equal to DT_s and an opening time equal to (1-D) T_s [15]. D is the duty cycle of the switch (D € [0 1]) and T_s is the switching time which is equal to $(1/f_s)$ as shown in figure 1.18.
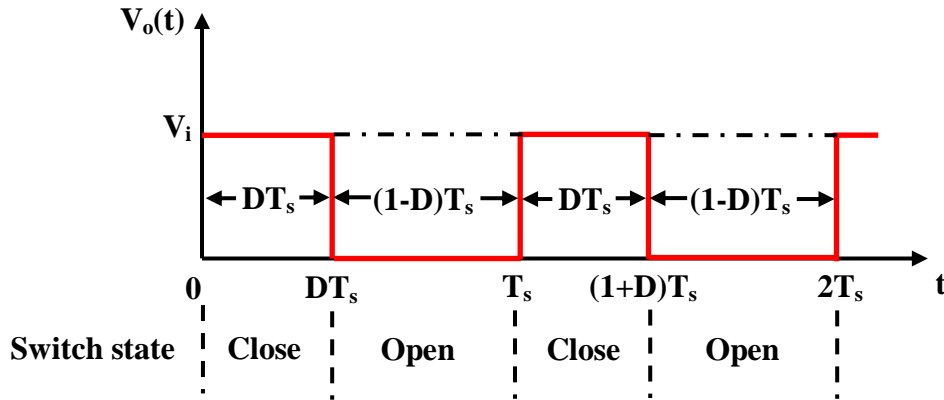
Fig. 1.18. DC-DC Converter output voltage waveform.

Generally speaking, three different types of DC-DC power converters are most frequently used within a given PV system depending on the conversion ratio M, which is the ratio between the output voltage V_o and the input voltage V_i ($M = V_o / V_i$). When M is greater than 1, the converter is called step up or boost converter. When M is less than 1, the converter is called step down or buck converter. When M can be greater or less than 1, the converter is called step up & step down or buck-boost converter [15, 36].

Among the DC-DC topologies existed, the boost converter has seen widespread adoption in PV systems. It is difficult to identify all studies that have used boost converters in PV grid-connected or stand-alone applications for reasons of simplicity, high efficiency and the presence of the input inductor which guarantees the compatibility with the primary source and improves the global performance. In the content of this thesis, a DC-DC boost converter is adopted as interface between the PV array and the load, for this we will discuss in detail the operating principle of boost converter in the next section.

1.7.1. Operating principle of DC-DC boost converter
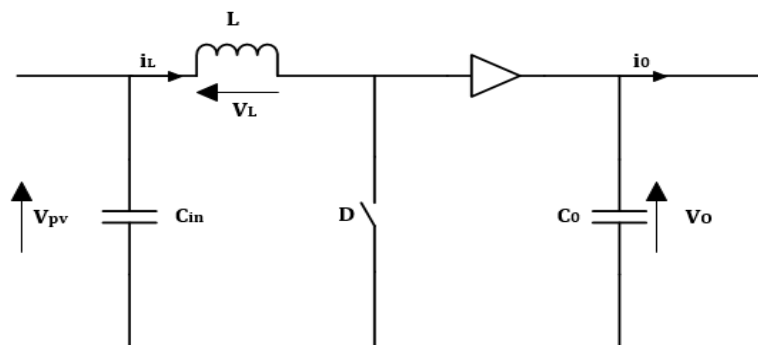
Fig. 1.19. DC-DC boost converter circuit.

27

A boost converter is a device which step-up the input voltage and gains a higher output voltage. The input and output of the boost are DCs and the output keeps its polarity [6]. This converter is very simple in structure, design and control. It can be implemented with an inductor, a power electronic switch (usually MOSFET or IGBT), a diode and a capacitor [26, 11, 16, 38]. Figure 1.19 shows the basic construction of a boost converter circuit.

To understand the operating principal of the boost converter, the circuit must be critically analyzed and mathematically modeled whether the status of the switch is on or off. The equivalent boost circuits during switch-on and switch-off intervals for ideal switch are shown in Figure 1.20 and Figure 1.21 respectively. If we assume that Ts is the switching period, DT_s will be the time when the switch is ON and (1-D) T_s will be the time when the switch is OFF.

During the time DT_s, the switch is closed (Figure 1.20), the diode operates on a reverse-bias so the current will go through the inductor and to the source. In this case the inductor L stores the energy of the power source while the capacitor C_o discharges to supply the load.
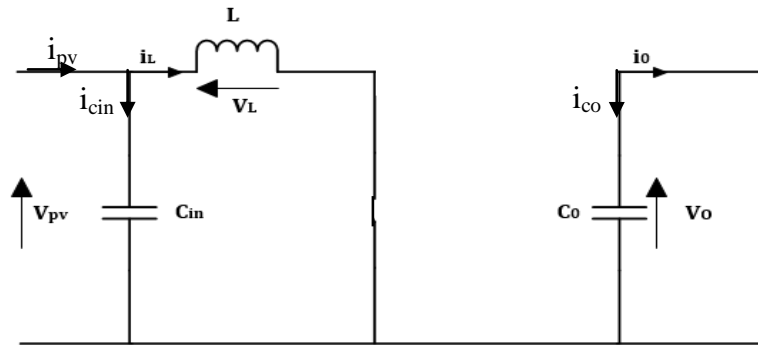
Fig. 1.20. Equivalent boost circuits during switch-on.

In this case, the DC-DC boost converter operation can be described by the well-known system of equations as follows:

$$i_{Cin}(t) = C_{in}\frac{dV_{PV}(t)}{dt} = i_{pv}(t) - i_L(t)$$

$$V_L(t) = L\frac{di_L(t)}{dt} = V_{pv}(t) \tag{1.12}$$

$$i_{Co}(t) = C_o\frac{dV_o(t)}{dt} = -i_o(t)$$

On the other hand and during the time (1-D) T_s, the converter switch is off. The diode in this case acts in a forward-biased scenario, which offers a path for the energy stored in the

inductor L and that of the source to be transferred to the output capacitor C_o and the load. The equivalent circuit of boost converter in this phase is given in Figure 1.21.
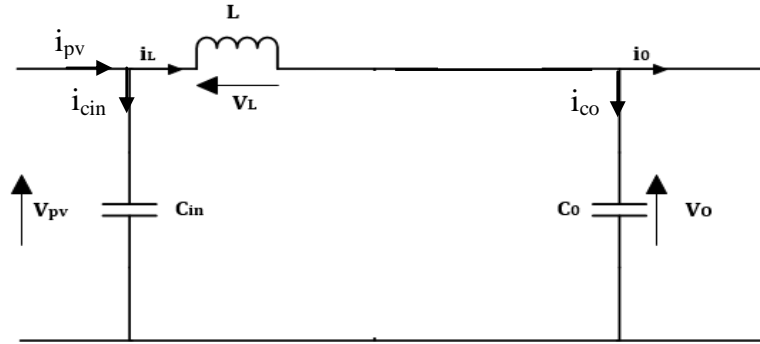
Fig. 1.21. Equivalent boost circuit during switch-off.

The DC-DC boost converter operation during $t \in [DT_s, T_s]$ can be described by the following equations as.

$$i_{Cin}(t) = C_{in} \frac{dV_{PV}(t)}{dt} = i_{pv}(t) - i_L(t)$$

$$V_L(t) = L \frac{di_L(t)}{dt} = V_{pv}(t) - V_o(t) \tag{1.13}$$

$$i_{Co}(t) = C_o \frac{dV_o(t)}{dt} = i_L(t) - i_o(t)$$

1.7.2. Approximate model of DC-DC boost converter

The basic equations (1.12) and (1.13) represent the DC-DC Boost converter for a period DTs and (1-D)Ts respectively. The converter oscillating between these two states with a high frequency, we must find an approximate dynamic representation valid for the two time intervals.

The following approach allows us to decompose the expression of the average value of the derivative of the dynamic variable y over the two time periods DT_s and $(1-D)T_s$ [39]:

$$< \frac{dy}{dt} > T_s = \frac{dy}{dt}_{(DT_s)} . DT_s + \frac{dy}{dt}_{((1-D)T_s)} . (1-D)T_s \tag{1.14}$$

Where $< \frac{dy}{dt} >$ is the average value of the derivative of y over a period T_s.

This relation is valid if $\frac{dy}{dt}_{(DT_s)}$ and $\frac{dy}{dt}_{((1-D)T_s)}$ are constant over the periods DT_s and $(1-D)\ T_s$ respectively.

By applying the relation (1.14) on the systems of equations (1.12) and (1.13) and by considering that the variation of the dynamic variables i_C, V_L is of linear form, we find the approximate model of the Boost converter over a whole period as:

$$C_{in}\frac{dV_{PV}}{dt}T_s = DT_s(i_{pv} - i_L) + (1 - D)T_s(i_{pv} - i_L)$$

$$L\frac{di_L}{dt}T_s = DT_sV_{pv} + (1 - D)T_s(V_{pv} - V_o) \tag{1.15}$$

$$C_o\frac{dV_o}{dt}T_s = -DT_s\frac{V_o}{R} + (1 - D)T_s\left(i_L - \frac{V_o}{R}\right)$$

Simplifying the previous equations, gives the dynamic modeling of the DC-DC Boost converter represented by equations (1.16).

$$\frac{dV_{PV}}{dt} = \frac{1}{C_{in}}(i_{pv} - i_L)$$

$$\frac{di_L}{dt} = -(1 - D)\frac{V_o}{L} + \frac{V_{pv}}{L} \tag{1.16}$$

$$\frac{dV_o}{dt} = (1 - D)\frac{i_L}{C_o} - \frac{V_o}{RC_o}$$

If we set V_{pv}, i_L and V_o as system state variables, we obtain:

$$X = \begin{bmatrix} x_1 \\ x_2 \\ x_3 \end{bmatrix} = \begin{bmatrix} V_{pv} \\ i_L \\ V_o \end{bmatrix} \tag{1.17}$$

The system of equations (1.16) can be written as equation (1.18):

$$\dot{X} = \frac{dX}{dt} = f(x, t) + g(x, t)D \tag{1.18}$$

Where:

$$\dot{X} = \begin{bmatrix} dV_{pv}/dt \\ di_L/dt \\ dV_o/dt \end{bmatrix}, \quad f(x) = \begin{bmatrix} \frac{1}{C_{in}}(i_{pv} - x_2) \\ \frac{1}{L}(x_1 - x_3) \\ \frac{1}{C_o}\left(x_2 - \frac{x_3}{R}\right) \end{bmatrix}, \quad g(x) = \begin{bmatrix} 0 \\ \frac{1}{L}x_3 \\ -\frac{1}{C_o}x_2 \end{bmatrix}$$

The detailed parameters of the DC-DC boost converter used in the suggested study in this thesis are given in Table 1.2.

Table 1.2. DC-DC boost converter parameters.

Description	Boost parameters
Capacitor C_{in}	200 µF
Capacitor C_o	20 µF
Indictor L	$15e^{-3}$ mH
Resistive load R	20 Ω
Switching frequency	10 KHz

1.8. Summary

In this chapter, a study on the principle of converting solar energy into electrical energy is presented. The chapter providing a general view on photovoltaic cell, starting by a brief historical about her foundation and development to the main parameters that are used to characterize her performance, without forgetting to present its equivalent electrical circuit based on a mathematical analysis. Furthermore, the low output power of the single PV cell is discussed to pointing a necessity to connect number of cells in series and in parallel with protection diodes to form a PV module and array to meet the desired load power either in standalone or grid connected PV applications.

The effect of temperature and solar radiation on the I-V and P-V characteristics of PV array is also discussed in this chapter to show the importance of using an adaptation stage to ensuring, through a control strategy, the transfer of the power delivered by the PV generator to the load so that it is as close as possible to the maximum power available. As the PV system is proposed in this work is a stand-alone system, the focus was on the DC-DC boost converter. The electrical circuit of this converter was presented and operating concept was thoroughly explained.

The various techniques for tracking the maximum power point, which aim to keep the maximum power available continuously despite changes in weather conditions, will be the subject of the following chapter.

References

[1.1].   E. Becquerel, "On electron effects under the influence of solar radiation". Comptes Rendues 9, 1839.

[1.2].   M. Green, "Photovoltaics: Coming of age, Photovoltaic Specialists Conference". Conference Record of the Twenty First IEEE. IEEE, 1-8.1990.

[1.3].   W.G. Adams, and R. Day, "The Action of Light on Selenium". Proceedings of the Royal Society of London, 25(171-178), pp. 113-117.1876.

[1.4].   D. Chapin, C. Fuller, and G. Pearson, "A new silicon p-n junction photocell for converting solar radiation into electrical power". Journal of Applied Physics, 25(5), pp. 676-677. 1954.

[1.5].   J. Perlin, "A History of Photovoltaics", 2008.

[1.6].   M. A. Alqarni, "A High Efficiency Photovoltaic Inverter System Configuration with Maximum Power Point Tracking". Doctoral thesis, Brunel University London, March 2016.

[1.7].   I. A. Abdalla, "Integrated PV and Multilevel Converter System for Maximum Power Generation under Partial Shading Conditions". Doctoral thesis, University of Leeds, School of Electronic and Electrical Engineering, February 2013.

[1.8].   B. N. Alajmi, "Design and Control of Photovoltaic Systems in Distributed Generation". Doctoral thesis, University of Strathclyde, Department of Electronic and Electrical Engineering, January 2013.

[1.9].   Y. Liu, "Advanced Control of Photovoltaic Converters". Doctoral thesis, University of Leicester, April 2009.

[1.10].   H. Attoui, "Contribution à la synthèse de nouvelles stratégies de commande des systèmes d'énergie renouvelable". Doctoral thesis, University of Ferhat Abbas Setif, 2018.

[1.11].   A. Ghamrawi, "Optimisation et gestion des flux énergétiques d'un générateur solaire photovoltaïque". Doctoral thesis, University of Poitiers, December 2018.

[1.12].   T. Radjai, "Commandes Avancées des Convertisseurs Utilisés dans les Systèmes Photovoltaïques". Doctoral thesis, University of Ferhat Abbas Setif, April 2017.

[1.13]. O. Gergaud, B. Multon and H. Ben Ahmed, "Analysis and Experimental Validation of various Photovoltaic System Models", 7th International ELECTRIMACS Congress, Montreal (Canada), pp.1-6, August 2002.

[1.14]. M. Jieming, "Optimization Approaches for Parameter Estimation and Maximum Power Point Tracking (MPPT) of Photovoltaic Systems". Doctoral thesis, University of Liverpool, August 2014.

[1.15]. B. Bendib, "Une nouvelle approche de modélisation et de commande des systèmes photovoltaïques autonomes". Doctoral thesis, University of Ferhat Abbas Setif, November 2017.

[1.16]. B. Talbi, "Contribution à l'Amélioration de la Commande d'un Système de Pompage Photovoltaïque". Doctoral thesis, University of Ferhat Abbas Setif, June 2018.

[1.17]. A. Labouret and M. Villoz, "Energie Solaire Photovoltaïque ". 4ème édition. France: Dunod, 2009.

[1.18]. M. Petibon Stéphane, "Nouvelles architectures distribuées de gestion et de conversion de l'énergie pour les applications". Doctoral thesis, University of Toulouse III- Paul Sabatier, January 2009.

[1.19]. R. Kadri, "Contribution à l'amélioration de la capture de l'énergie solaire photovoltaïque dans l'habitat résidentiel : nouvelles structures de puissance et de commande ". Doctoral thesis, University of Poitiers, December 2010.

[1.20]. B. Boukezata, " Etude et commande d'une chaine de conversion d'énergie d'un système solaire photovoltaïque ". Doctoral thesis, University of Ferhat Abbas Setif, 2017.

[1.21]. N. Femia, et al, "Power Electronics and Control Techniques for Maximum Energy Harvesting in Photovoltaic Systems ". Taylor & Francis Group, 2013.

[1.22]. G. M. Masters, "Renewable and Efficient Electric Power Systems". University of Stanford. 2004.

[1.23]. R. E. Meng, "Methods for Investigating Interactions between Multiple Maximum Power Point Trackers in Photovoltaic Systems". Doctoral thesis, University of Leicester, April 2013.

[1.24]. J. G. Garza. "Modelling and Control of Integrated PV-Converter Modules under Partial Shading Conditions". Doctoral thesis, University of Leeds, December 2013.

[1.25]. E. Suryanto Hasyim, S. R. Wenham, and M. A. Green, "Shadow tolerance of modules incorporating integral bypass diode solar cells". Sol. Cells, vol. 19, no 2, p. 109‑122, December. 1986.

[1.26]. S. Hadji, "Optimisation de la conversion énergétique pour les systèmes à énergie Photovoltaïque". Doctoral thesis, University of Ferhat Abbas Setif, October 2018.

[1.27]. N. E. Zakzouk, "Photovoltaic System Design and Control". Doctoral thesis, University of Strathclyde, 2015.

[1.28]. L. Castaner and S. Silvestre, "Modelling photovoltaic systems using PSpice". Catalonia University, Spain, 2002.

[1.29]. N. Derbel and Q. Zhu, "Modeling, identification and control methods in renewable energy systems". Book, 2019.

[1.30]. L. Vechiu, "Modélisation et Analyse de l'Intégration des Énergies Renouvelables dans un Réseau Autonome", University of Havre, 2005.

[1.31]. A. Belkaid, "Conception et implémentation d'une commande MPPT de haute performance pour une chaine de conversion photovoltaïque autonome". Doctoral thesis, University of Ferhat Abbas Setif, October 2015.

[1.32]. A. Cid Pastor, "Conception et Réalisation de Modules Photovoltaïques Electroniques". Doctoral thesis, September 2006.

[1.33]. D. Meekhun, "Réalisation d'un système de conversion et de gestion de l'énergie d'un système photovoltaïque pour l'alimentation des réseaux de capteurs sans fil autonomes pour l'application aéronautique". Doctoral thesis, University of Toulouse.

[1.34]. O. L. Santos, "Contribution to the DC-AC conversion in photovoltaic systems: module oriented converters". Doctoral thesis, University of Toulouse, February 2015.

[1.35]. K. S. Nathan, "A Novel DC-DC Converter for Photovoltaic Applications". Doctoral thesis, University of Cambridge, September 2018.

[1.36]. M. H. Rashid, "Power Electronics Handbook: Devices, Circuits and Applications". 3rd ed. MA, USA: Elsevier and Butterworth-Heinemann, 2011.

[1.37]. F. Aashoor, "Maximum power point tracking techniques for photovoltaic water pumping system". Doctoral thesis, University of Bath, May 2015.

[1.38]. M. A. Alsumiri, "Sliding Mode Control of Renewable Energy Generation Systems". Doctoral thesis, University of Liverpool, May 2015.

[1.39]. S. M. Ait cheikh, "Etude, Investigation et conception d'algorithmes de commande appliqués aux systèmes photovoltaïques". Doctoral thesis, National Polytechnic School. December 2007.

Chapter 2:

Literature Review on Maximum Power Point Tracking Techniques

Table of Contents

2.1. Introduction

Under uniform irradiance level and constant cell temperature, a PV module has a non-linear I–V and P-V characteristic curve on which there is a single optimal operating point, called the maximum power point (MPP).

To confirm that the PV system operates at the MPP, a maximum power point tracking (MPPT) control technique has been implemented which enables the maximum power to be delivered during the operation of the PV array and which tracks the variations in maximum power caused by the changes in the atmospheric conditions, thereby we guarantee an increase in the overall efficiency of the system.

In fact, determining the MPP is not always easy, since it depends on fluctuations in climatic conditions. A review and analysis of several MPPT techniques have been carried out in [2.1, 2.2, 2.3, 2.4, 2.5] to quantify the performance of each control algorithm compared to the others, some of these MPPT are very simple while other approaches are more complicated and more difficult to implement.

2.2. Maximum power point tracking issue

In the case of direct connection to the load, the operating point of a solar panel is the intersection of the two characteristic curves of the panel and the load. This point does not correspond to that of maximum power in most cases. As the characteristic of the solar panel is non-linear, the location of the MPP on the P-V curve varies in an unpredictable manner it cannot be defined beforehand due to changes in irradiation and temperature (figure 2.1).
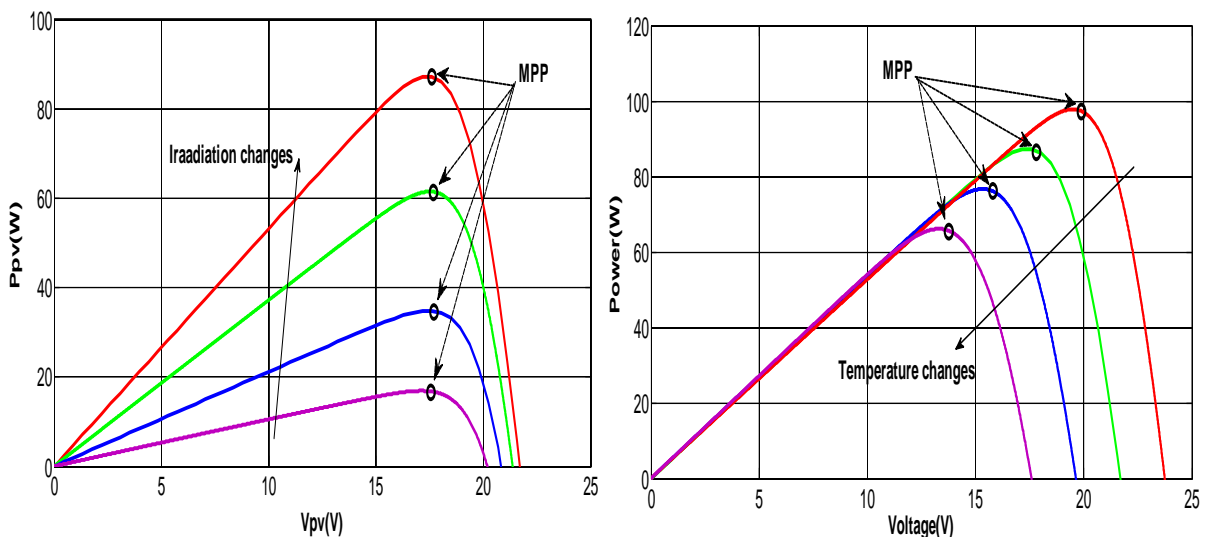
Fig. 2.1. Influence of the climatic conditions on the MPP.

In order to control the operating point, an adaptation stage is added between the photovoltaic generator and the load. This stage which aims to minimize the difference between the maximum available power and the power actually recovered, is only a DC-DC power converter controlled by a maximum power point tracking technique (MPPT) as figure 2.2 show. It is generally based on the adjustment of the duty cycle of the converter until it is placed on the MPP in all climatic conditions.
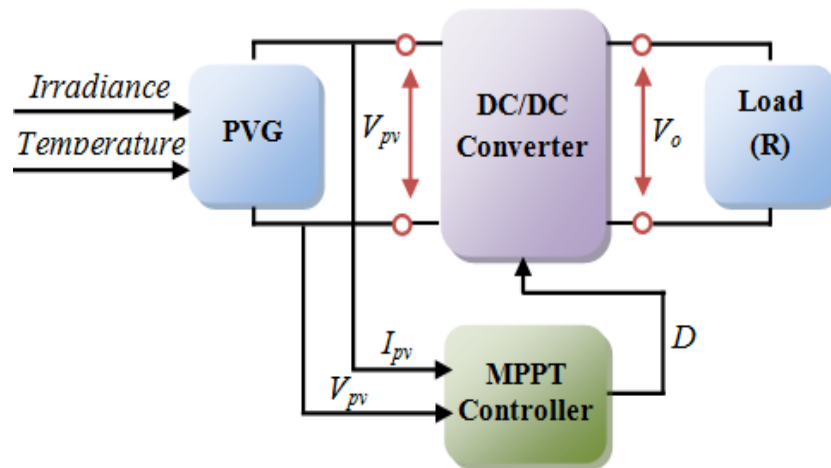
Fig. 2.2. Block diagram of the photovoltaic system.

To evaluating the performance of a new or modified MPPT control techniques, several criteria should be considered, the most important of them are:

✓ **Dynamic response:** To be efficient, the response of a MPPT control technique needs to be fast to track the MPP during the rapid changes in the atmospheric conditions (solar irradiation and temperature). The higher the tracking speed of the MPPT algorithm, the lower the loss in solar energy in the system.

✓ **Steady state error:** The MPPT controller should stop tracking, once the MPP is located and should force the system to maintain operation at this optimal operating point as long as possible. In most MPPT controllers and in steady state, the operating point appears fluctuations around the MPP. These fluctuations cause losses, this is why an MPPT controller must minimize these fluctuations as much as possible to allow the system to operate as close as possible to the MPP and subsequently, increase the overall PV system efficiency.

✓ **Tracking efficiency:** Defining the tracking efficiency is a very important step, to quantify how successfully an MPPT control algorithm tracks the MPP and to what extent it contributes to increase the overall performance of the PV system compared to other methods. The atmospheric conditions are able to change in a large proportion during a day.

Hence, each MPPT technique must be evaluated over a range of different operating conditions when comparing MPPT algorithm performance. A well-designed MPPT control system should provide good performance in different atmospheric conditions.

✓ **Stability:** Since the characteristics of the solar panel as well as the static converters used in photovoltaic systems are non-linear, the stability is a very important factor for the evaluation of the MPPT techniques.

✓ **Robustness:** Change in irradiance and/ or temperature can lead to an error in tracking the MPP and therefore the instability of the photovoltaic system. An MPPT controller must take these disturbances into account to be robust.

2.3. Literature review on Maximum Power Point Tracking (MPPT)

Numerous MPPT Algorithms with different levels of complexity, accuracy, efficiency, time response, cost, and implementation difficulty have been proposed for maximizing the energy utilization efficiency of the PV arrays in the literature [2.6, 2.7, 2.8]. In this chapter, different MPPT strategies are analyzed before introducing the principles of our new strategy. The aim of our approach is to list the existing and identify the limits of each method as well as the possible improvement perspectives.

According to the originality and the limitations associated to these strategies, we propose a classification into two families. The first group includes the conventional MPPT techniques in which we introduce some of the most used algorithms, while the second family groups the intelligent MPPT techniques in which we suggest some possible improvements.

2.3.1. Conventional MPPT techniques

Among the conventional MPPT techniques mentioned in the literature to reach MPP, perturbation and observation (P&O), incremental conductance (IncCond) and hill climbing (HC), are the most widely used because of simplicity, ease of implementation, and low cost.

For a better understanding of the performance of these techniques, we explain in the following paragraphs their different principles.

2.3.1.1. Perturbation and observation algorithm (P&O)

The perturbation and observation algorithm is considered to be the most commonly used MPPT algorithm among the other techniques because of its simplicity, low cost and ease of implementation [2.2, 2.9, 2.10, 2.11]. It is based on the concept that on the P-V curve, the

change in the PV array output power is equal to zero ($\Delta P_{pv} = 0$) on the top of the curve as illustrated in figure 2.3. From its name, the P&O algorithm operates by continuously perturbing PV system either by incrementing or decrementing the operating PV output voltage and observing its effect on the output power of the PV array. According to this observation, the algorithm decides on the act to do during the next iteration. Four situation cases for P&O are considered in figure 2.3 and summarized in Table 2.1.

　　　As illustrated in P-V curve of figure 2.3, we can see that when there is a same variation positive or negative in both of the PV output power and voltage ($\Delta P_{pv} > 0$ and $\Delta V_{pv} > 0$) or ($\Delta P_{pv} < 0$ and $\Delta V_{pv} < 0$), the operation point of the system is located at the left side of the MPP, in this case the increasing in the PV output voltage is required to track the MPP. Otherwise, when the variation in P_{PV} output power and V_{PV} output voltage is different ($\Delta P_{pv} < 0$ and $\Delta V_{pv} > 0$) or ($\Delta P_{pv} > 0$ and $\Delta V_{pv} < 0$), the operation point of the system is located at the right side, in this case the decreasing in the PV output voltage is required to track the MPP. From these various analyses, it is easy to locate the position of the operation point of the PV system compared to the MPP on the P-V curve. Thereafter, through an appropriate control, the operating point can move towards the maximum power point.
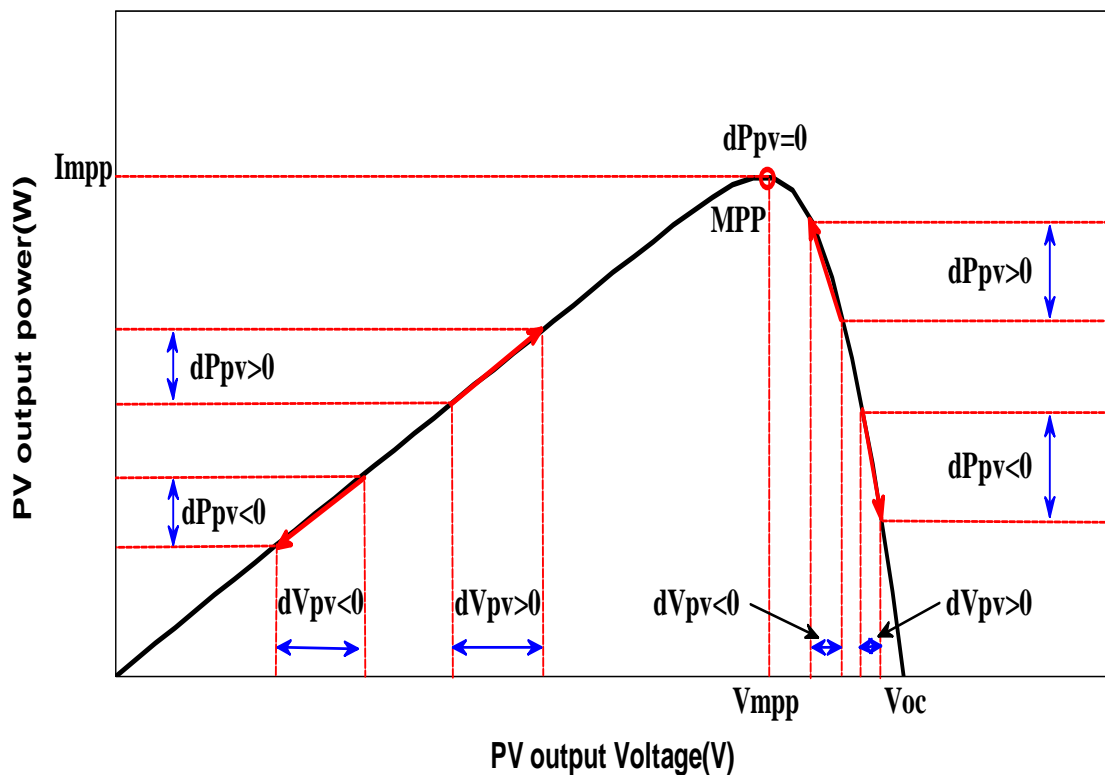
Fig. 2.3. Operating principle of the P&O algorithm based MPPT controller.

Table 2.1. P&O operating principle.

Case N°	ΔV	ΔP	$\dfrac{\Delta P}{\Delta V}$	Tracking direction	Control act
1	+	+	+	good	V=V+ ΔV
2	-	-	+	bad	V=V+ ΔV
3	+	-	-	bad	V=V- ΔV
4	-	+	-	good	V=V- ΔV
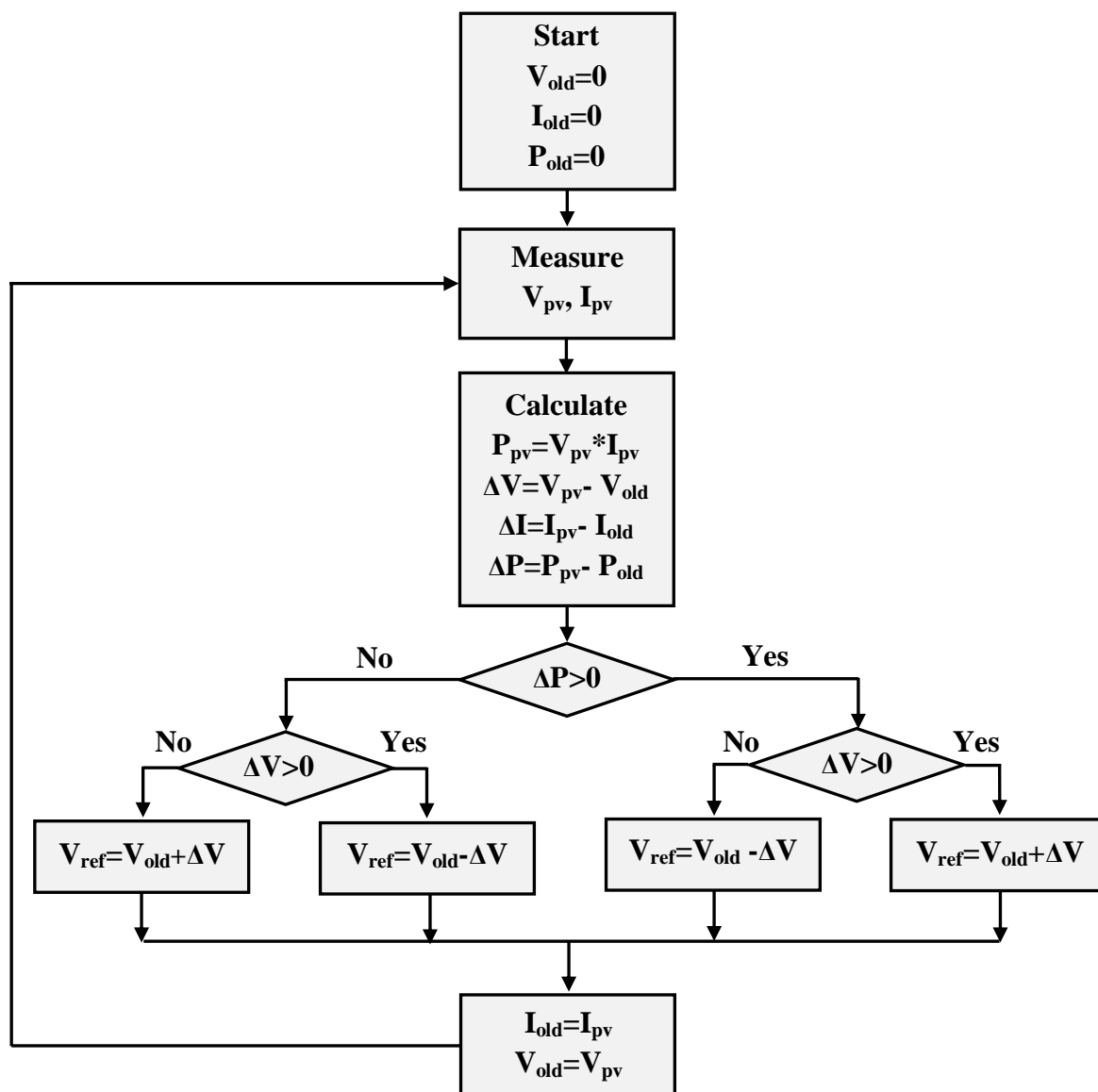
Fig. 2.4. Flowchart of P&O algorithm.

The flowchart of the conventional P&O algorithm is presented in figure 2.4. For this type of control, both of current and voltage of the PV panel are required to determine the PV output power every moment.

Conventional P&O algorithm based on the fixed step size perturbation have two primary demerits. The first is the oscillation around the MPP at steady state, which gives rise to the waste of some amount of available energy [2.12, 2.13, 2.14]. Where the small step size helps causes a low oscillations, but significantly slows the tracking progressions. Unlike the large step size leads to faster response but with higher oscillations at steady-state conditions. Improved versions of P&O algorithms exist to overcome this oscillation problem. For example, one study suggested a variable step size perturbation that starts high and decreases as it converges to the MPP [2.15]. Other studies suggested variable values for the perturbation introduced with the P&O method [2.16, 2.17].

The second disadvantage of the P&O algorithm is the low quality tracking during rapidly changing weather conditions. The MPPT algorithm moves away from the real MPP due to the quick change in the weather conditions. To summarise this problem, the algorithm is not intelligent enough to distinguish if the new output power value is higher because of the new irradiation amount or because of the value of the new duty cycle. So improvements have been made to overcome these issues. Authors in Ref. [2.13] correct the trajectory of the P&O algorithm to trend close to the real MPP by separating the effect of irradiation change from the effect of the tracker perturbation. References [2.10, 2.18, 2.19] propose modified P&O algorithm called dP-P&O by inserting an additional power measurement in the middle of MPPT sampling period, in order to prevent deviation from the MPP as well as to enhance the tracking. A pair of other studies proposed an improved MPPT based on Mamdani fuzzy logic technique in order to separate the effect between the irradiation and perturbation changes [2.20, 2.21].

2.3.1.2. Incremental Conductance algorithm (IncCond)

The incremental conductance algorithm was introduced in 1995 by Hussein [2.24], in order to improve the tracking accuracy and dynamic performance in rapidly changing atmospheric conditions of the P&O algorithm [2.8, 2.22, 2.23, 2.24]. Even though the improvements are limited [2.25], it is one of the most widely used MPPT algorithm.

As the P&O method, the IncCond algorithm is also based on the fact that, the derivative of PV array output power with respect to its output voltage is zero ($dP_{pv} / dV_{pv} = 0$) at the

MPP and at any irradiation and temperature level. The derivative is negative on the right of MPP and positive on the left of the MPP as explained by the following equations:

$$\frac{dP_{PV}}{dV_{PV}} = 0 \qquad \text{At the MPP}$$

$$\frac{dP_{PV}}{dV_{PV}} < 0 \qquad \text{At the right of the MPP} \tag{2.1}$$

$$\frac{dP_{PV}}{dV_{PV}} > 0 \qquad \text{At the left of the MPP}$$

Since:

$$\frac{dP_{PV}}{dV_{PV}} = \frac{d(I_{PV} V_{PV})}{dV_{PV}} = I_{PV} + V_{PV} \frac{dI_{PV}}{dV_{PV}} = I_{PV} + V_{PV} \frac{\Delta I_{PV}}{\Delta V_{PV}} \tag{2.2}$$

Equation (2.1) can be written as:

$$\frac{\Delta I_{PV}}{\Delta V_{PV}} = -\frac{I_{PV}}{V_{PV}} \qquad \text{At the MPP}$$

$$\frac{\Delta I_{PV}}{\Delta V_{PV}} < -\frac{I_{PV}}{V_{PV}} \qquad \text{At the right of MPP} \tag{2.3}$$

$$\frac{\Delta I_{PV}}{\Delta V_{PV}} > -\frac{I_{PV}}{V_{PV}} \qquad \text{At the left of the MPP}$$
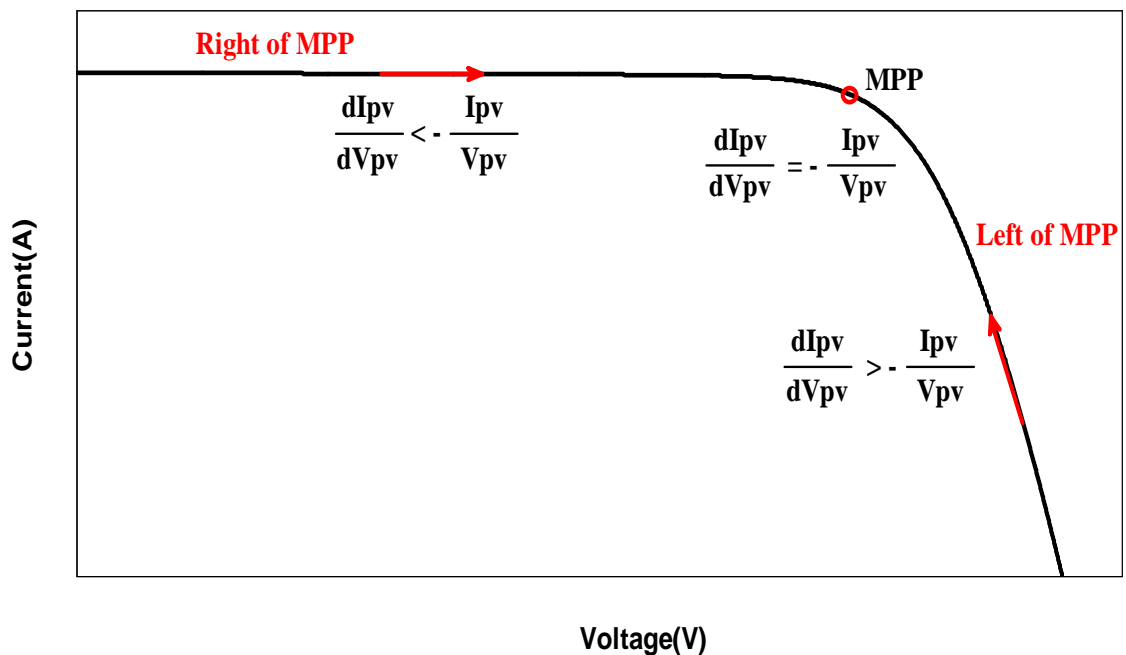
Fig. 2.5. Operating principle of the IncCond algorithm.
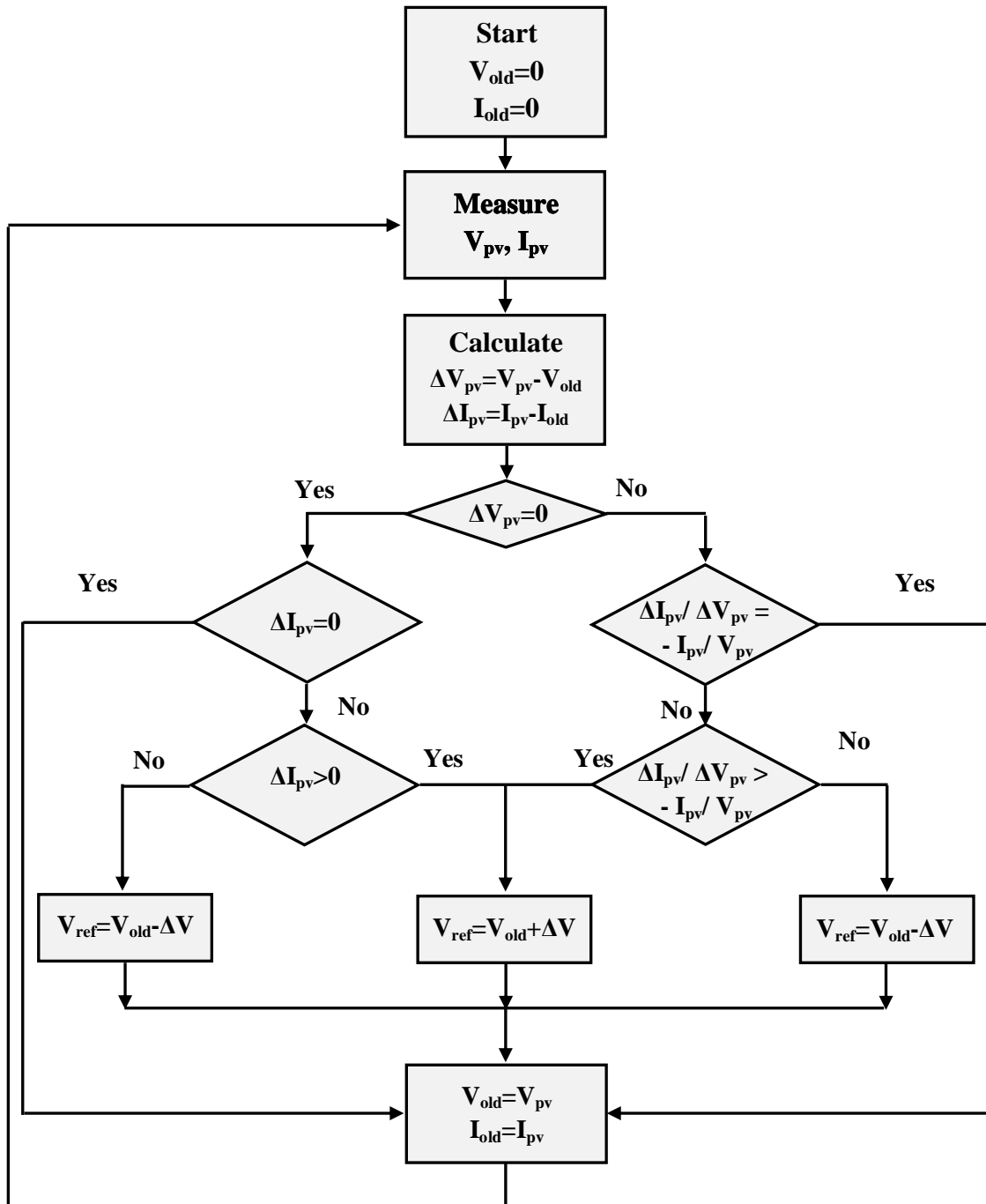
Fig. 2.6. Flowchart of IncCond algorithm.

The last equation makes it possible to locate the MPP by only comparing the instantaneous conductance (I_{PV}/V_{PV}) to the incremental conductance (dI_{PV}/dV_{PV}) (figure 2.5). The flowchart in figure 2.6 illustrates how this method works. Theoretically, there is no steady stat oscillation around the MPP. The verification of the Eq. 2.3 with the verification of $dI_{pv} = 0$ eliminates the oscillations around the MPP and also maintains the PV output voltage constant once the MPP is reached. However, in practical implementation, the Eq. 2.3 is rarely

equal to zero at the MPP. Therefore, this non-zero value can be detected by accepting a small error, where the value of the error depends on the required sensitivity of the MPPT [2.22], which allows modify the relation (2.3) in the following equation:

$$\frac{\Delta I_{PV}}{\Delta V_{PV}} + \frac{I_{PV}}{V_{PV}} = \xi \qquad \text{At the MPP}$$

$$\frac{\Delta I_{PV}}{\Delta V_{PV}} + \frac{I_{PV}}{V_{PV}} = \xi < 0 \qquad \text{At the right of MPP} \qquad (2.4)$$

$$\frac{\Delta I_{PV}}{\Delta V_{PV}} + \frac{I_{PV}}{V_{PV}} = \xi > 0 \qquad \text{At the left of the MPP}$$

In this case, the operating point is fixed close to the MPP, and this method falls back on the same disadvantages of the P&O algorithm. In addition, the execution time of the algorithm is longer because the latter is more complex which generates a delay in the detection of climate change. In some research paper, an improvements have been made to overcome the drawbacks of IncCond algorithm, such modified IncCond algorithm by proposed a new variable step-size which only depends on the PV power change (ΔP), thus eliminating its division by the PV voltage change (ΔV) [2.32, 2.33, 2.34], or using a fuzzy logic estimator to estimate the optimal size of the duty cycle change from the irradiance change by minimizing the error between the instantaneous conductance and the incremental conductance [2.26, 2.27].

2.3.1.3. Hill Climbing algorithm (HC)
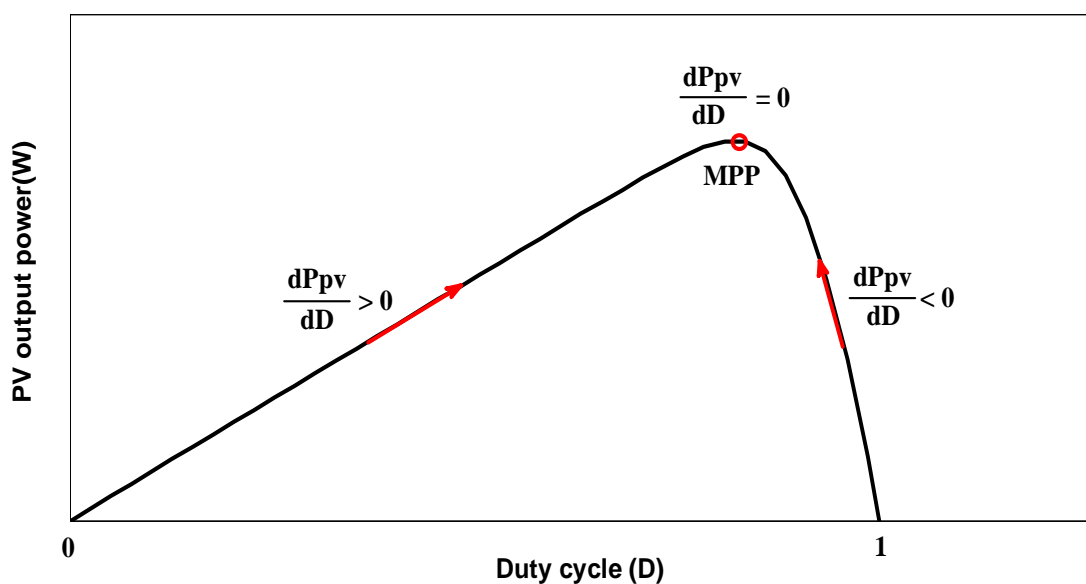
Fig. 2.7. Operating principle of HC algorithm.

45

Most MPPT algorithms presented before are based on the adjustment of the output voltage of the solar panel even though the real controlled variable for the converter is the duty cycle D. The hill climbing method is based on the relationship between the power delivered by the PV panel and the duty cycle applied to the static converter [2.2, 2.28, 2.29, 2.30]. Mathematically, the MPP is achieved when dP_{pv}/dD is forced to be zero, as shown in figure 2.7. The flowchart of this method is depicted in figure 2.8.
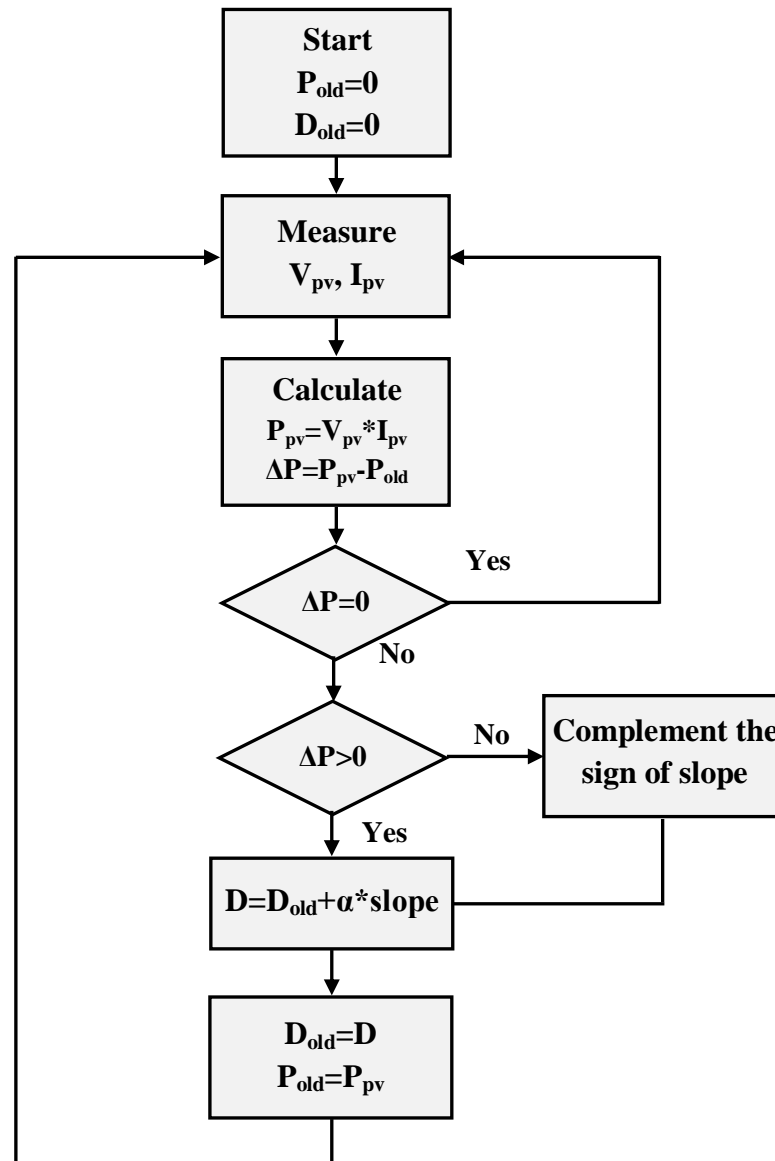
Fig. 2.8. Flowchart of HC algorithm.

Depending on the direction that must given to the tracking process to achieve the MPP, the slope variable takes two values +1 or -1, where α is the perturbation step of the duty cycle. Periodically, the power $P_{pv}(n)$ is compared to the value determined previously $P_{pv}(n-1)$, based on the result of the comparison, the sign of the slope value changes or remains the same. This

has the effect of increasing or decreasing the value of the duty cycle. However, once the MPP is reached, the same drawbacks as P&O and IncCond methods are appeared regarding to the oscillations around the MPP at the steady state condition and power loss during the fast variation of the weather conditions. Several techniques in the literature have addressed improving hill climbing algorithm. In [2.31], a technique has been developed to overcome oscillation around the MPP based on the estimation of the boost converter duty cycle associated with the conventional hill climbing. Another technique was implemented in [2.30] by fuzzifying the rules of the hill climbing search method to reduce its disadvantages, with a relatively simple approach.

2.3.2. Intelligent MPPT techniques

The use of intelligent techniques is experiencing a great boom today whether for modeling or systems control, this thanks to their adaptability to changes in system parameters and their robustness to disturbances and modeling errors.

The non-linear characteristic of photovoltaic systems, in addition to their affected by climatic conditions that are very random, are the subject of much researches interest that works to improve the performance of these systems using intelligent techniques. Below we review the most important of these techniques.

2.3.2.1. Fuzzy Logic based MPPT controller (FLC)
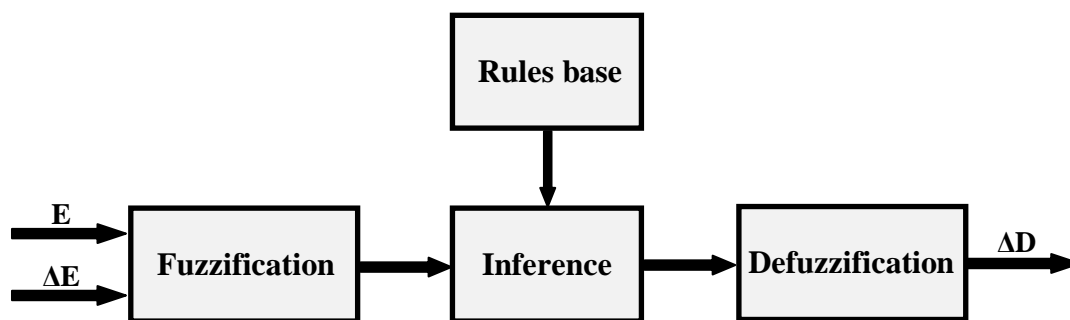
Fig. 2.9. Fuzzy controller structure.

Recently, fuzzy logic-based control has received a lot of attention from a number of researchers in MPPT applications for PV systems either independently or along with other methods [2.20, 2.35, 2.36, 2.37, 2.38]. This technique has the advantage of being does not require an accurate mathematical model to implement and able to operate with little imprecise

inputs. Moreover, the ability to deal with the nonlinearity of the system. However, a good knowledge of the behavior of the system is required for the development of such regulator.

Generally, the fuzzy logic controller is consists of three stages (shown in figure 2.9) that can be described as: fuzzification, inference engine (rule-based table lookup) and defuzzification [2.39].

✓ **Fuzzification stage:** In this stage, the inputs are converted from numerical to linguistic variables based on a membership function similar to figure 2.10. Several membership functions can be defined for the same variable such as: negative big (NB), negative small (NS), zero (Z), positive small (PS) and positive big (PB) [2.40]. In practice the membership functions can have a number of different shapes depending on the application. They can be triangular, trapezoidal, Gaussian, bell-shaped or sigmoidal. Trapezoidal or triangular membership functions are usually used in systems that require significant dynamic variation in a short period of time, a Gaussian or other membership function is always selected if the system requires very high control accuracy [2.39]. The accuracy of the fuzzy logic depends on the number of the fuzzy subset; whenever the fuzzy subset has increased the accuracy has increased.
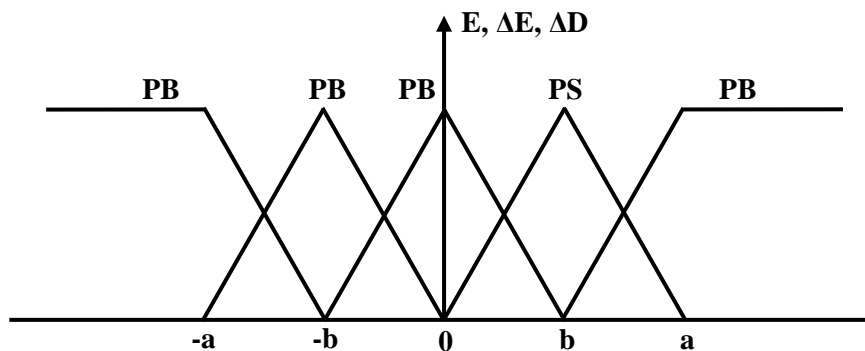
Fig. 2.10. Membership function for inputs and output of fuzzy logic controller.

Based on the fact that at MPP $\Delta P/\Delta V = 0$, and this whatever the weather conditions. Therefore, the first input will be the variation of the power compared to the voltage (the slope of the P-V characteristic) called the error (E), which shows whether the operating point at time k is on the left or on the right of the MPP in the P-V characteristic of the PV generator. As a second input, information on the direction and speed of convergence would be necessary, so as a second input the variation of the error (ΔE) is used (the slope change). These variables can be calculated as follow:

$$E(k) = \frac{P(k) - P(k-1)}{V(k) - V(k-1)} \tag{2.5}$$

$$\Delta E(k) = E(k) - E(k - 1) \tag{2.6}$$

At the output, the control is carried out by adjusting the duty cycle (ΔD) to drive the DC-DC converter in order to bring the operating point to the maximum point.

✓ **Inference stage (rule-based table lookup):** It is a step that involves defining a logical relationship between the inputs and the output. In fact, systems' using fuzzy logic use rules that the designer writes based on experience and system knowledge, which they have the following form:

IF « E condition » AND « ΔE condition » THEN « ΔD conclusion »

The number of base rules can be defined based on the number of membership in the fuzzy set and the inputs. For example if the system contains two inputs and each of them contains five memberships then the total base rules will be 5*5 = 25 base rule. The higher the number of memberships, the better the system efficiency will be, but the system implementation will become more complex [2.10].

Thanks to these fuzzy rules and by responding to the specifications of the system, an inference matrix giving a linguistic variable assigned to the output ΔD can be drawn up depends on different combinations of E and ΔE (Table 2.2).

There are several techniques for performing the fuzzy interface process, such as, the Mamdani method, Takagi-Sugeno Kang (TSK) method, Tsukamot method and Larsen method. The Mamdani method is usually more popular for most control engineering applications because this method is computationally more efficient and has better interpolative properties than the other interface methods [2.39].

Table 2.2. Example of the inference table.

ΔD		ΔE				
		NB	NS	Z	PS	PB
E	NB	Z	Z	NB	NB	NB
	NS	Z	Z	NS	NS	NS
	Z	NS	Z	Z	Z	PS
	PS	PS	PS	PS	Z	Z
	PB	PB	PB	PB	Z	Z

✓ **Defuzzification stage:** the last step in the process of the fuzzy inference is the defuzzification, and it is reverse of the fuzzification process. The output of the fuzzy inference process result from the combination of the control inputs is still linguistic variable. Hence the defuzzification process is needed to convert the fuzzy output from a linguistic variable to a numerical variable [2.10], and offers an analog signal that will drive the power converter to operate at the MPP. There are several defuzzification techniques which are used: Mean of maximum method (MOM), Height method (HM) and the most commonly used technique is Centre of gravity method (COG) [2.42].

Compared to conventional algorithms, the fuzzy logic based MPPT controller exhibits generally a better performance, good stability and fast response especially under different atmospheric conditions [2.43, 2.44, 2.45]. However, successful implementation of the FLC is heavily relied on the amount of designer's knowledge of the system who sets up the membership function and the rule-base table. In [2.46], an adaptive FLC was proposed to regularly change the membership function and the rule base table for improving the control system. Another improvement was suggested and validated experimentally in [2.47, 2.48] by using an asymmetrical FLC based MPPT algorithm for PV systems.

2.3.2.2. Artificial Neural Network (ANN) based MPPT controller

Another type of artificial intelligence technologies that have become popular and expanded in MPP tracking for PV systems to achieve high efficiency is the artificial neural network (ANN). The architecture of an ANN commonly have three stages or layers: input, output, and hidden layers between these layers where the processing takes place as shown in figure 2.11. The user or control engineer has the flexibility to choose the number of nodes in each layer.
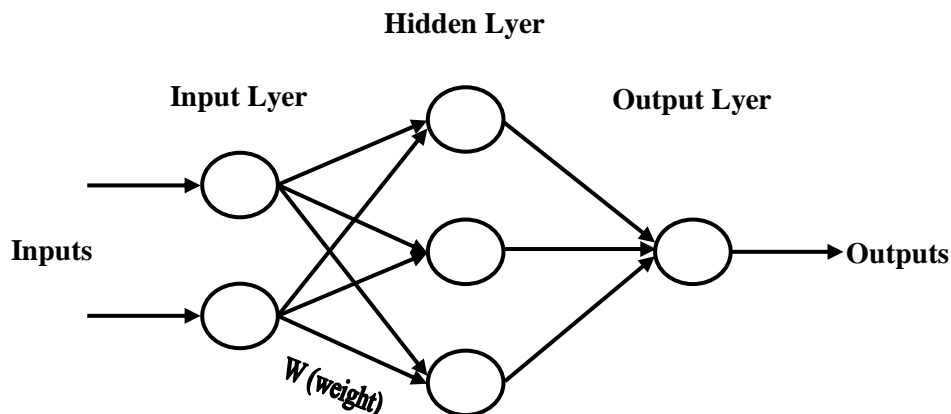

Fig. 2.11. Artificial neural network representation.

For the input variables, it can be the PV array parameters like open-circuit voltage V_{oc} and short-circuit current I_{sc}, atmospheric data like the temperature and irradiance, or any combination of these variables. After these inputs are processed in the hidden layer, the output most likely is a duty cycle signal that drives the power converter to operate at or close to the MPP as possible based on the algorithm used in the hidden layer and how well the neural network has been trained. The neural network technique needs to be well trained to perform at a high quality and to accurately identify the MPP. The training process happens on a long run, where all the PV data is recorded continuously over months or even years into the neural network database. The result of this training is an algorithm in the hidden layer to make relationships between the inputs and the outputs, where every link between nodes is weighted precisely [2.8, 2.49].

Artificial neural network technique shows a fast and accurate convergence to the MPP and a high effectiveness under varying atmospheric conditions especially instantaneous climate changes and partial shading [2.2, 2.50]. However, the major drawback of this method is that each PV array has its unique characteristics, so the neural network controller must be trained for the PV array in use separately depending on the knowledge of the user in choosing the right algorithm parameters, without generalized to work on several types at the same time unless trained to. Moreover, the characteristics of a PV array change with time therefore, neural networks should be trained periodically to maintain high quality tracking. These entire drawbacks make this technique features by high complexity and requires a costly microprocessor to implement.

To overcome these limitations, an ANN-based MPPT technique is proposed in [2.51] which utilize two cascaded ANNs to minimize the number of training sets. Some other researches use an adaptive neuro-fuzzy inference system (ANFIS) which combines neural network and fuzzy logic to achieve a suitable MPP tracker [2.52, 2.53, 2.54].

2.3.2.3. Sliding Mode based MPPT controller (SMC)

Starting from late 1970s and continuing today [2.41], sliding mode control (SMC) considered as one of the most well-known nonlinear control techniques because of its fast convergence and high robustness. Moreover, it is insensitive to system parameter changes, disturbance and load variations [2.55]. SMC is a variable structure control strategy; its design involves two basic stages. The first stage is to determine the sliding surface that ensures the convergence property towards the desired surface. The second stage aims to establish an

optimum design of the control law that forces the system trajectory to reach and stay in the vicinity of a predetermined sliding surface in finite time [2.56, 2.57]. The state trajectory consists of two distinct parts: Convergence mode and Sliding mode as shown in figure 2.12.
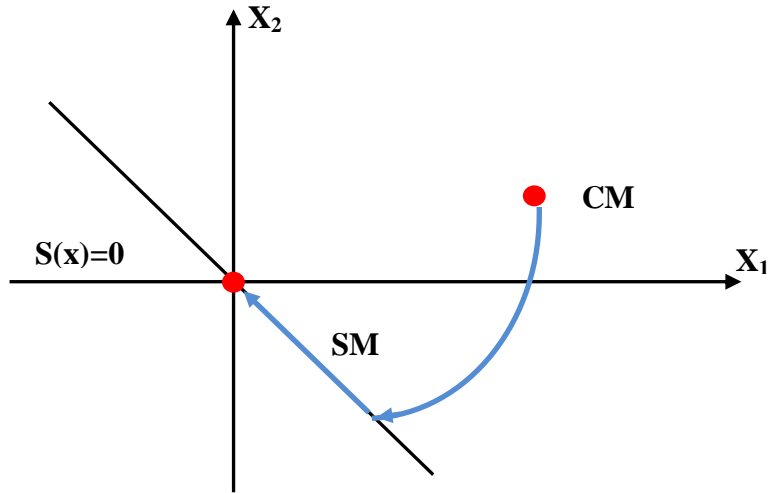
Fig. 2.12. The state trajectory modes.

✓ **Convergence mode (CM):** this is the mode during which the variable to be adjusted moves from any point on the phase plane to the sliding surface S(x) =0. The attractiveness to the sliding surface is ensured by the discrete control law D_d.

✓ **Sliding mode (SM):** this is the mode during which the operation point is maintained on the sliding surface and displaces it towards the origin. This mode is ensured by the equivalent control low D_{eq}.

The design of the SMC can be carried out in three main stages which are very dependent on each other. These steps concern:

✓ **Choice of surface:** As agreed, the MPP of the PV system is achieved when the following equality is satisfied:

$$\frac{dP_{pv}}{dI_{pv}} = \frac{dI_{pv}\,V_{pv}}{dI_{pv}} = V_{pv} + I_{pv}\frac{dV_{pv}}{dI_{pv}} = 0 \tag{2.7}$$

Accordingly, the sliding surface can be chosen as:

$$S = V_{pv} + I_{pv}\frac{dV_{pv}}{dI_{pv}} \tag{2.8}$$

If $S > 0$, so $(dP_{pv}/dI_{pv}) > 0$ which means that the operating point is to the right of the MPP.

If $S < 0$, so $(dP_{pv}/dI_{pv}) < 0$ which means that the operating point is to the left of the MPP.

✓ **Control law design:** The general control law D consists of two parts, the discrete control D_d and the equivalent control D_{eq}.

$$D = D_d + D_{eq} \tag{2.9}$$

The discrete control D_d, determined to ensure the attractiveness to the sliding surface and defined as follows:

$$D_d = K * sgn(S) \tag{2.10}$$

Where: K is a positive constant.

The equivalent control D_{eq}, serves to maintain the operation point on the sliding surface and displace it towards the origin, it defined as follows:

$$D_{eq} = 1 - \frac{V_{pv}}{V_o} \tag{2.11}$$

So, the overall control law D has the expression mentioned in the following equation (2.12), where the corresponding block diagram using Matlab/Simulink [MT] tool is shown in figure 2.13.

$$D = K * sgn(S) + 1 - \frac{V_{pv}}{V_o} \tag{2.12}$$
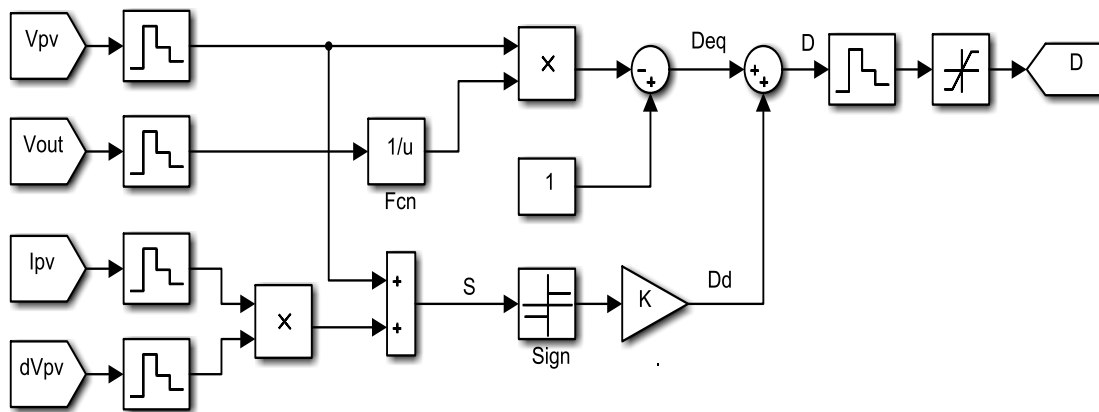
Fig. 2.13. Block diagram of sliding mode controller.

✓ **Checking for the existence of sliding mode:** Let be the positive definite quadratic Lyapunov function $V_L = \frac{1}{2}S^2$.

In order to ensure the attractiveness of the surface S=0 over the entire operating range; it's enough that the time derivative of V_L must be negative.

$$\dot{V}_L = S * \dot{S} < 0 \tag{2.13}$$

Where the surface derivative is given by:

$$\dot{S} = \frac{dS}{dt} = \left[\frac{dS}{dx}\right]^T \dot{x} = \left[\frac{dS}{dx}\right]^T \left[\frac{dI_{pv}}{dt}\right] \tag{2.14}$$

From equation (2.8) we have:

$$\left[\frac{dS}{dx}\right]^T = 2\frac{dV_{pv}}{dI_{pv}} + I_{pv}\frac{d^2V_{pv}}{dI_{pv}^2} \tag{2.15}$$

And from equation (1.1), we can deduce the output PV voltage V_{pv} as follows:

$$V_{pv} = \frac{N_s AKT}{q}\log\left(\frac{I_{ph} - I_{pv} + I_o}{I_o}\right) \tag{2.16}$$

From equation (2.16) we have:

$$\frac{dV_{pv}}{dI_{pv}} = \left(-\frac{N_s AKT}{q}\right)\left(\frac{1}{I_{ph} - I_{pv} + I_o}\right) \quad < 0 \tag{2.17}$$

$$\frac{d^2V_{pv}}{dI_{pv}^2} = \left(-\frac{N_s AKT}{q}\right)\left(\frac{1}{(I_{ph} - I_{pv} + I_o)^2}\right) \quad < 0 \tag{2.18}$$

From Eq. (2.17) and (2.18) we conclude that $\left[\frac{dS}{dx}\right]^T$ is always negative, which means the sign of $\dot{S}$ depends on the sign of $\dot{x} = \frac{dI_{pv}}{dt}$.

$$\dot{x} = \frac{dI_{pv}}{dt} = -\frac{V_o}{L}(1 - D) + \frac{V_{pv}}{L} \tag{2.19}$$

$$= -\frac{V_o}{L}\left(1 - 1 + \frac{V_{pv}}{V_o} - K * sgn(S)\right) + \frac{V_{pv}}{L}$$

$$= \frac{V_o}{L} * K * sgn(S) > 0$$

So, $\dot{S} = \left[\frac{dS}{dx}\right]^T \dot{x} < 0$ and from it, $\dot{V}_L = S * \dot{S} < 0$

We conclude that the sliding mode exists and the system is asymptotically stable, whatever the location of the operating point. The control law applied obliges the system trajectory to move from any initial state of the sliding surface in a finite time and thereafter keep it on it.

As the control law generated by the SMC combines two terms, it's not continuous. This sudden change or switching in the control law leads to the chattering phenomenon which induces many undesirable oscillations which may lead the system into instability [2.58, 2.59, 2.60]. Therefore, to maintain the amplitude of oscillation at low level, chattering must be decreased or eliminated. To achieve this objective, many chattering suppression methods have been suggested in the literature. In [2.59] sliding mode based layer concept and Lyapunov function approach is used. Other researches propose double integral sliding mode [2.61], second order sliding mode control [2.62], terminal sliding mode control (TSMC) [2.63] and fast terminal sliding mode control (FTSMC) as solution to break this drawback [2.64].

2.4. Summary

In this chapter, the maximum power point tracking issue is presented and explained in order to extract the maximum power from the PV panel and thus increase the efficiency of the PV system. Besides that, this chapter reviewed the operating principle of the most commonly MPPT techniques that are discussed in the literature along with their advantages and disadvantages through a substantial bibliographic investigation. The MPPT techniques can be classified into two categories: conventional techniques (P&O, IncCond, HC and…) and intelligent techniques (FLC, ANN, SMC and…). It's true that intelligent techniques are more effective and they have a quick response especially during the changes in atmospheric conditions, but they are more complex compared to conventional techniques which are generally simple, cheap and less effective.

The search for an efficient MPPT technique (faster, easy to implement and more stable) remains the objective of researchers and is the subject of a large number of studies. In the next chapter, a new efficient and strong tracking technique is proposed and implemented based on the synergistic approach in order to eliminate or minimize the effect of the chattering phenomenon resulting from the switching in the control law generated by sliding mode control technique.

References

[2.1].　　A. P. Bhatnagar and B. R. K. Nema, "Conventional and global maximum power point tracking techniques in photovoltaic applications: A review". J. Renew. Sustainable Energy, vol. 5, pp. 1-23, 2013.

[2.2].　　T. Esram and P. L. Chapman, "Comparison of photovoltaic array maximum power point tracking techniques". IEEE Trans. Energy Convers, pp. 439–449, 2007.

[2.3].　　B. Subudhi, and R. Pradhan, "A Comparative Study on Maximum Power Point Tracking Techniques for Photovoltaic Power Systems". IEEE Trans. on Sustainable Energy, vol. 4, pp. 89-98, 2013.

[2.4].　　M. A. Eltawil and Z. Zhao, "MPPT techniques for photovoltaic applications". Renewable Sustainable Energy Rev, vol. 25, pp. 793-813, 2013.

[2.5].　　K. Ishaque and Z. Salam, "A review of maximum power point tracking techniques of PV system for uniform insolation and partial shading condition". Renew Sustain Energy Rev, vol. 19, pp. 475–88, 2013.

[2.6].　　R. Entwistle, "Methods for Investigating Interactions between Multiple Maximum Power Point Trackers in Photovoltaic Systems". Doctoral thesis, University of Leicester, April 2013.

[2.7].　　K. S. Nathan, "A Novel DC-DC Converter for Photovoltaic Applications". Doctoral thesis, University of Cambridge, September 2018.

[2.8].　　B. Bendib, "Une nouvelle approche de modélisation et de commande des systèmes photovoltaïques autonomes". Doctoral thesis, University of Ferhat Abbas Setif, November 2017.

[2.9].　　M. A. Alqarni, "A High Efficiency Photovoltaic Inverter System Configuration with Maximum Power Point Tracking". Doctoral thesis, Brunel University London, March 2016.

[2.10].　F. Aashoor, "Maximum power point tracking techniques for photovoltaic water pumping system". Doctoral thesis, University of Bath, May 2015.

[2.11].　T. Radjai, "Commandes Avancées des Convertisseurs Utilisés dans les Systèmes Photovoltaïques". Doctoral thesis, University of Ferhat Abbas Setif, April 2017.

[2.12]. W. Wu, N. Pongratananukul , W. Qiu, K. Rustom, T. Kasparis, and I. Batarseh, "DSP-based multiple peak power tracking for expandable power system". IEEE Appl. Power Electron. Conf. Expo. , 525-530, 2003.

[2.13]. R. Kadri, J. P. Gaubert, and G. Champenois, "An improved maximum power point tracking for photovoltaic grid-connected inverter based on voltage-oriented control". IEEE Transactions on Industrial Electronics, vol. 58, pp. 66–75, 2011.

[2.14]. A. K. Abdelsalam, A. M. Massoud, S. Ahmed, and P. Enjeti, "High-Performance Adaptive Perturb and Observe MPPT Technique for Photovoltaic-Based Microgrids". IEEE Transactions on Power Electronics, vol. 26, pp. 1010–1021, 2011.

[2.15]. W. Xiao and W.G. Dunford, "A modified adaptive hill climbing MPPT method for photovoltaic power systems". Power Electronics Specialists Conference, 2004.

[2.16]. C. Hua, and J. Lin, "Fully digital control of distributed photovoltaic power systems". IEEE International Symposium on Industrial Electronics, pp. 1-6. 2001.

[2.17]. K. Noppadol, W. Theerayod , S. Phaophak, "Implementation of MPPT using variable step-size P&O algorithm for PV applications". IEEE International Symposium On Communication and Information Technologies, pp. 212-215, 2006.

[2.18]. D. Sera, T. Kerekes, R. Teodorescu, and F. Blaabjerg, "Improved MPPT method for rapidly changing environmental conditions". IEEE International Symposium on Industrial Electronics, Vol. 2, pp. 1420–1425, 2006.

[2.19]. D. Sera, R. Teodorescu, J. Hantschel, and M. Knoll, "Optimized maximum power point tracker for fast-changing environmental conditions". IEEE Trans. Ind. Electron, vol. 55, 2629, 2008.

[2.20]. T. Radjai, J. P. Gaubert, L. Rahmani, and S. Mekhilef, "Experimental verification of P&O MPPT algorithm with direct control based on Fuzzy logic control using cuk converter: Photovoltaic System". International Transactions on Electrical Energy Systems, vol. 25, pp. 3492-3508, 2015.

[2.21]. B. Boukezata, A. Chaoui, J. P. Gaubert, M. Hachemi, "An improved fuzzy logic control MPPT based P&O method to solve fast irradiation change problem". Journal of Renewable and Sustainable Energy 8, 2016.

[2.22]. K. H. Hussein, et al., "Maximum photovoltaic power tracking: an algorithm for rapidly changing atmospheric conditions". Generation, Transmission and Distribution, IEEE Proceedings, vol. 142, pp. 59-64, 1995.

[2.23]. A. Safari and S. Mekhilef, "Simulation and hardware implementation of incremental conductance MPPT with direct control method using cuk converter". IEEE Trans. Ind. Electron. 58, pp.1154–1161, 2011.

[2.24]. K. S. Tey and S. Mekhilef, "Modified incremental conductance MPPT algorithm to mitigate inaccurate responses under fast-changing solar irradiation level". Sol. Energy 101, 333–342, 2014.

[2.25]. S.B. Kjaer, "Evaluation of the Hill Climbing and the Incremental Conductance Maximum Power Point Trackers for Photovoltaic Power Systems". IEEE Transactions on Energy Conversion, vol.27, no.4, pp.922–929, 2012.

[2.26]. T. Radjai, L. Rahmani, S. Mekhilef, et J. P. Gaubert, "Implementation of a modified incremental conductance MPPT algorithm with direct control based on a fuzzy duty cycle change estimator using dSPACE". Solar Energy, vol. 110, p. 325‑337, 2014.

[2.27]. T. Radjai, J. P. Gaubert and L. Rahmani, "The new FLC-variable incremental conductance MPPT with direct control method using cuk converter". IEEE International Symposium on Industrial Electronics (ISIE), (pp. 2508-2513), 2014.

[2.28]. Z. Shiqiong, and al, "A novel maximum power point tracking algorithms for stand-alone photovoltaic system". International Journal of Control, Automation and Systems, vol. 8, pp. 1364-1371, 2011.

[2.29]. I. A. Abdalla, "Integrated PV and Multilevel Converter System for Maximum Power Generation under Partial Shading Conditions". Doctoral thesis, University of Leeds, February 2013.

[2.30]. B. N. Alajmi, "Design and Control of Photovoltaic Systems in Distributed Generation". Doctoral thesis, University of Strathclyde, Department of Electronic and Electrical Engineering, January 2013.

[2.31]. C. N. Fapi, P. Wira, M. Kamta, T. Hyacinthe, B. Abderrezak, "Real-Time Experimental Assessment of Hill Climbing MPPT Algorithm Enhanced by Estimating a Duty Cycle for PV System". International Journal of Renewable Energy Research, pp. 1180-1189. September 2019.

[2.32]. N. E. Zakzouk, "Photovoltaic System Design and Control". Doctoral thesis, University of Strathclyde, 2015.

[2.33]. F. Liu and al., "A Variable Step Size INC MPPT Method for PV Systems". IEEE. Trans. Industrial Electronics, Vol. 55, No. 7, pp. 2622-2628, 2008.

[2.34]. Q. Mei, and al., "A Novel Improved Variable Step-size Incremental-Resistance MPPT Method for PV Systems". IEEE Trans. Ind. Electronics, pp. 2427-2434, 2011.

[2.35]. F. Chekired, C. Larbes, D. Rekioua, F. Haddad, "Implementation of a MPPT fuzzy controller for photovoltaic systems on FPGA circuit". Energy Procedia, pp. 541‑549, 2011.

[2.36]. C. R. Algarin, J. T. Giraldo and O. R. Alvarez, "Fuzzy Logic Based MPPT Controller for a PV System". Energies, vol. 10, pp. 20-36, 2017.

[2.37]. B. Talbi and al., "Design and hardware validation of modified P&O algorithm by fuzzy logic approach based on model predictive control for MPPT of PV systems". Journal of Renewable and Sustainable Energy 9, 2017.

[2.38]. X. Li, H. Wen, Y. Hu, L. Jiang, "A novel beta parameter based fuzzy-logic controller for photovoltaic MPPT application". Renewable Energy, pp. 416-427, 2019.

[2.39]. Y. Bai and al., "Advanced fuzzy logic technologies in industrial applications". Springer, 2007.

[2.40]. M. G. Simoes, N. Franceschetti, and M. Friedhofer, "A fuzzy logic based photovoltaic peak power tracking control". IEEE International Symposium on Industrial Electronics, pp. 300-305, 1998.

[2.41]. M. A. Alsumiri, "Sliding Mode Control of Renewable Energy Generation Systems". Doctoral thesis, University of Liverpool, May 2015.

[2.42]. K. Michels, F. Klawonn, R. Kruse, and A. Nürnberger, "Fuzzy control: fundamentals, stability and design of fuzzy controllers". Springer, 2007.

[2.43]. T. Kottas, Y. Boutalis, A. Karlis, "New maximum power point tracker for PV arrays using fuzzy controller in close cooperation with fuzzy cognitive networks", IEEE Trans. on Energy Conversion, vol. 21, pp. 793-803, 2006.

[2.44]. A. Al Nabulsi and R. Dhaouadi, "Efficiency optimization of a dsp-based standalone pv system using fuzzy logic and dual-mppt control". IEEE Trans. Ind. Informat., vol. 8, pp. 573–584, 2012.

[2.45]. A. El Khateb, N. Abd Rahim, J. Selvaraj, and M. Uddin, "Fuzzy-logic-controllerbased sepic converter for maximum power point tracking". IEEE Trans. Ind. Appl., vol. 50, pp. 2349–2358, 2014.

[2.46]. N. Patcharaprakiti and al., "Maximum power point tracking using adaptive fuzzy logic control for grid-connected photovoltaic system", Renewable Energy, pp. 1771-1788, 2005.

[2.47]. C. L. Liu, J. H. Chen, Y. H. Liu, Z. Z. Yang, " An Asymmetrical Fuzzy-Logic-Control-Based MPPT Algorithm for Photovoltaic Systems". Energies, vol. 7, 2177-2193, 2014.

[2.48]. P. C. Cheng and al., "Optimization of a Fuzzy-Logic-Control-Based MPPT Algorithm Using the Particle Swarm Optimization Technique". Energies, vol. 8, 5338-5360, 2015.

[2.49]. S. M. Ait cheikh, "Etude, Investigation et conception d'algorithmes de commande appliqués aux systèmes photovoltaïques". Doctoral thesis, National Polytechnic school. December 2007.

[2.50]. V. P. and M. A. Mathews, "Modelling and Analysis of Artificial Intelligence Based MPPT Techniques for PV Applications". IEEE International Conference on Advances in Green Energy, pp. 56-65, 2014.

[2.51]. L. M. Elobaid, A. K. Abdelsalam, and E. E. Zakzouk, "Artificial Neural Network Based Maximum Power Point Tracking Technique for PV Systems", IEEE Conference on Industrial Electronics Society, pp. 937-942, 2012.

[2.52]. A. Chikh, A. Chandra, "Adaptive neuro-fuzzy based solar cell model". IET Renew. Power Gener. 8, pp. 679–686, 2014.

[2.53]. B. Bendib, et al, "An Intelligent MPPT Approach Based on Neural-network Voltage Estimator and Fuzzy Controller, Applied to a Stand-alone PV System". IEEE International Symposium on Industrial Electronics, pp.404-409, 2014.

[2.54]. H. Afghoul, et al, "Tracking the Maximum Power from a PV Panels Using of Neuro-fuzzy Controller ", IEEE International Symposium on Industrial Electronics, pp. 1-6, 2013.

[2.55]. K. Vrdoljak, N. Peric, I. Petrovic. "Sliding mode based load-frequency control in power systems". Electric power systems research, 80(5), pp. 514-527, 2010.

[2.56]. Y. Irfan, K. Y. Ersagun, "Fast and robust voltage control of DC–DC boost converter by using fast terminal sliding mode controller". IET Power Electronics, vol. 9, 2015.

[2.57]. A. Belkaid, "Conception et implémentation d'une commande MPPT de haute performance pour une chaine de conversion photovoltaïque autonome". Doctoral thesis, University of Ferhat Abbas Setif, October 2015.

[2.58]. N. Zerroug and al., "DSP-based implementation of fast terminal synergetic control for a DC–DC Buck converter". J. of the Franklin Institute, pp. 2329–2343, 2018.

[2.59]. M. Rezkallah and al., "Lyapunov Function and Sliding Mode Control Approach for the Solar-PV Grid Interface System". IEEE Tra. on Ind. Electronics, 2017.

[2.60]. V. Bregeault, " Quelques Contributions à la Théorie de la Commande par Modes Glissants'. PhD Thesis, Ecole Centrale de Nantes, 2010.

[2.61]. P. Raseswari, S. Bidyadhar,: "Double Integral Sliding Mode MPPT Control of a Photovoltaic System". IEEE Transactions on Control Systems Technology, 2015.

[2.62]. H. Sahraoui, L. C. Alaoui, S. Drid, P. Bussy, "Second Order Sliding Mode Control of DC-DC Converter used in the Photovoltaic System According an Adaptive MPPT". International Journal of Renewable Energy Research, vol.6, 2016.

[2.63]. C. Chian-Song, O. Ya-Lun, K. Chan-Yu, "Terminal sliding mode control for maximum power point tracking of photovoltaic power generation systems". Solar Energy 86(10), pp. 2986–2995, 2012.

[2.64]. A. Zaidi, K. Dahech, T. Damak, "Maximum Power Point Tracking of Photovoltaic Systems Based on Fast Terminal Sliding Mode Controller". International Journal of Renewable Energy Research, Vol.6, No.4, 2016.

Chapter 3:

Synergetic Approach Based

MPPT Controller

Table of Contents

3.1. Introduction

All MPPT's difficulties and drawbacks, whether conventional or intelligent technique, inspired from the depth study in previous chapter in particular, speed of the MPPT in tracking the optimal power, oscillation behavior, stability and robustness against environment changes, have guided to move to improve the performance of the PV system by introducing more advanced control approches. To achieve this objective, one of the most promising robust control strategies named Synergetic Control (SC) is adopted.

In this chapter, we propose a new nonlinear strategy based on Synergetic Control theory to track the maximum power point (MPP) for stand-alone PV system under different atmospheric conditions. The control strategy consists a solution developed to eliminate or reduce the chattering drawback provided by sliding mode controller (SMC), where it allows generating continuous control law instead of a switching term. A DC/DC boost converter (whose specifications are illustrated in Table1.1) is introduced in the content of this work as an interface between a PV array (whose specifications are illustrated in Table 1.2) and a resistive load.

The design of the synergetic MPPT controller is explained and mathematically described in the content of this chapter. The developed MPPT controller was tested both in simulations using Matlab/Simulink^{MT} tool, and experimentally, using a dSPACE based experimental test bench, and compared with the sliding mode-based MPPT controller. The MPPT efficiency is calculated using the EN 50530 standard test with different ramp gradients values from the slow to the very fast. The main goal of the proposed MPPT controller is to ensure the system stability at the maximum power, good robustness and fast dynamic response simultaneously.

3.2. Synergetic control overview

Synergetic control theory was first developed and introduced in general terms by Prof. Anatoly Klesnikov and his team [3.1]. This approach does not require linearization of the model and employs a nonlinear model for synthesizing the command (control law).

The design of Synergetic Control is very similar to that of the sliding mode control (SMC). It depends on the same invariance property of systems found in SMC, but without its chattering drawback because it provides a continuous control law unlike the conventional SMC which combine two terms, one ensures the attractiveness of the system states to the sliding surface while the other one maintains the operating point on sliding surface and

displace it to the origin. This sudden change or switching in the control law leads to the chattering phenomena as it mentioned in many researches [3.2, 3.3, 3.4].

Synergetic Control theory has been successfully applied initially in power electronics control [3.5, 3.6], in battery charging system [3.7], then recently in control of the epidemic system [3.8, 3.9] and in the control of wind turbine system [3.10]. The synthesis of synergistic control in the general case is reviewed in the next section.

3.3. Synthesis of Synergetic control

To detail the general principle, mechanism and working of synergetic strategy and then demonstrate how they are to be operationalised through empirical modeling, let us first consider the system to be controlled is described by a non linear differential equation of this form:

$$\dot{x} = \frac{dx}{dt} = f(x, D, t) \tag{3.1}$$

Where **x** represents the system state vector, **D** the control vector and **f** a continuous differentiable nonlinear function.

Synergetic controller design starts by selecting a macro-variable (MV) given in the following equation:

$$\Psi = \Psi(x, t) \tag{3.2}$$

Where Ψ is the macro-variable and $\Psi(x, t)$ is a user defined function of system state variables. The characteristics of the macro-variable can be chosen by the designer according to the desired performance and the control specifications such as the control objective, the settling time, limitations in the control output, and so on. In the trivial case, the macro-variable can be a simple linear combination of the state variables. The same process can be repeated, defining as many macro-variables as control channels [3.1, 3.11].

The objective of the synergetic controller is to direct the system trajectory to operate on a designer chosen manifold (attractor):

$$\Psi = 0 \tag{3.3}$$

Once the trajectory reaches the desired manifold, the synergetic controller will keep it there.

The macro-variable is evolved in a desired manner by introducing a constraint that is expressed in the following equation:

$$T_S \left(\frac{d\Psi}{dt}\right) + \Psi = 0; \quad T_S > 0 \tag{3.4}$$

Mathematically, the solution of equation (3.4) gives the following function:

$$\Psi(t) = \Psi_0 e^{-\frac{t}{T_s}} \tag{3.5}$$

According to equation (3.5), the macro-variable $\Psi(t)$ converges towards the attractor $\Psi=0$ for different initial conditions of Ψ_0. Where **Ts** is a positive value which will affect smoothly at the system convergence speed to the desired equilibrium point.

Differentiating the macro-variable along equation (3.1) leads to equation (3.6):

$$\frac{d\Psi}{dt} = \left(\frac{d\Psi}{dx}\right)\left(\frac{dx}{dt}\right) \tag{3.6}$$

By combining equations (3.1), (3.4), and (3.6) we get:

$$T_S \left(\frac{d\Psi}{dx}\right) f(x, D, t) + \Psi = 0 \tag{3.7}$$

Finally, when solving equation (3.7), we can describe the output control law as flow:

$$D = g(x, t, \Psi(x, t), T_S) \tag{3.8}$$

It is obvious from Eq. (3.8), that the control law is continuous and depends not only on the system state variables (x, t), but also on the adequate selection of the **MV** and time constant **Ts** to ensure the overall system stability and the good transient and steady state performances.

In what follows, we applied the concept of the SC explained above for the MPPT controller design in PV system.

3.4. Synergetic MPPT controller design

The configuration of the proposed standalone PV system used in this study consists of PV array, DC-DC boost converter, resistive load and a non-linear controller allows maximum power tracking as shown in figure 3.1. The dynamic model of the DC-DC boost converter

used and shown in figure 3.1 can be described by the differential equations developed in the section (1.7) of the first chapter given as:
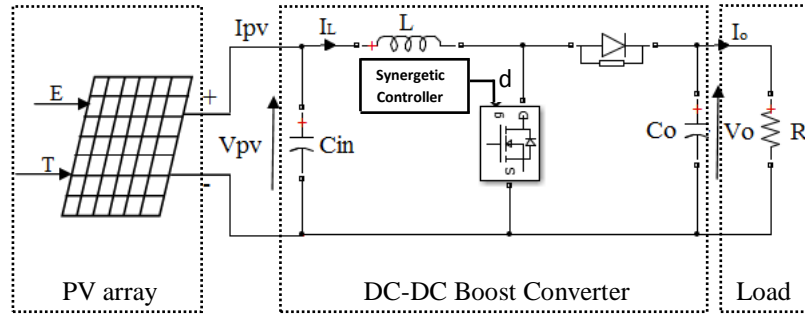

Fig. 3.1. Photovoltaic system structure.

$$\frac{dV_{pv}}{dt} = \frac{1}{C_{in}}\left(i_{pv} - i_L\right) \tag{3.9}$$

$$\frac{dI_{pv}}{dt} = -(1-D)\frac{V_o}{L} + \frac{V_{pv}}{L} \tag{3.10}$$

$$\frac{dV_o}{dt} = (1-D)\frac{I_L}{C_o} - \frac{V_o}{RC_o} \tag{3.11}$$

Where: C_{in} is the input capacity, C_o is the output capacity, L is the inductance, R is the resistive load, $D \in [0\ 1]$ is the duty ratio, which is also the control output law and V_o is the output voltage.

The objective of using MPPT controller is to reach the MPP under different weather conditions, with high efficiency. To apply the Synergetic Control strategy as MPPT technique on the selected system, we start by selecting a macro-variable. This selection is based on the output power of the PV array as follows:

$$\Psi(x, t) = \frac{dP_{pv}}{dI_{pv}} \tag{3.12}$$

Hence, the manifold is defined as:

$$\Psi = \frac{dP_{pv}}{dI_{pv}} = \frac{dI_{pv}\,V_{pv}}{dI_{pv}} = V_{pv} + I_{pv}\frac{dV_{pv}}{dI_{pv}} = 0 \tag{3.13}$$

By applying equation (3.6) we find:

$$\frac{d\Psi}{dt} = \left(\frac{d\Psi}{dI_{pv}}\right)\left(\frac{dI_{pv}}{dt}\right) \tag{3.14}$$

Compensating equation (3.14) in equation (3.4) give us:

$$T_S \left[\left(\frac{d\Psi}{dI_{pv}} \right) \left(\frac{dI_{pv}}{dt} \right) \right] + \Psi = 0 \tag{3.15}$$

Where:

$$\frac{d\Psi}{dI_{pv}} = 2 \frac{dV_{pv}}{dI_{pv}} + I_{pv} \frac{d^2 V_{pv}}{dI_{pv}^2} \tag{3.16}$$

The output PV voltage V_{pv} can be deduced from the equation (1.1) of the first chapter, as follows (by considering $R_{sh} \gg$ and $R_s \ll$):

$$V_{pv} = \frac{N_s AKT}{q} \; ln \left(\frac{I_{ph} - I_{pv} + I_o}{I_o} \right) \tag{3.17}$$

From (3.17) we can conclude:

$$\frac{dV_{pv}}{dI_{pv}} = \frac{N_s AKT}{q} \left(- \frac{1}{I_{ph} - I_{pv} + I_o} \right) \tag{3.18}$$

$$\frac{d^2 V_{pv}}{dI_{pv}^2} = \left(- \frac{N_s AKT}{q} \right) \left(\frac{1}{(I_{ph} - I_{pv} + I_o)^2} \right) \tag{3.19}$$

The substitution of equations (3.10) and (3.16) into the equation (3.15) gives the control law equation described in equation (3.20):

$$D(t) = 1 - \frac{\Psi L}{V_o T_S \left(2\frac{dV_{pv}}{dI_{pv}} + I_{pv} \frac{d^2 V_{pv}}{dI_{pv}^2} \right)} - \frac{V_{pv}}{V_o} \tag{3.20}$$
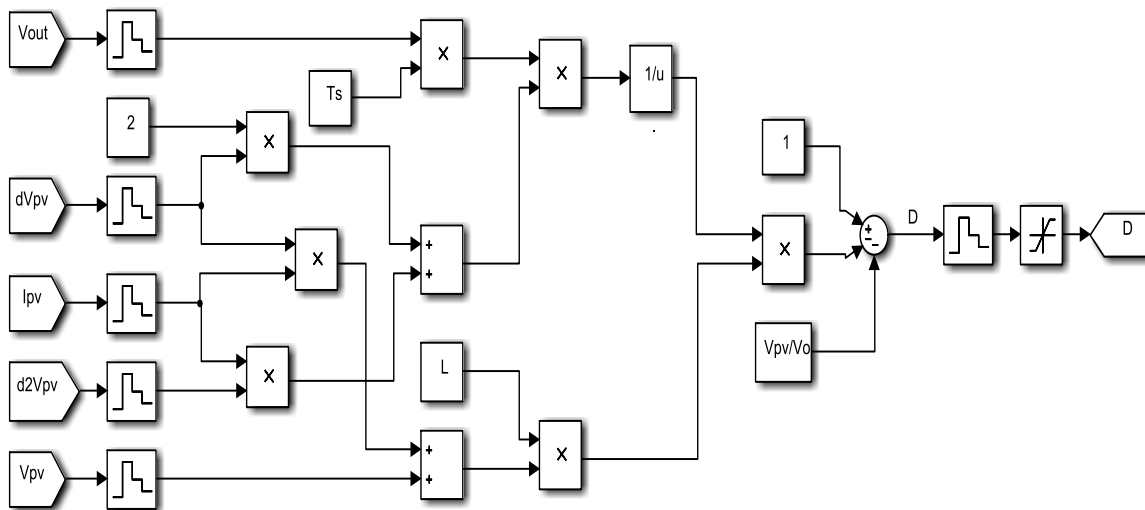

Fig.3.2. Simulink block diagram of synergetic controller.

From equation (3.20), we see that the Synergetic controller will force the controlled variable trajectory approaching directly and with no sudden change to the desired manifold $\Psi=0$ and serves to keep it there. For that we say that the control law generated by the synergetic approach is continuous instead of a switching term like SMC, by thus the chattering phenomenon can be either reduced or eliminated. The block diagram of the proposed synergetic strategy is given in figure 3.2.

Stability Proof

The system stability is ensured using the Lyapunov's theory. Let the Lyapunov's function be defined positive as follows:

$$V_L = \frac{1}{2}\Psi^2 \qquad > 0 \tag{3.21}$$

We say that the system is stable if the derivative of the Lyapunov's function is less than zero. The derivative of V_L is given by:

$$\frac{dV_L}{dt} = \Psi\left(\frac{d\Psi}{dt}\right) = \Psi\left[\left(-\frac{1}{T_s}\right)\Psi\right]$$

$$= \left(-\frac{1}{T_s}\right)\Psi^2 \leq 0 \tag{3.22}$$

According to equation (3.22), the derivative of the Lyapunov's function is always negative, which ensures system stability.

3.5. Results and discussion

In order to validate and evaluate the effectiveness of the proposed synergetic based MPPT controller, the model of the PV system, shown in figure 3.1, has been first implemented in Matlab/Simulink environment for simulation. Next, the proposed MPPT controller is implemented in dSPACE RTI 1104 real-time platform and several tests were performed on an experimental test bench to obtained simulation results.

3.5.1. Simulation results

To verify the performance of the proposed MPPT controller, the PV model system has been designed in Matlab/Simulink as shown in figure 3.3. It includes the PV array, the DC-

DC boost converter controlled by the proposed MPPT controller and a resistive load. The PV modules specifications and the system specifications used in the simulation are shown in table 1.1 and table 1.2 respectively.

The simulation results obtained by the developed controller are compared to that obtained by sliding mode controller at Standard Climatic Conditions STC (Irradiance = 1000W/m² and temperature = 298 K).
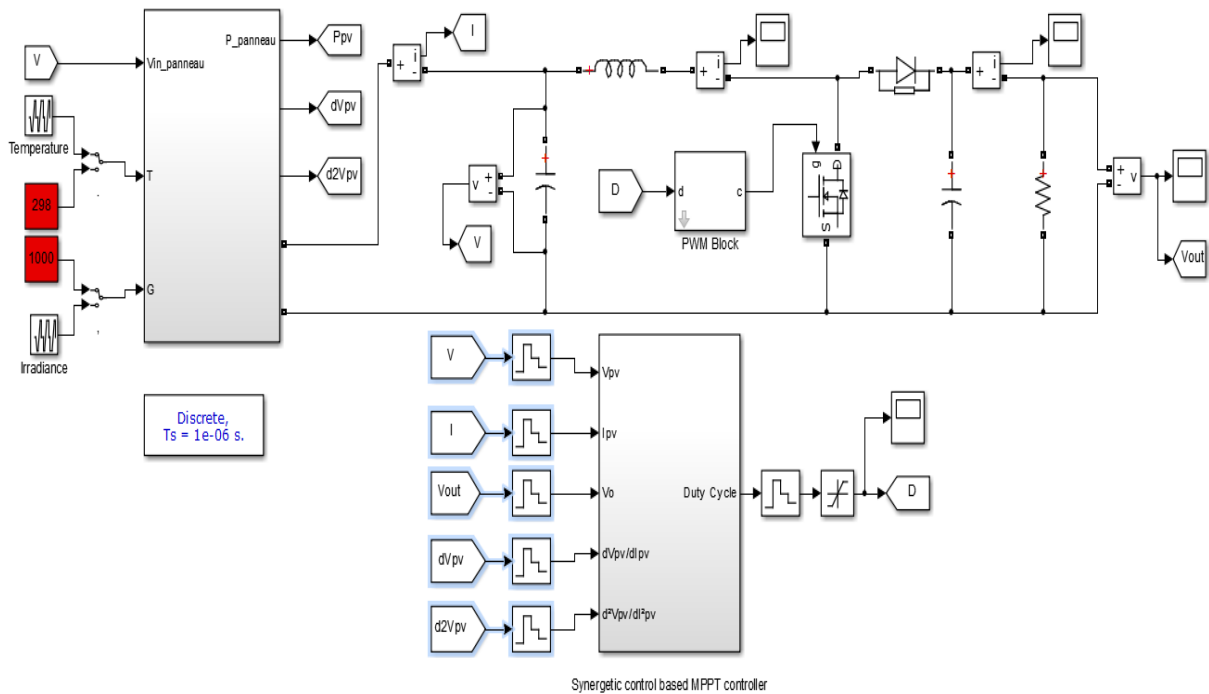

**Fig.3.3.** Implementation of PV system in Matlab/Simulink.

Figure. 3.4 (a) shows the output power of all above mentioned methods, these results have confirmed the good performance and the high effectiveness of the proposed controller in transient and steady state. We can note clearly, in a transient state, that the synergetic approach ensures the convergence to the MPP more rapidly compared to sliding mode controller and in the right direction. At the same time, the duty cycle of the proposed technique converges to the optimal value in limited time as shown in figure 3.4 (b) and the macro-variable is maintained very close to zero as shown in figure 3.4 (c), by this we guarantee the ability to reach the optimum point (dP_{pv}/dI_{pv} =0). Moreover, in a steady state, once the output power of the PV system is maintained at the maximum, a significant reduce of the oscillation around the MPP is appeared and as result, the power extracted using synergetic approach is much larger compared to the power extracted using SMC technique as shown obviously in attached zoom in figure 3.4 (a).
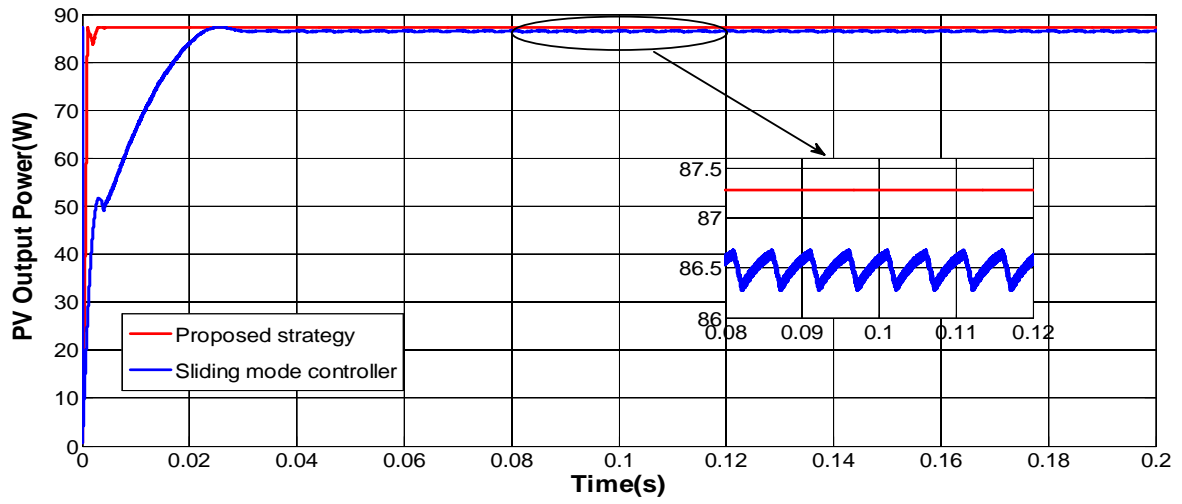
(a)
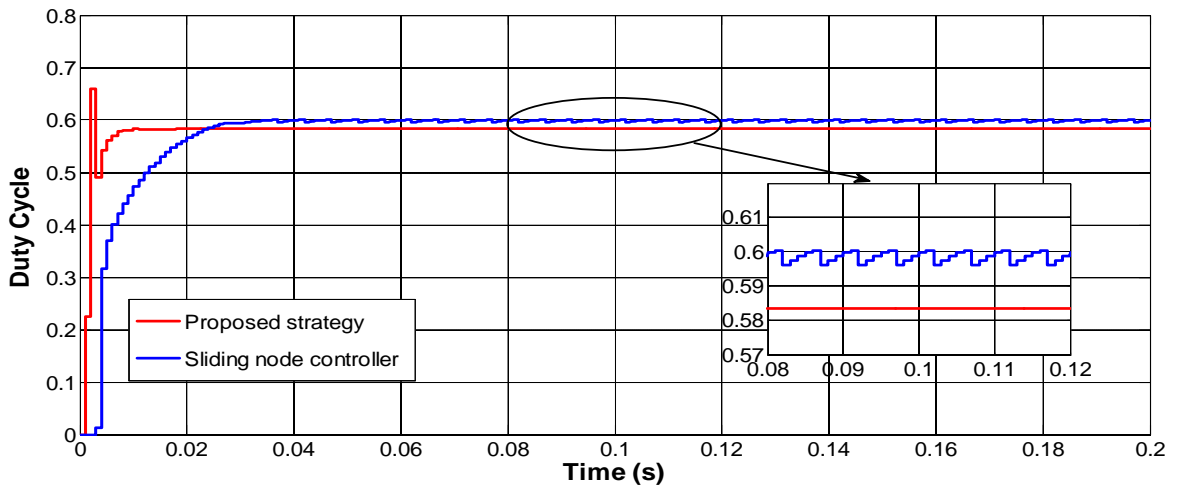
(b)
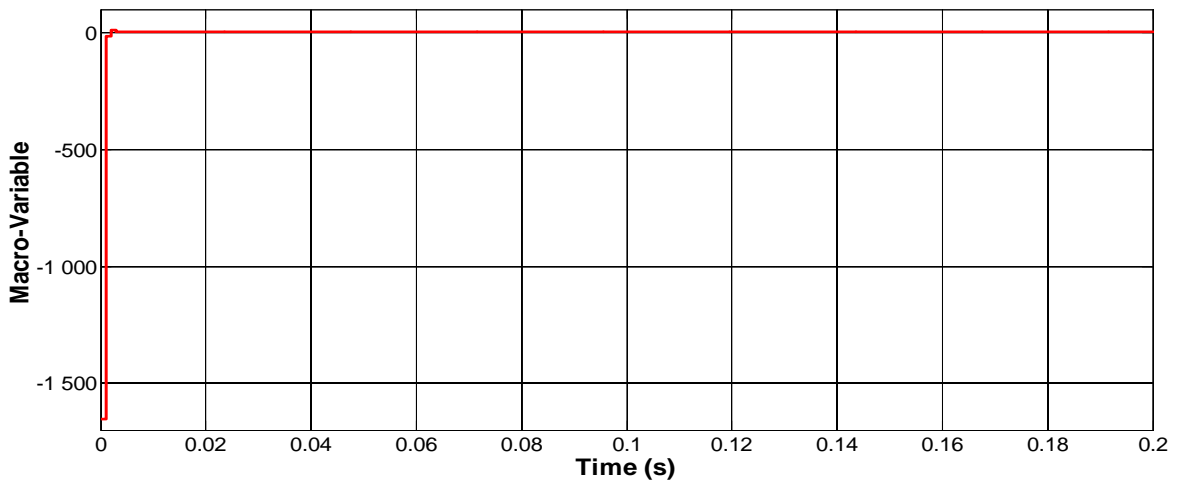
(c)

Fig.3.4. Simulation results of the proposed strategies at STC (S=1000 W/m², T = 298 K, (a) Output power (P$_{pv}$), (b) Duty cycle (D), (c) Macro-variable (Ψ).

In order to evaluate the robustness of the proposed MPPT controller under variable atmospheric conditions, the sun insolation 700 W/m² is applied to the PV system. Then, it is stepped up to 1000 W/m² and finally it is stepped down to 500 W/m² as shown in figure 3.5 (a). The tracking result of this step change of both techniques is shown in figure 3.5 (b). While figure 3.5 (c) and (d) illustrate the duty cycle, the output voltage (V_{out}), the PV voltage (V_{pv}) and the PV current (I_{pv}) of the proposed synergetic controller at the same step change.

In the first step change introduced at 0.1s we stepped up the irradiance from 700 W/m² to 1000 W/m² in short time equal to 0.05s. On the obtained results we can make a detailed analysis. In transient state, the SMC takes a relatively long time to reach the MPP without an overshoot. The settling time in this case is equal to 0.08 s. While the SC reaches the MPP at the same time that the irradiance settled at 1000 W/m² as it is shown in zoom1of figure 3.5 (b). In steady state, once the power extracted by SMC will be stable, the oscillations around the MPP introduce a power with an average value equal to 86.95 W which creates a static error equal to 0.33 W. On the other hand, the average value of the power extracted by SC is estimated to 87.28 W which provides almost neglected static error. The second step change is distinguished by a stepped down of irradiance at 0.25 s from 1000 W/m² to 500 W/m² in relatively long time, compared to the time of the first step change which equals 0.15 s. In this case, SMC shows a fast tracking where the settling time is estimated by 0.003 s (Zoom3 of figure 3.5 (b)) and this is caused by the slow change in the irradiance but it is still not able to extract the maximum power estimated by 43.8 W under 500 W/m² which creates a static error equal to 0.2 W. On the other hand, the proposed strategy managed to reach the MPP at 0.4 s, which is the same time that the irradiance is stable at 500 W/m². The average value of the power extracted in steady state is 43.79 W which creates a static error around 0.01W.

To examine the performance of the proposed MPPT controller under temperature variations, we suddenly change the temperature from 303 K to 288 K, then to 323 K as shown in figure 3.6 (a). The tracking result of these changes is shown in figure 3.6 (b). While figure 3.6 (c) and (d) illustrate the duty cycle, the output voltage (V_{out}), the PV voltage (V_{pv}) and the PV current (I_{pv}) of the proposed controller at the same step change.
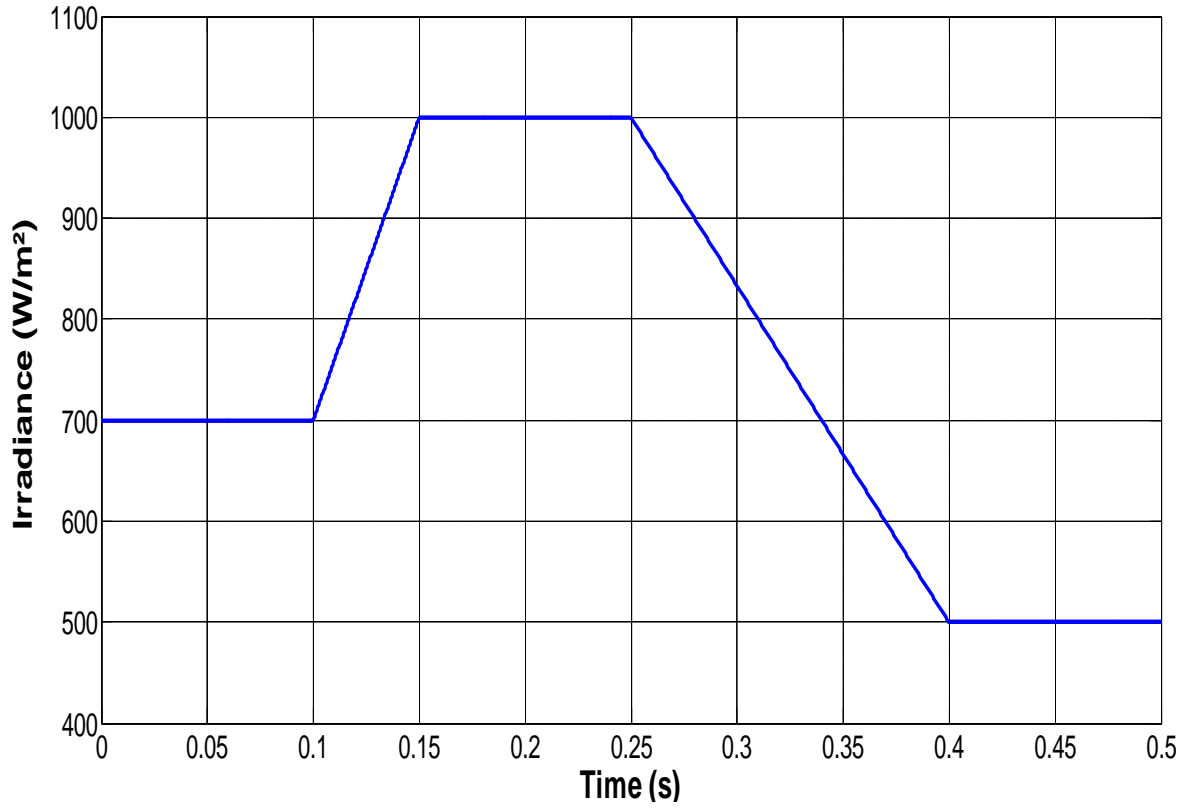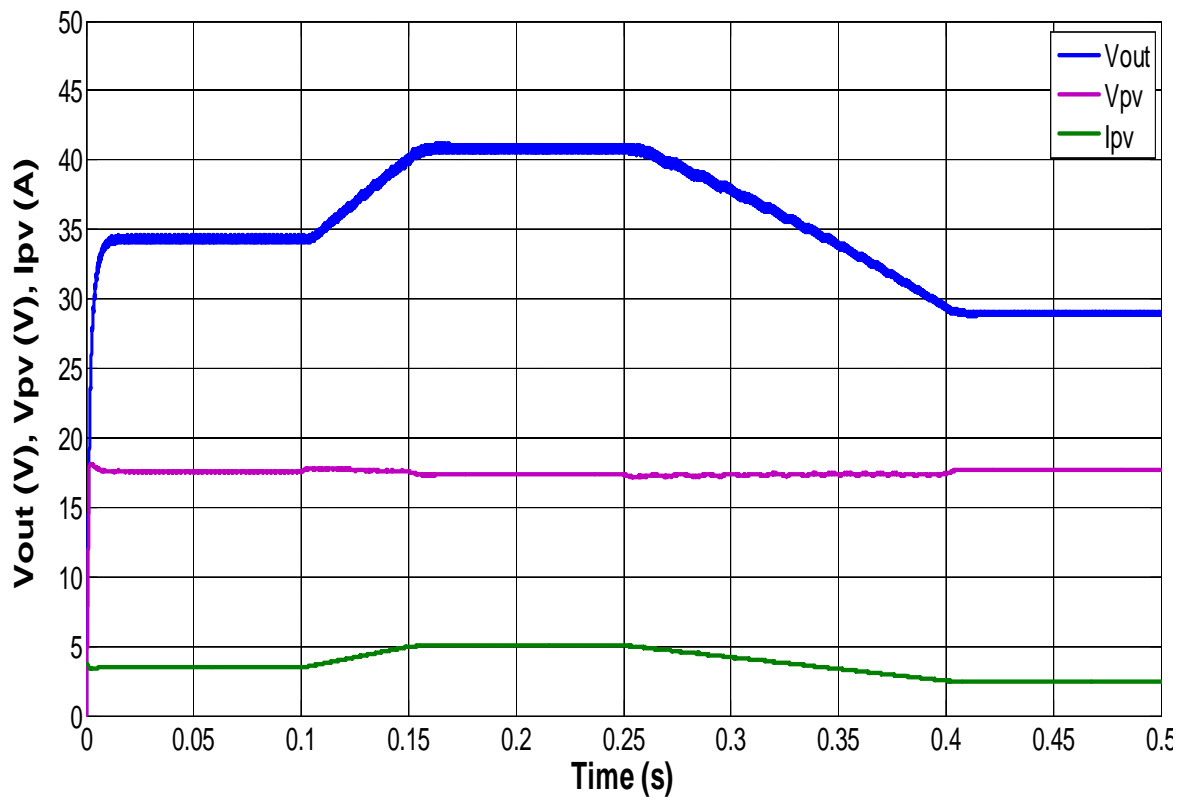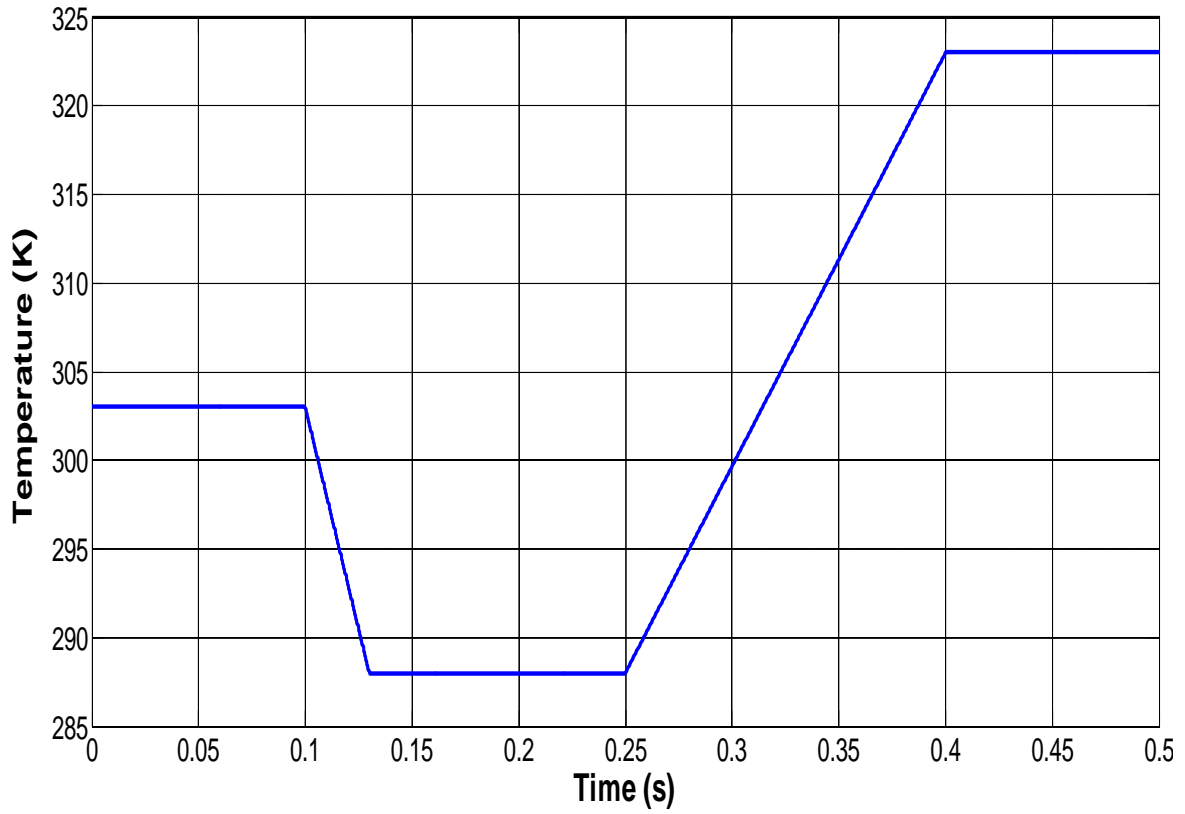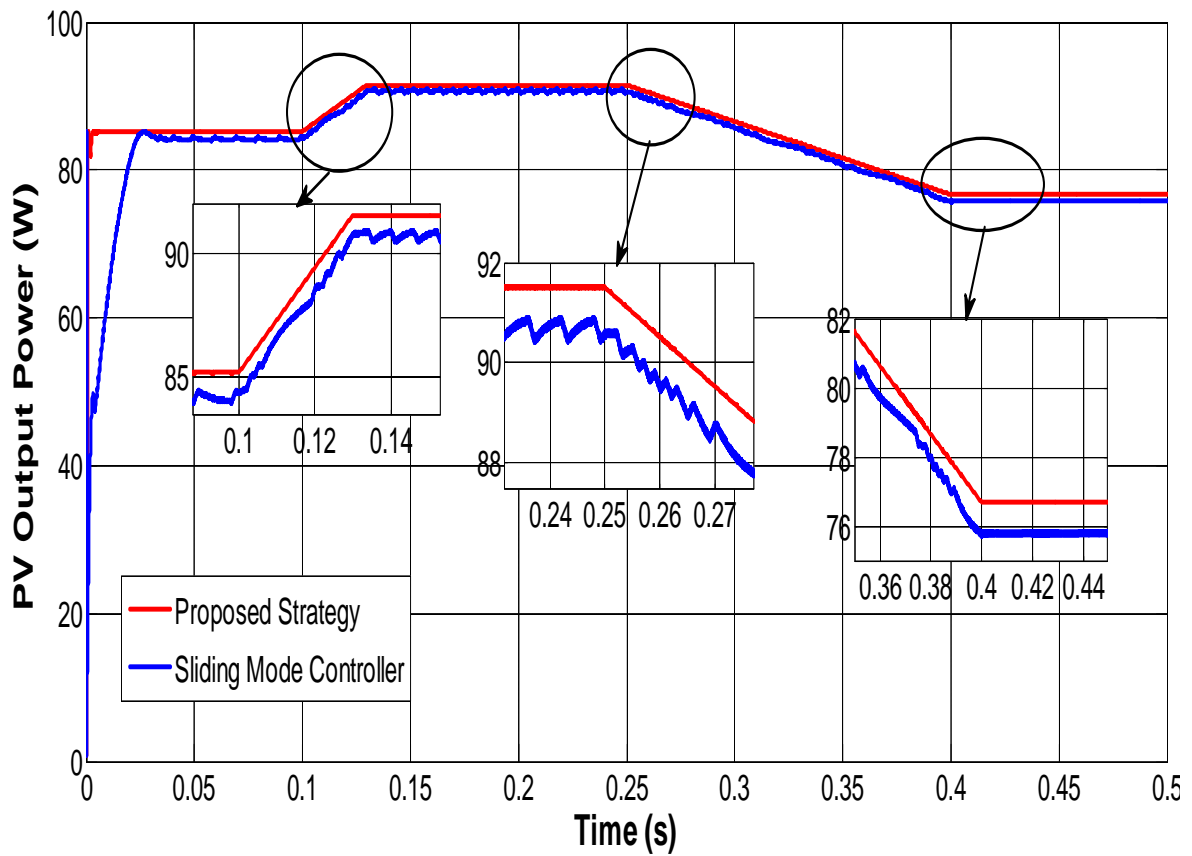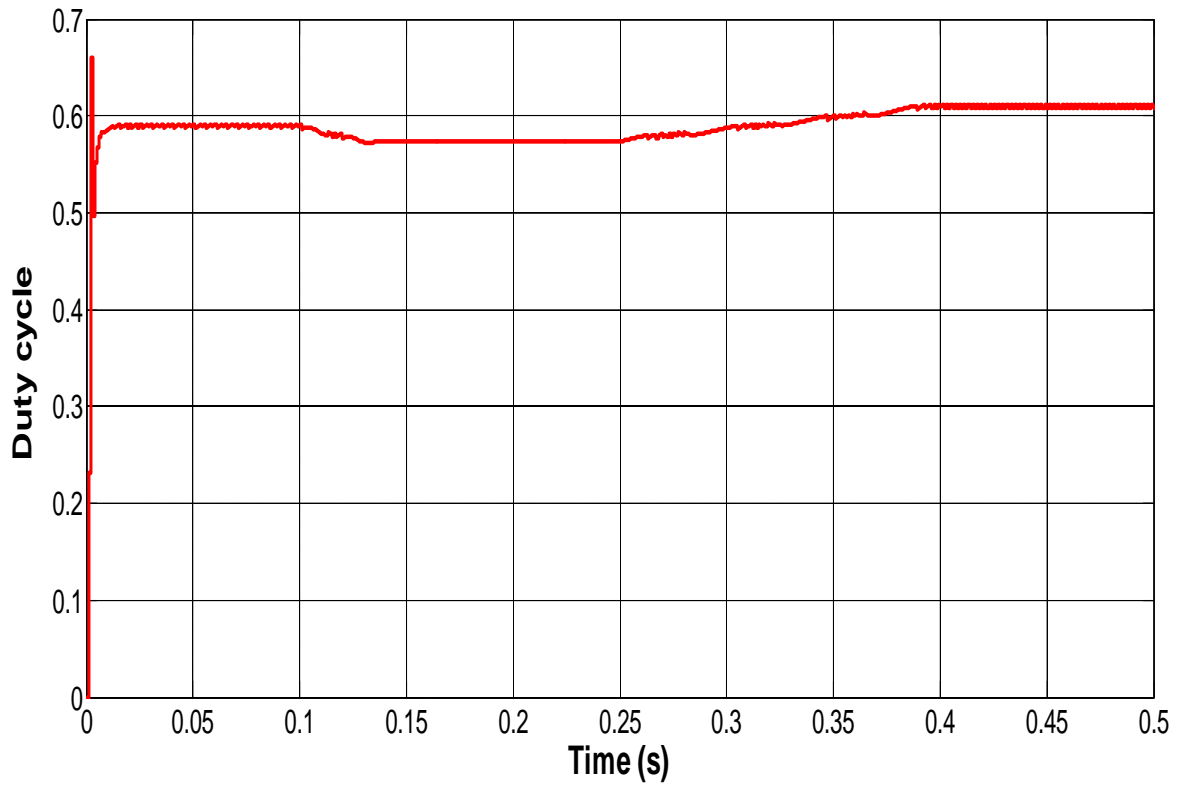
(a)
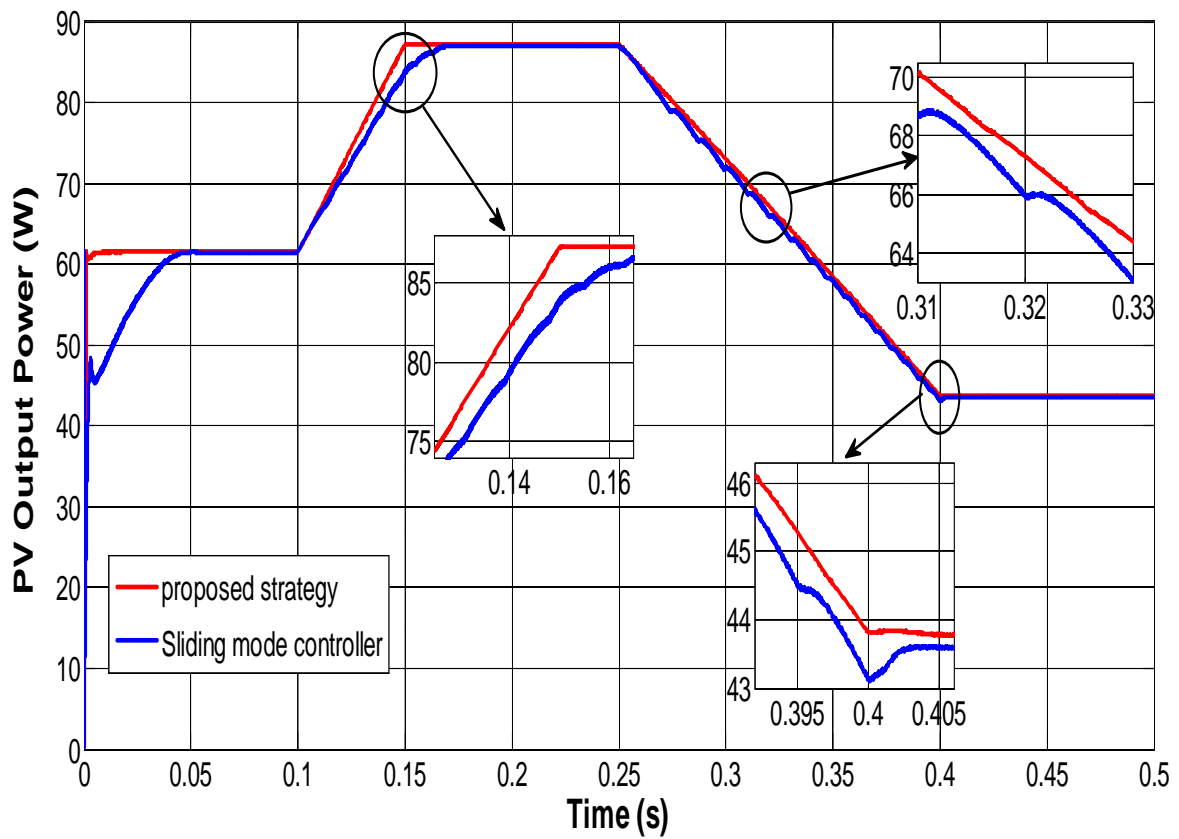
(b)
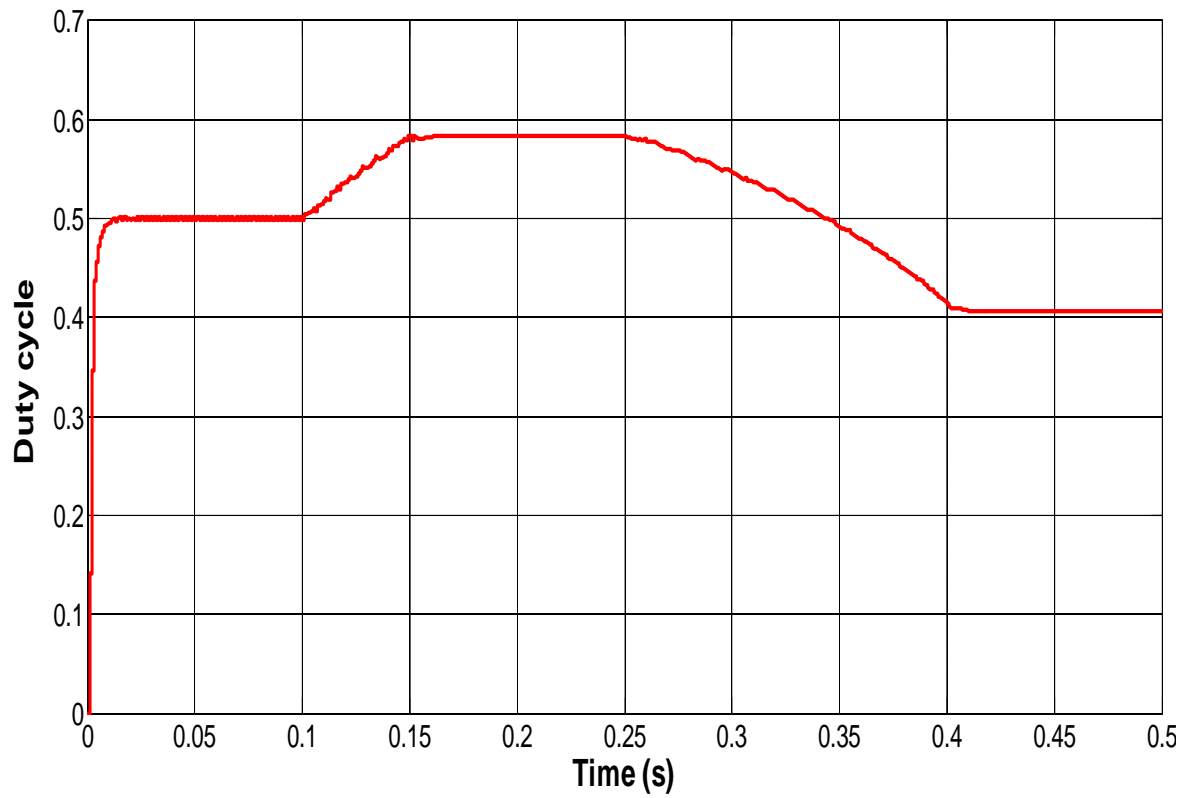
(c)

(d)

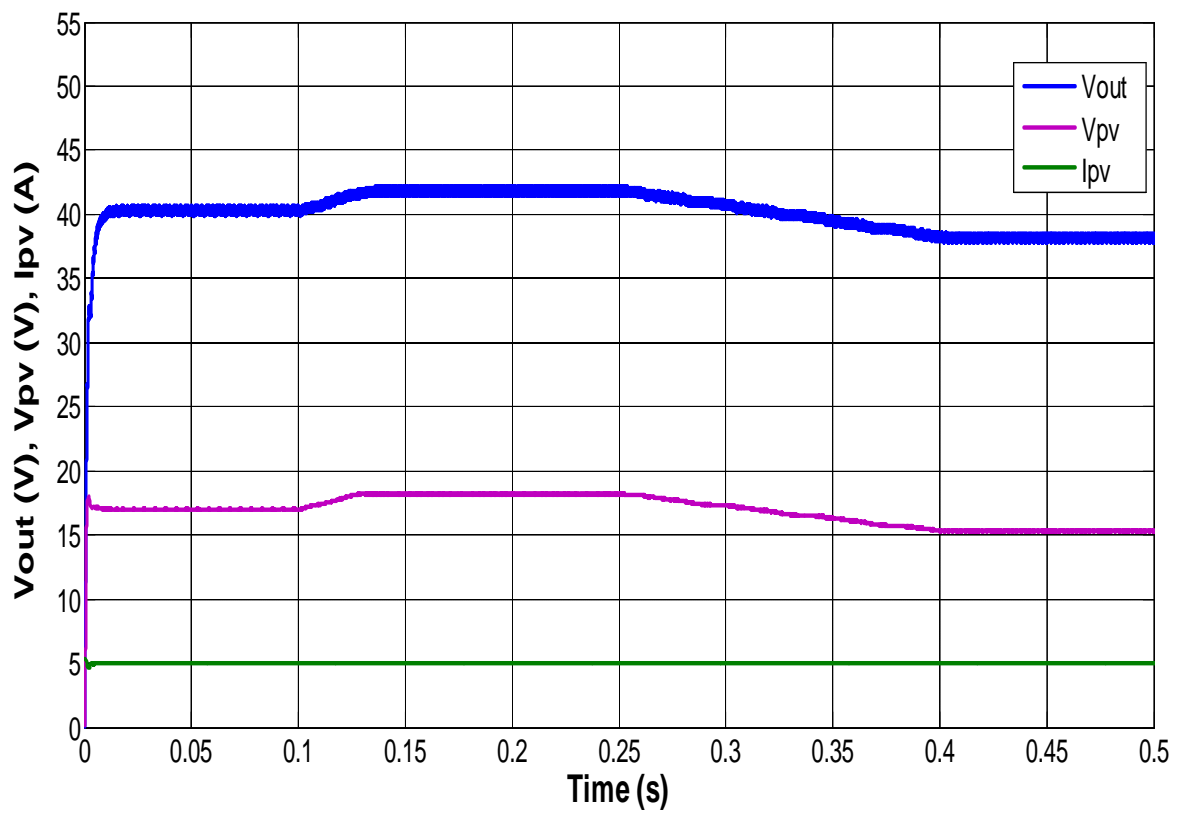**Fig.3.5.** Simulation with step change of irradiance (T=298 K).

(a)

(b)

(c)

(d)

Fig.3.6. Simulation with step change of temperature (S=1000W/m²).

In both cases of temperature change, the SMC shows a fast tracking to the M-PP but not with the same accuracy given by Synergetic controller as it is shown in attached zoom of figure 3.6 (b). In steady state and by using SMC, sizeable oscillations were appeared around the MPP to give a power with an average value equal to 90.75 W, in the first step change, which provides a static error equal to 0.75 W. A power with an average value equal to 75.78 W is obtained in the second step change which provides a static error equal to 0.92 W. On the other hand, the use of the proposed MPPT controller based on synergetic approach makes the extraction of the maximum power possible and with highly reduced oscillations, which achieves almost neglected static error, where the average power value equals 91.5 W in the first step change and 76.7 W in the second step change.

Thus, all the obtained simulation results have confirmed the strong robustness, in transient and steady state conditions, of the proposed synergetic MPPT controller against the SMC technique. The SC ensures the convergence to the MPP quickly under different tests and towards the environment changes without affecting inversely at the output power.

3.5.2. Validation and experimental results
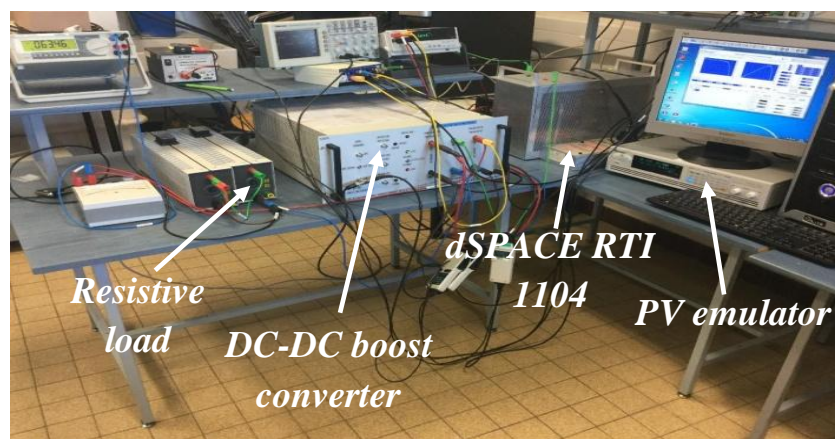
Fig.3.7. Experimental test bench of PV system with the developed MPPT controller.

An experimental test bench, figure 3.7, has been developed in LIAS-ENSIP-laboratory, France, to confirm the validity of the proposed synergetic-based MPPT controller. It consists of the following equipment's: a programmable DC power supply with solar array simulation: 62020H-150S manufactured by the company Chroma to simulate two Kyocera KC85T panels (whose specifications are illustrated in Table 1.1) connected in series to generate 177W at PV peak power, a DC-DC boost converter with a switching frequency of 10 kHz (Table 1.2) and a linear resistive load. The synergetic-based MPPT algorithm is digitally implemented on a dSPACE RTI 1104 system real-time platform through a Matlab/Simulink environment.
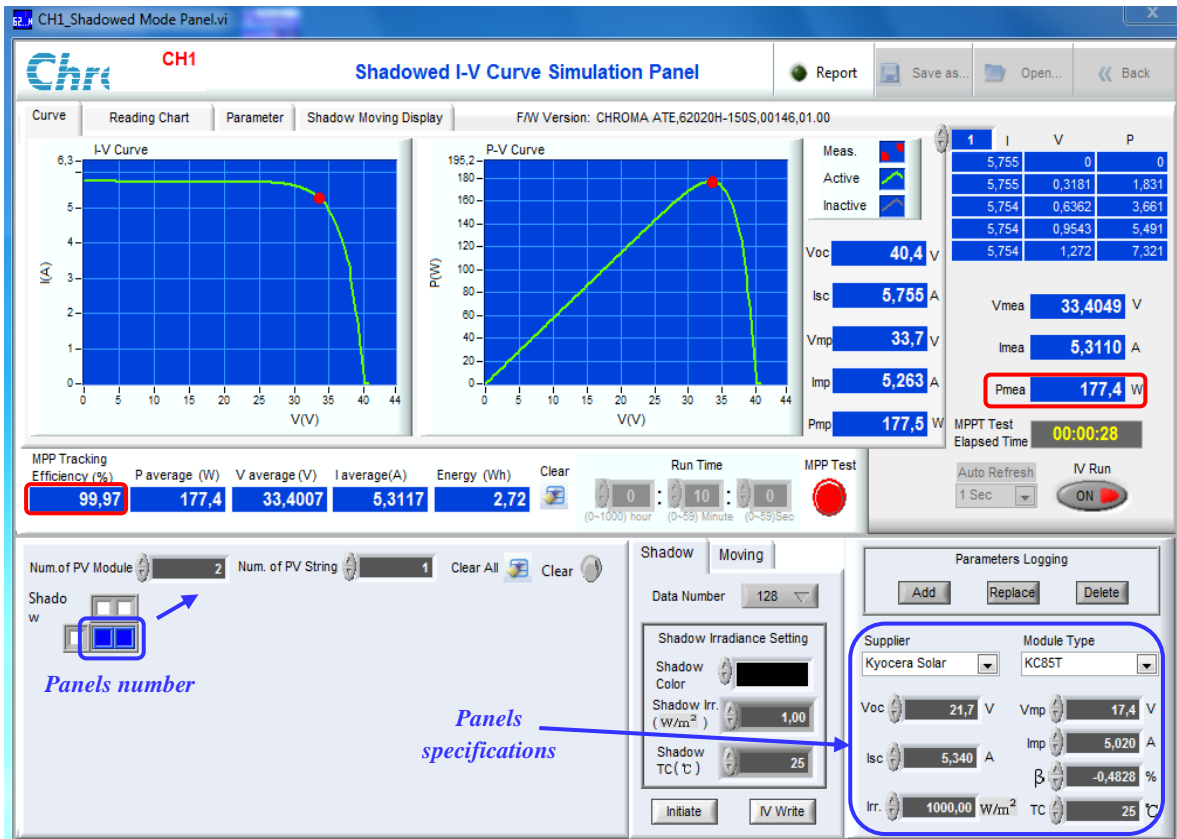
(a)
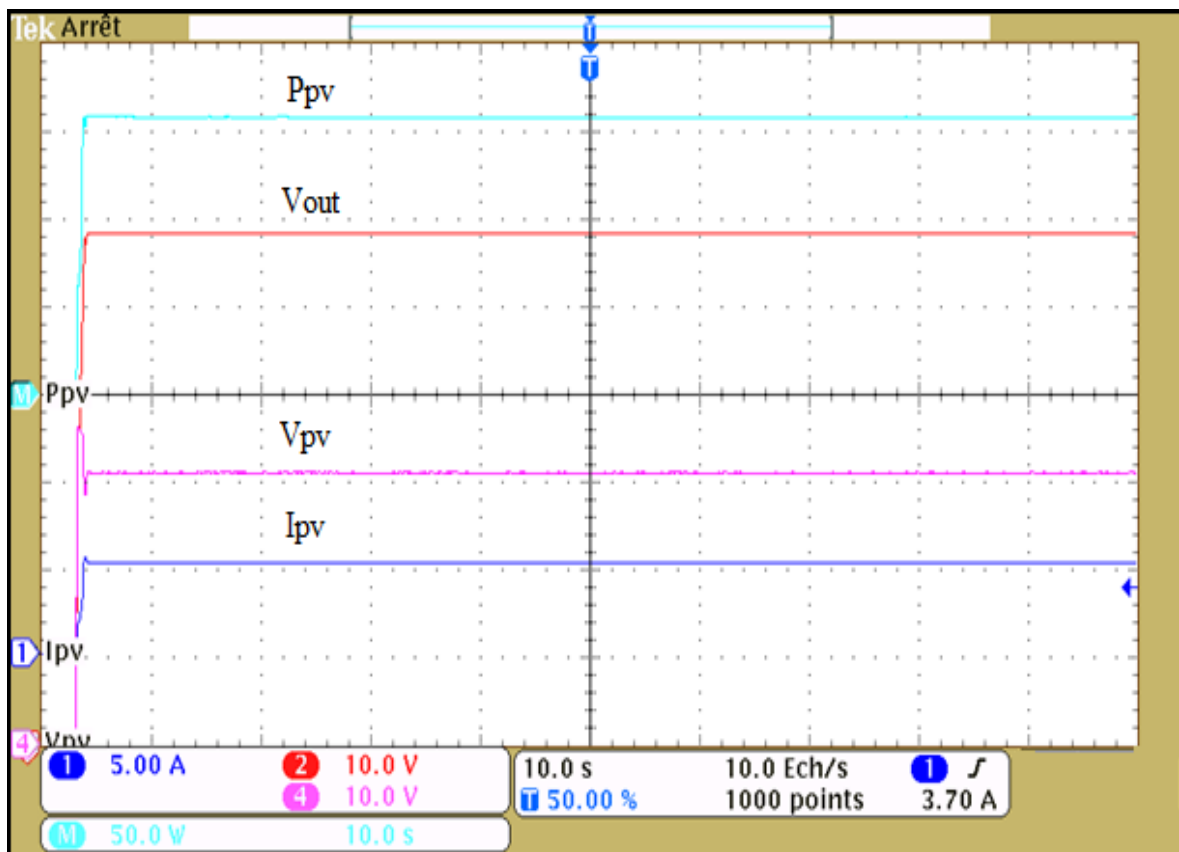
(b)
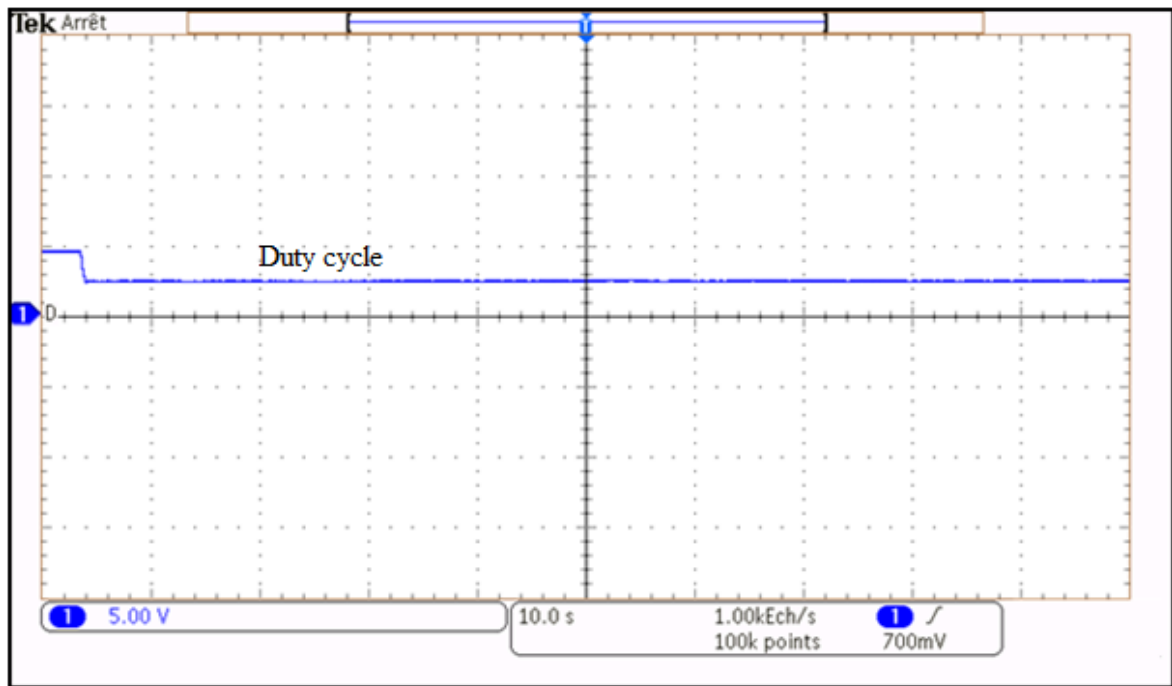
(c)
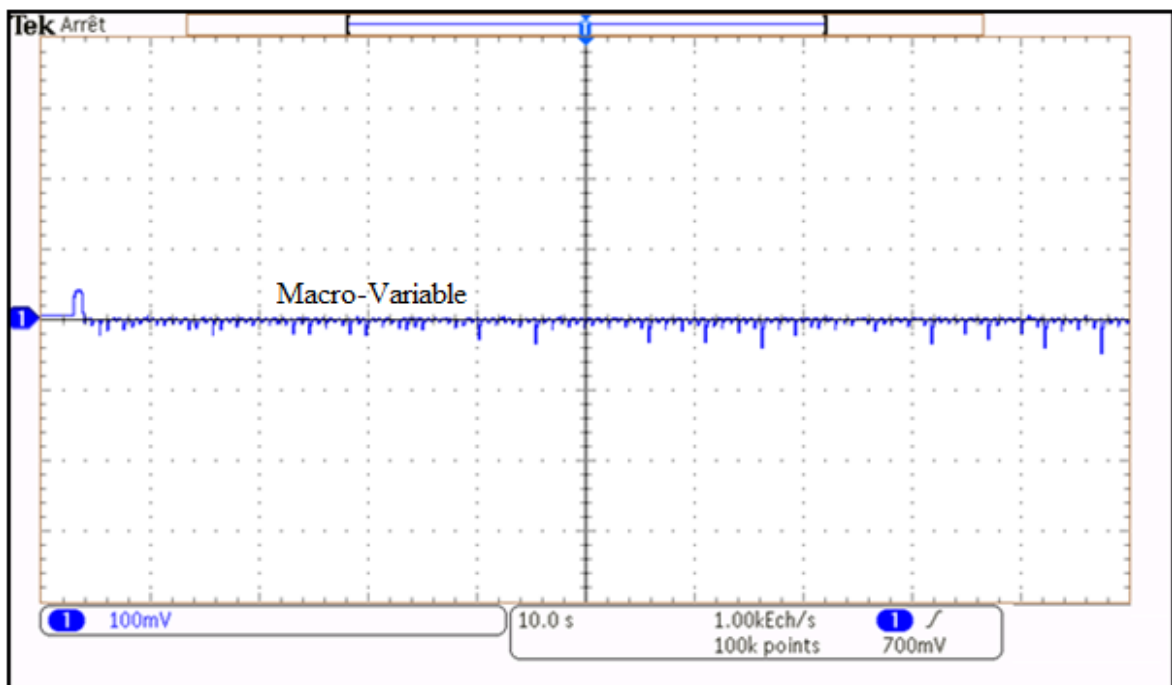
(d)

Fig.3.8. Experimental results at STC (Irradiance = 1000 W/m² and Temperature = 298 K).

(a) P-V characteristic plotted on the Chroma emulator in the STC.

(b) Experimental results of P_{pv}, I_{pv}, V_{pv} and V_{out}.

(c) Experimental results of the duty cycle.

(d) Experimental results of the macro variable.

The experimental results under standard test conditions (Irradiance = 1000 W/m² and Temperature = 298 K) are presented in figure 3.8 (b). The proposed synergetic MPPT controller is able to maintain the output power *Ppv*, current *Ipv*, voltage *Vpv* and the output voltage *Vout* constant. Figs. 3.8 (c) and (d) show the experimental results of the duty cycle and the macro-variable respectively.

Fig. 3.9. Experimental results under a step change of irradiation (T=298 K).

Fig. 3.10. Experimental results under a step change of temperature (S=1000 W/m²).

In order to examine the performance of the proposed MPPT controller, the dynamic behavior under a step change of irradiance and temperature, in the experimental test, is presented in figure 3.9 and figure 3.10 respectively.

In figure 3.9, the irradiance is increased from 200 W/m² to 500 W/m² at 3.5 s and increased from 500 W/m² to 1000 W/m² at 7 s. After a very short transient, the output power *Ppv*, current *Ipv*, voltage *Vpv* and the output voltage *Vout* are maintained constant with good stability.

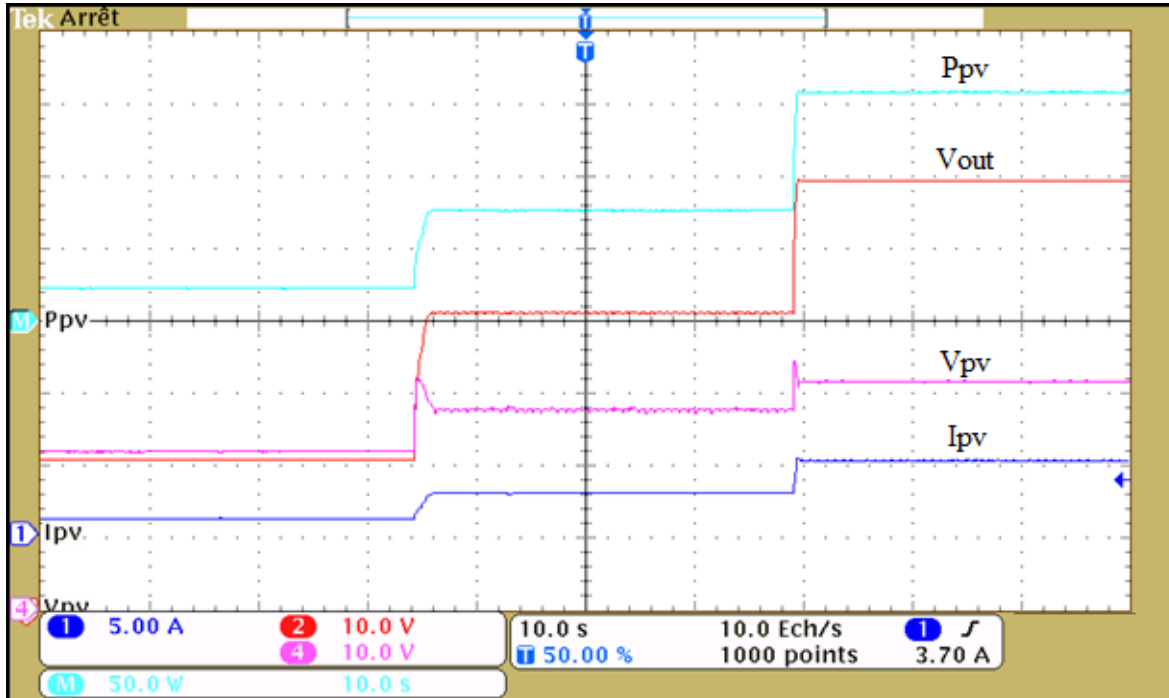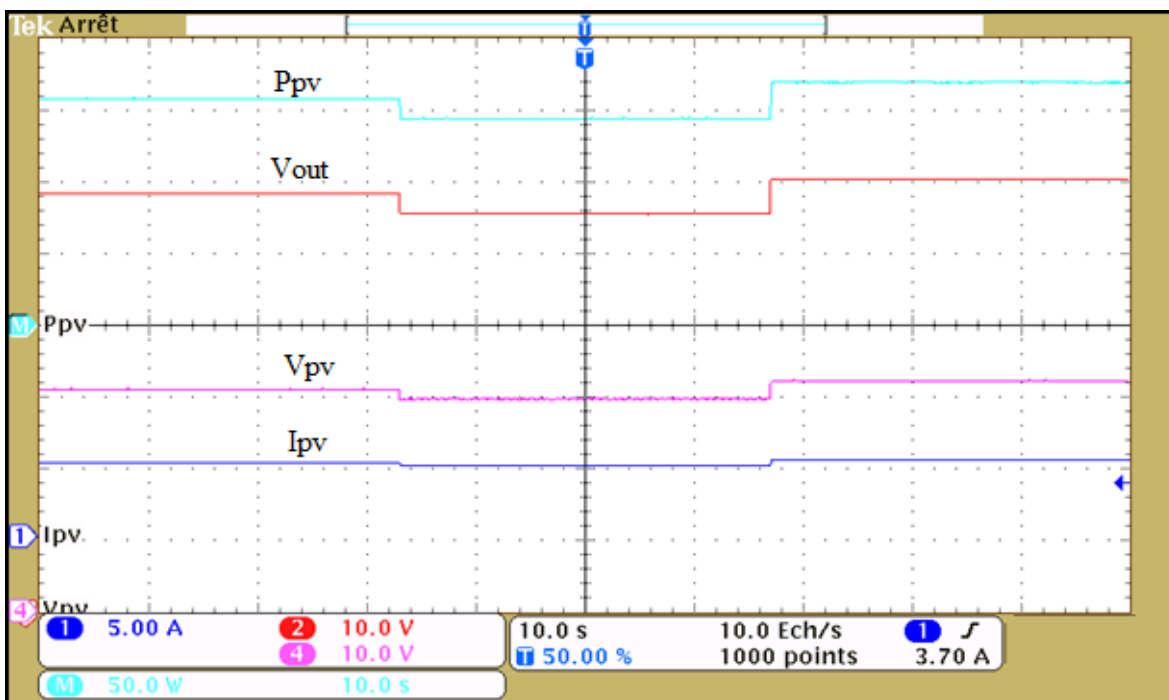Figure 3.10 shows experimental results under a step change of temperature using the proposed synergetic MPPT controller. In this experimental test, the temperature is increased from 298 K to 313 K and decreased from 313 K to 283 K at constant irradiance of 1000 W/m². From this figure, it can be observed that the stability of the system is successfully achieved by maintaining the output power *Ppv*, current *Ipv*, voltage *Vpv* and the output voltage *Vout* constant after a very short transient.

All experimental results are in concordance and very close to the previous simulation results. Thus, confirm the validity and the feasibility of the proposed synergetic-based MPPT controller. This approach provides high efficiency 99.97% at standard test conditions, as shown in figure 3.8 (a), with correct and fast tracking as shown in figure 3.8 (b). Oscillations around the MPP are approximately eliminated and the macro variable is maintained very close to zero (see figure 3.8 (d)). At the same time, the duty cycle converges to the optimal value to reach the MPP as shown in figure 3.8 (c). Moreover, the experimental results show the effectiveness and the good robustness of the PV system with the proposed MPPT against the variation of external conditions, irradiance (figure 3.9) and temperature (figure 3.10).

3.5.3. The EN 50530 MPPT efficiency test

To further evaluate the developed strategy, the EN 50530 European standard test for measuring the dynamic MPPT efficiency is used [3.12]. It's implemented by providing triangular irradiance waveforms sequentially but with different ramp gradients values from 0.5 W/m²/s to 100W/m²/s, so thus covered a comprehensive set of irradiance changes from the slow to the very fast.

In this work, we use the EN50530 standard test with two different irradiance levels from 300 to 1000 W/m² (medium to high irradiance), but without repeating the same triangular waveforms as mentioned in the original document [3.12], because MPPT techniques as agreed keep the same responds during the same ramp (up and down). We applied three

sequences with different ramp gradients: 10, 35 and 70 W/m²/s (slow, fast, and very fast) respectively, the irradiation remains constant for a certain period of time at the high level as well as the low as shown in figure 3.11.The power tracking result of the proposed strategy and the sliding mode controller is presented in figure 3.12, certain parts are zoomed in to be clearer.

During a slow solar irradiance change (10 W/m²/s); the tracking power obtained by the proposed strategy is almost perfect and the ability to extract the maximum power is very high compared to sliding mode controller as shown in Zoom 1. The SMC also provides a good performance when the irradiance changes slowly as shown in Zoom 2, it's true that the tracking power deviate from the right direction compared to synergetic controller but after each relatively large period which makes the disturbances along the tracking smaller. In the second sequence, the solar irradiance changes faster: 35 W/m²/s (increase and decrease), the synergetic controller is still able to maintain the good and the accurate tracking while the deviations of the tracking power from the correct direction provided by SMC become more (each 0.75 s) as illustrated in Zoom 3, which make more oscillations. During the third sequence, the increasing and the decreasing of irradiance is very fast (70 W/m²/s), the deviations of SMC become much more than the previous sequence (each 0.45 s) and as a result the oscillations along the tracking increase more and more while the proposed controller still copes with the very fast change with high performance as shown in Zoom 4.
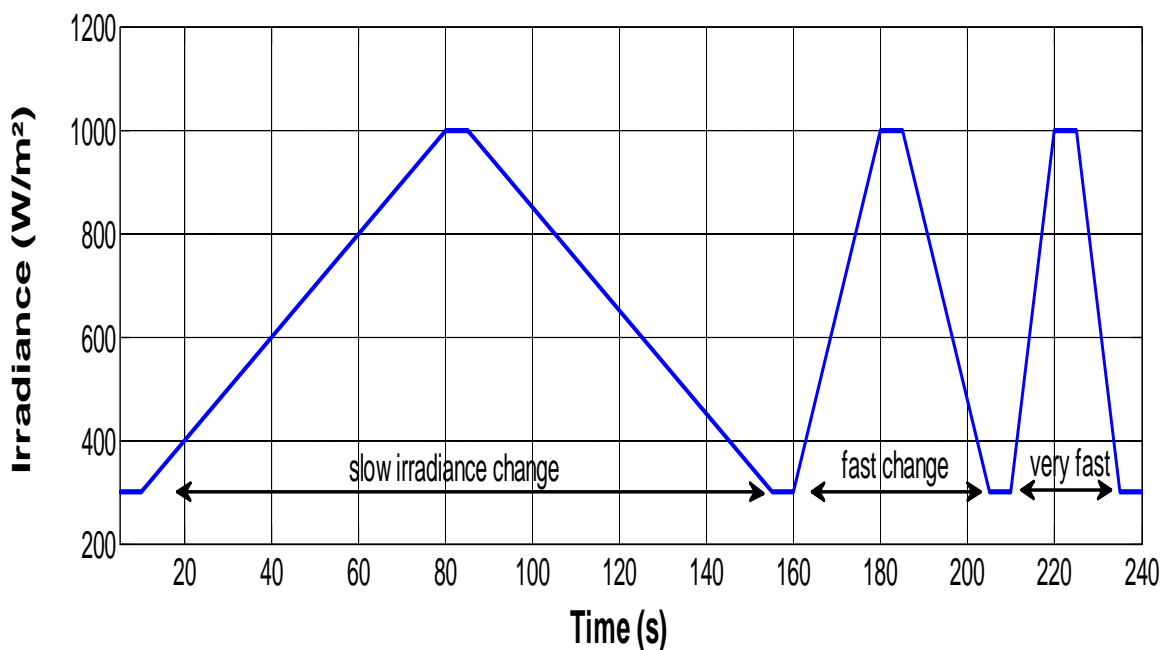
Fig. 3.11. Triangular irradiance waveforms for the EN 50530 standard test of dynamic MPPT efficiency.
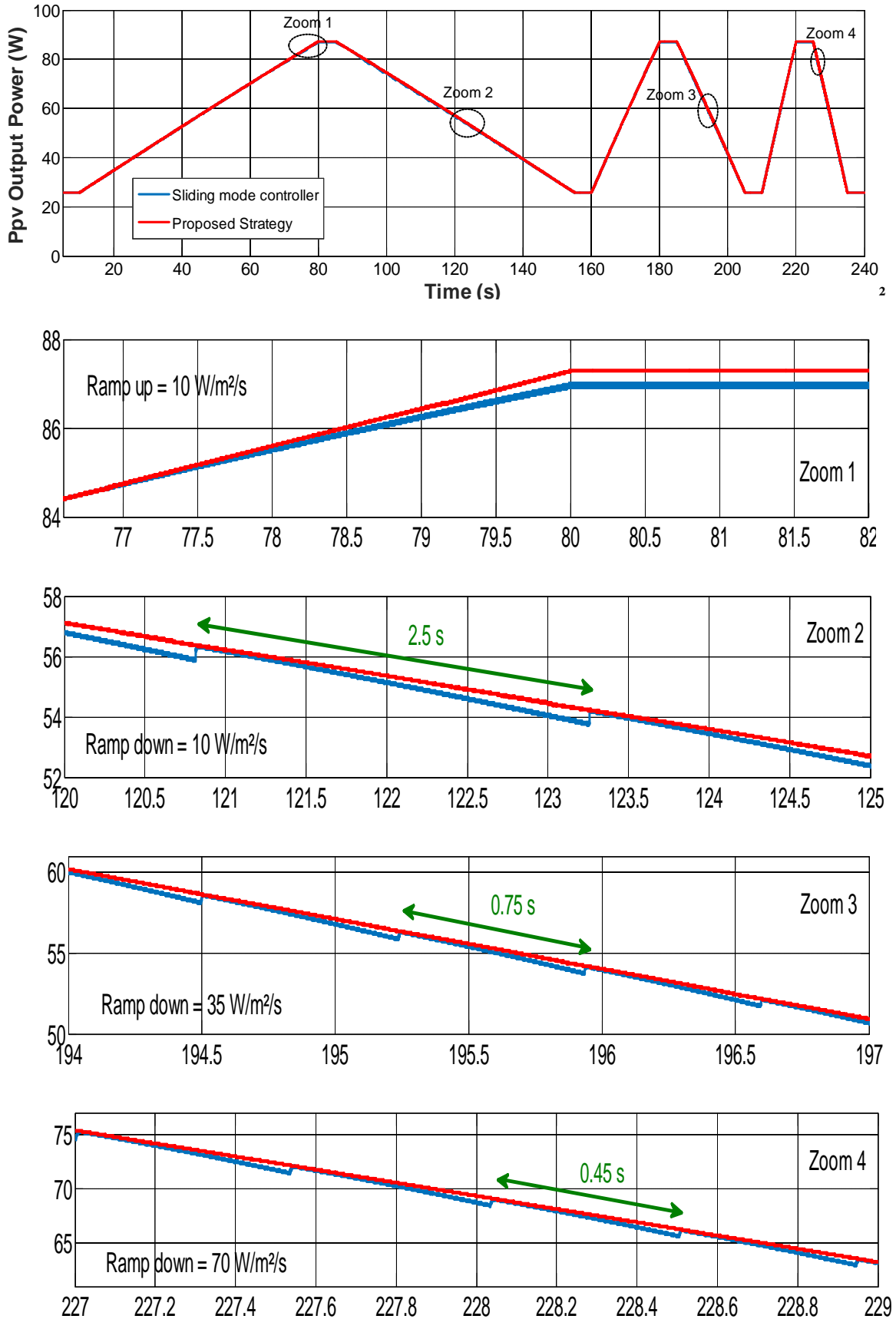
Fig. 3.12. Power tracking result of the synergetic controller and the sliding mode controller.

The MPPT efficiency is measured using the following formula [3.13]:

$$\eta_{MPPT} = \frac{P_{out}(t)}{P_{max}(t)} \tag{3.23}$$

So the average efficiency is calculated according to equation (3.24):

$$\eta_{MPPT,avg} = \frac{\int P_{out}(t)dt}{\int P_{max}(t)dt} \tag{3.24}$$

Where P_{out} is the output power extracted from the PV array and P_{max} is the theoretical maximum power. Although the efficiency is volatile in certain parts of the approved profile in the EN 50530 standard test especially in low irradiance and fast changes, the proposed strategy achieves an average tracking efficiency of 99.93 % under all stages of changing weather whereas the SMC achieves 99.12 % as shown in figure 3.13.
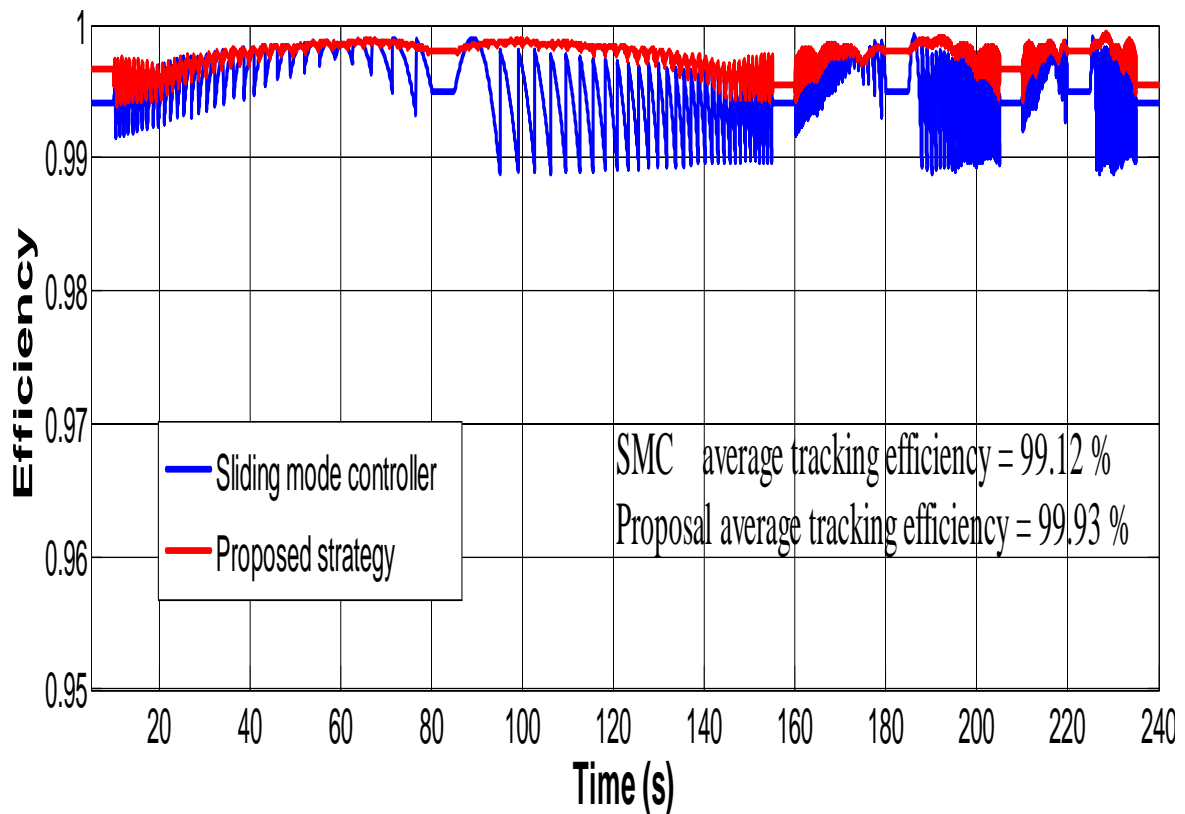
Fig. 3.13. The efficiency of the synergetic controller and the SMC under the EN50530 standard test.

3.6. Summary

In this chapter, a new nonlinear Maximum Power Point Tracking (MPPT) controller based on the synergetic control theory applied to a stand-alone PV system is presented. A DC-DC boost converter is used as an interface between the PV array and the load. The proposed controller was tested both in simulation and experimentally. The EN 50530 standard test was used with different gradients values to calculate the MPPT efficiency under irradiance changes.

The simulation results, obtained using Matlab/Simulink^{MT} tools, prove the good performance in transient and steady state of the proposed synergetic-based MPPT controller, under different temperature and solar irradiance. Moreover, it is much better than sliding mode-based MPPT controller. The synergetic MPPT controller overcomes the problems that exist in the conventional and intelligent algorithms, not only regarding to the fast and accurate tracking but also regarding to the oscillations around the MPP. These features are confirmed by experimental results obtained using dSPACE RTI 1104 real-time platform. In fact, various atmospheric conditions are tested to prove the high efficiency of the proposed synergetic MPPT controller.

References

[3.1].   A. Kolesnikov, G. Veselov, "Modern Applied Control Theory: Synergetic Approach in Control Theory". TSURE Press, vol. 2, 2000.

[3.2].   V. Bregeault, " Quelques Contributions à la Théorie de la Commande par Modes Glissants". PhD Thesis, Ecole Centrale de Nantes, 2010.

[3.3].   D. Zehar, A. Chérif, K. Benmahammed, K. Behih, "Fast Terminal Synergetic Control of Underactuated System". International Multi-Conference on Systems, Signals & Devices, 2018.

[3.4].   N. Zerroug , "Contribution au Contrôle Robuste des Convertisseurs DC-DC". PhD Thesis, Batna University, 2018.

[3.5].   E. Santi, A. Monti, L. Donghong, K. Proddutur, A. Dougal, "synergetic control for DC–DC boost converter: implementation options". IEEE Trans. Ind. Appl., vol.39, pp. 1803–1813, 2003.

[3.6].   Z. Bouchama, M. N. Harmas,K. Zehar, "Finite Time Nonlinear Control for DC-DC Converters". Soft Computing and Electrical Engineering, vol. 1, pp.36-45, 2019.

[3.7].   Z. Jiang, R. A. Dougal, "Synergetic control of power converters for pulse current charging of advanced batteries from a fuel cell power source". IEEE Trans. Power Electron, vol. 19, pp. 1140–1150, 2004.

[3.8].   A. Boonyaprapasorn, S. Natsupakpong, P. S. Ngiamsunthorn, K. Thung-od, "An application of finite time synergetic control for vaccination in epidemic systems". Proceedings of IEEE Conference on Systems, Process and Control, 2017.

[3.9].   A. Hachana, M. N. Harmas, "Synergetic and Higher Order Sliding Mode Control of Blood Glucose Regulation in Diabetes Patients". Journal of Dynamic Systems Measurement and Control, vol. 140, 2018.

[3.10].   R. Ettouil, K. Chabir, M. N. Abdelkrim, "Optimal Synergetic Control for Wind Turbine System". International Journal of Engineering and Science, vol. 7, pp. 44-48, 2018.

[3.11].   N. Zerroug and al., "DSP-based implementation of fast terminal synergetic control for a DC–DC Buck converter". J. of the Franklin Institute, pp. 2329–2343, 2018.

[3.12]. R. Brundlinger and al., "prEN 50530 The New European standard for performance characterisation of PV inverters". 24th European Photovoltaic Solar energy conf., , pp. 3105-3109, 2009.

[3.13]. A. Jubaer, S. Zainal, "A Modified P&O Maximum Power Point Tracking Method with Reduced Steady State Oscillation and Improved Tracking Efficiency". IEEE Transactions on Sustainable Energy, vol. 7, pp. 1506-1515, 2016.

Chapter 4:

Fast Terminal Synergetic Based MPPT Controller

Table of Contents

4.1. Introduction

Recently, the synergetic approach has attracted many researchers where it was classified as one of the most promising robust control technique due to the satisfactory results that have been proven theoretically and experimentally in various fields [3.1]. This strategy has been successfully applied in DC–DC power converters [3.1, 3.2, 3.3], in battery charging system [3.4], in control of the epidemic system [3.5] and also in photovoltaic system to track the MPP under different temperatures and solar irradiances [3.6, 3.7]. In most of the above mentioned applications, the synergetic control law in its classical version offers an asymptotic convergence, which means that the system errors converge theoretically to zero in an infinite time.

In order to reach the equilibrium point in a finite time and reduce the steady state error as much as possible, Fast Terminal Synergetic (FTS) approach has been introduced in several recently research works to overcome the problem of asymptotic stability and thus improve the robustness of the system [3.1].

According to this study, we present in this chapter a new non-linear control strategy based on Fast Terminal Synergetic Control (FTSC) to track the MPP of a stand-alone PV system. The first control objective of the developed MPPT strategy is to reach the MPP in limited time and without any fluctuations once the output power of the PV system is maintained at the maximum, by that we ensure the finite time stability. The second objective is to confirm the high effectiveness and the strong robustness of the proposed controller under non uniform atmospheric conditions or load changes. To evaluate the improvements provided by FTS-based MPPT controller, a comparative study with synergetic controller and conventional P&O algorithm is presented.

4.2. Fast Terminal Synergetic based MPPT controller

The configuration of the proposed standalone PV system used in this study consists of PV array, DC-DC boost converter, resistive load and a non-linear controller allows maximum power tracking as shown in figure 3.1 of the third chapter. The electrical characteristics of the PV array used for the suggested simulation at Standard Test Condition (1000 W/m² and T=298 K) are given in Table 1.1.

The dynamic model of the DC-DC boost converter used can be described by the differential equations developed in the section (1.7) of the first chapter given as:

$$\frac{dV_{PV}}{dt} = \frac{1}{C_{in}}\left(i_{pv} - i_L\right)$$

$$\frac{di_L}{dt} = -(1 - D)\frac{V_o}{L} + \frac{V_{pv}}{L} \tag{4.1}$$

$$\frac{dV_o}{dt} = (1 - D)\frac{i_L}{C_o} - \frac{V_o}{RC_o}$$

If we set V_{pv}, i_L and V_o as system state variables, we obtain:

$$X = \begin{bmatrix} x_1 \\ x_2 \\ x_3 \end{bmatrix} = \begin{bmatrix} V_{pv} \\ i_L \\ V_o \end{bmatrix} \tag{4.2}$$

The system of equations (4.1) can be rewritten as equation (4.3):

$$\dot{X} = \frac{dX}{dt} = f(x, t) + g(x, t)D \tag{4.3}$$

Where:

$$\dot{X} = \begin{bmatrix} dV_{pv}/dt \\ di_L/dt \\ dV_o/dt \end{bmatrix}, \quad f(x) = \begin{bmatrix} \frac{1}{C_{in}}\left(i_{pv} - x_2\right) \\ \frac{1}{L}(x_1 - x_3) \\ \frac{1}{C_o}\left(x_2 - \frac{x_3}{R}\right) \end{bmatrix}, \quad g(x) = \begin{bmatrix} 0 \\ \frac{1}{L}x_3 \\ -\frac{1}{C_o}x_2 \end{bmatrix}.$$

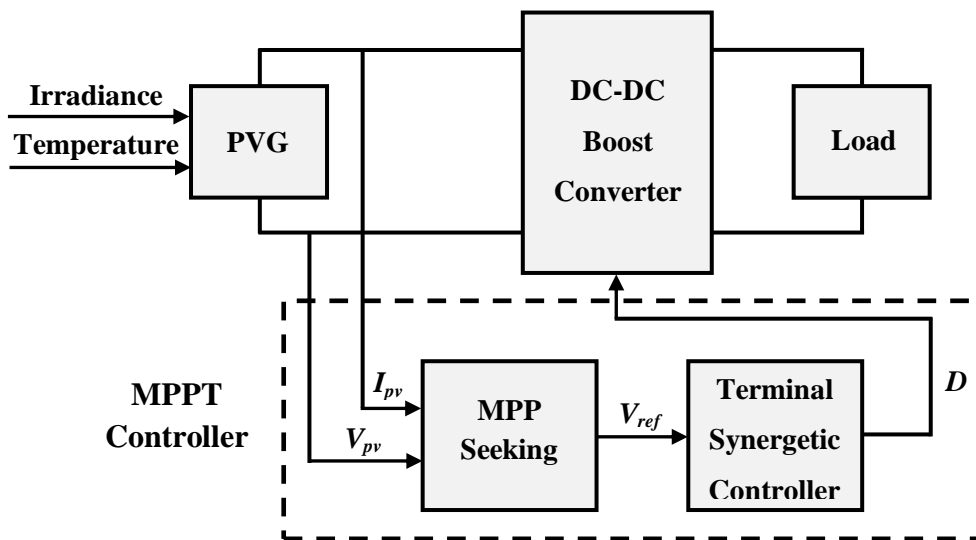The detailed parameters of the DC-DC boost converter used are given in Table 1.2.

Fig. 4.1. Configuration of the proposed MPPT controller.

To extract the total energy from the PV module regardless weather changes or load variations, a nonlinear MPPT based on FTS strategy is used. The structure of the control system is illustrated in figure 4.1. The MPPT controller consists of two blocks:

The first block (MPP seeking) calculates the reference voltage $\mathbf{V_{ref}}$ by following explanation below:

Depending on many previous studies, the maximum power point of the PV system is reached when:

$$\frac{dP_{pv}}{dI_{pv}} = \frac{d(I_{pv}\,V_{pv})}{dI_{pv}} = V_{pv} + I_{pv}\,\frac{dV_{pv}}{dI_{pv}} = 0 \tag{4.4}$$

The output PV voltage V_{pv} can be deduced from the equation (1.1) as follows:

$$V_{pv} = \frac{N_s AKT}{q}\ln\left(\frac{I_{ph}-I_{pv}+I_o}{I_o}\right) \tag{4.5}$$

Consequently, the derivative of V_{pv} gives the following expression:

$$\frac{dV_{pv}}{dI_{pv}} = -\frac{N_s AKT}{q}\left(\frac{1}{I_{ph}-I_{pv}+I_o}\right) \tag{4.6}$$

By substituting equations (4.5) and (4.6) in equation (4.4) we get:

$$\ln\left(\frac{I_{ph}-I_{pv}+I_o}{I_o}\right) = \frac{1}{I_{ph}-I_{pv}+I_o} \tag{4.7}$$

Solve equation (4.7) gives a linear dependence between the short circuit current (I_{ph}) and the PV current corresponding to the MPP (I_{ref}) [22]:

$$I_{ref} = 0.909I_{ph} \tag{4.8}$$

Finely substituting $\mathbf{I_{ref}}$ by its value in equation (4.5) gives the reference voltage corresponding to the MPP $\mathbf{V_{ref}}$ as follows:

$$V_{ref} = \frac{N_s AKT}{q}\ln\left(\frac{I_{ph}-I_{ref}+I_o}{I_o}\right) \tag{4.9}$$

The second block (Fast Terminal Synergetic Controller) takes the reference voltage $\mathbf{V_{ref}}$ as input to adjust the duty cycle of the boost converter to achieve the MPP. In the next section we provide a detailed study on how to formulate the problem to design the new Fast Terminal Synergetic Controller.

4.2.1. Problem formulation

The objective of this formulation is to obtain a control law which provides the desired values of PV output voltage ($x_1 = x_{1ref}$) and inductance current ($x_2 = x_{2ref}$).

Let us first defining the tracking error as follows:

$$e_i = x_i - x_{iref} \; ; \qquad i = 1,2 \tag{4.10}$$

Where:

$$x_{1ref} = V_{ref} \tag{4.11}$$

$$x_{2ref} = i_{pv} - C_{in} \, \dot{x}_{1ref} \tag{4.12}$$

The derivation of equation (4.10) and substituting equations (4.11) and (4.12) in it gives:

$$\dot{e}_1 = -\frac{e_2}{C_{in}} \tag{4.13}$$

$$\dot{e}_2 = \frac{x_3}{L}(d-1) + \frac{x_1}{L} - \dot{x}_{2ref} \tag{4.14}$$

If we put:

$$Z_1 = e_1 \tag{4.15}$$

$$Z_2 = -\frac{e_2}{C_{in}} \tag{4.16}$$

The derivation of equations (4.15) and (4.16) can be written as follows:

$$\dot{Z}_1 = Z_2 \tag{4.17}$$

$$\dot{Z}_2 = -\frac{\dot{e}_2}{C_{in}} \tag{4.18}$$

Once the problem is formulated, choosing an appropriate control law is the next step so that each of Z_1 and Z_2 converge to zero. In the next section, we applied the fast terminal synergetic theory to provide continuous control law D_{FTSC} able to guarantee a finite-time convergence and ensure required robustness.

4.2.2. Fast Terminal Synergetic controller design

The concept of FTSC needs to determine a nonlinear macro variable. In what follows, we applied this concept in the MPPT controller design in order to define a control law able to

guarantee an accurate tracking to the MPP in a finite-time. The selection of an appropriate macro variable is based on the problem formulation explained above and expressed as follows:

$$\Psi = \dot{Z}_1 + \alpha Z_1 + \beta Z_1^{\left(\frac{p}{q}\right)} \tag{4.19}$$

Where: $\alpha > 0$, $\beta > 0$, p and q are positive constants in which $q > p$. This controller will force the system trajectory approaching to the manifold $\Psi = 0$ in finite time (t_s) determined by the following expression [12, 22]:

$$t_s = \frac{q}{\alpha(q-p)} \ln\left(\frac{\alpha Z_1(0)^{\left(1-\frac{p}{q}\right)} + \beta}{\beta}\right) \tag{4.20}$$

Differentiating the macro-variable of equation (4.19) leads to Eq. (4.21):

$$\dot{\Psi} = \dot{Z}_2 + \alpha Z_2 + \beta\left(\frac{p}{q}\right)\dot{Z}_1 Z_1^{\left(\frac{p}{q}-1\right)} \tag{4.21}$$

By using the same procedure as in the synergetic approach, substituting equations (4.19) and (4.21) into equation (4.22) give the fast terminal synergetic control law (D_{FTSC}) expressed in equation (4.23).

$$T_s\dot{\Psi} + \Psi = 0; \qquad T_s > 0 \tag{4.22}$$

$$D_{FTSC} = 1 + \frac{L}{V_o}\left[C_{in}\left(\frac{\Psi}{T_s} + \alpha Z_2 + \beta\left(\frac{p}{q}\right)Z_2 Z_1^{\left(\frac{p}{q}-1\right)}\right) - \frac{V_{pv}}{L} + \dot{x}_{2ref}\right] \tag{4.23}$$

Under the control law determined in equation (4.23) with a nonlinear macro-variable (equation 4.19), the state variables Z_1 and Z_2 will reach zero and therefore the errors trajectory of the PV system will converge to the manifold $\Psi = 0$ in a finite time (equation 4.20) and so ensures the convergence to the MPP quickly in right direction.

4.2.3. Stability and robustness analysis

The control law must be designed to satisfy the stability condition. The stability and robustness issue of the controller are evaluated using the following Lyapunov function:

$$V = \frac{1}{2}\Psi^2 \tag{4.24}$$

Differentiating (4.24) leads to:

$$\dot{V} = \Psi\dot{\Psi} \tag{4.25}$$

Using (4.22) gives:

$$\dot{V} = \Psi\left(-\frac{1}{T_s}\Psi\right) = -\frac{1}{T_s}\Psi^2 \leq 0 \tag{4.26}$$

From equation (4.26), we make sure that $\dot{V} \leq 0$, which means the system's stability is guaranteed in all cases.

4.3. Simulation results and discussion

The PV system has been implemented in Matlab/Simulink^{MT} environment which includes a PV array, DC-DC boost converter controlled by the proposed FTS controller and a resistive load. To verify the effectiveness and the robustness of the proposed MPPT controller we studied the influence of atmospheric conditions on the one hand and the electric parameters on the other hand on the PV output power.

4.3.1. Influence of atmospheric conditions

Figure 4.2 shows the simulation results obtained by the developed FTSC against to that obtained by SC and the conventional P&O algorithm at STC (1000W/m², 298 K).

In a transient state, we can note from figure 4.2 (a) that the output power of all above mentioned methods converge to the MPP in the right direction but not at the same time. The developed controller ensures the finite time convergence and reaches the equilibrium point more quickly than the SC while the P&O algorithm requires more time before it stabilizes at the optimum. This is illustrated more by the fast convergence of the duty cycle to stabilize at the optimal value of the proposed technique compared to other techniques as shown in figure 4.2 (b). Moreover, the attached zoom in figure 4.2 (a) illustrates the output power of the PV system in a steady state for the three techniques. It's obvious that the oscillations appeared around the MPP using the P&O algorithm are almost eliminated using SC but without extracting the maximum energy and this is resulting from the asymptotic stability. While, the FTS controller is able to maintain the PV output power at the maximum and without oscillations around the MPP and this is due to the limited time convergence towards zero of the MV as shown in figure 4.3. All the obtained results have confirmed the good performance and the high effectiveness of the developed FTS controller in transient and steady states.
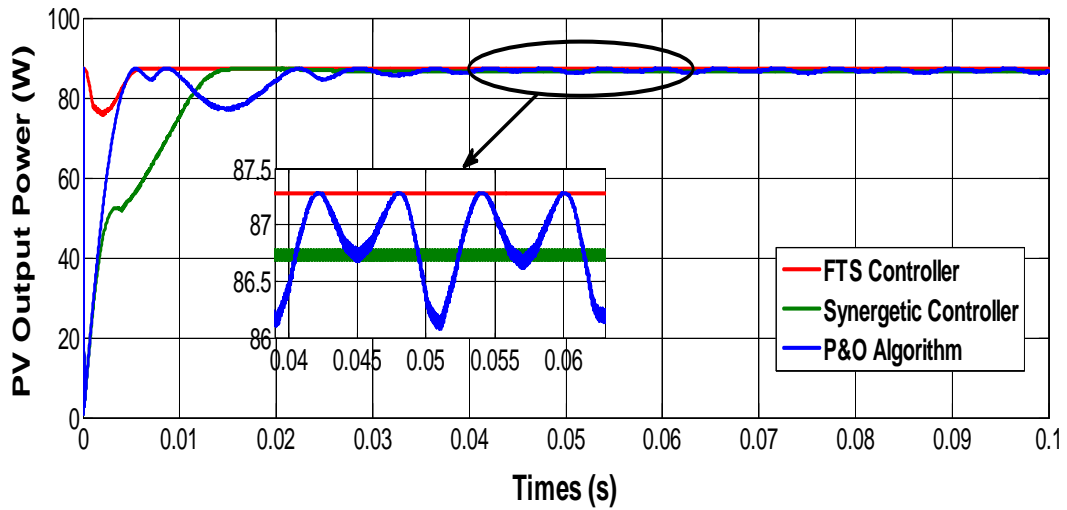
(a)
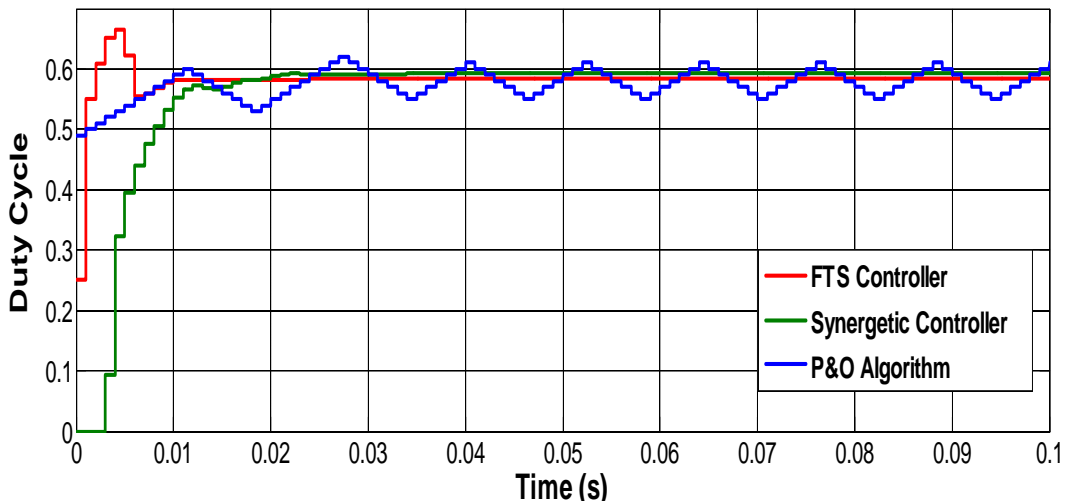
(b)

Fig.4.2. Simulation results of three MPPT controllers at STC (S=1000 W/m², T = 298 K)
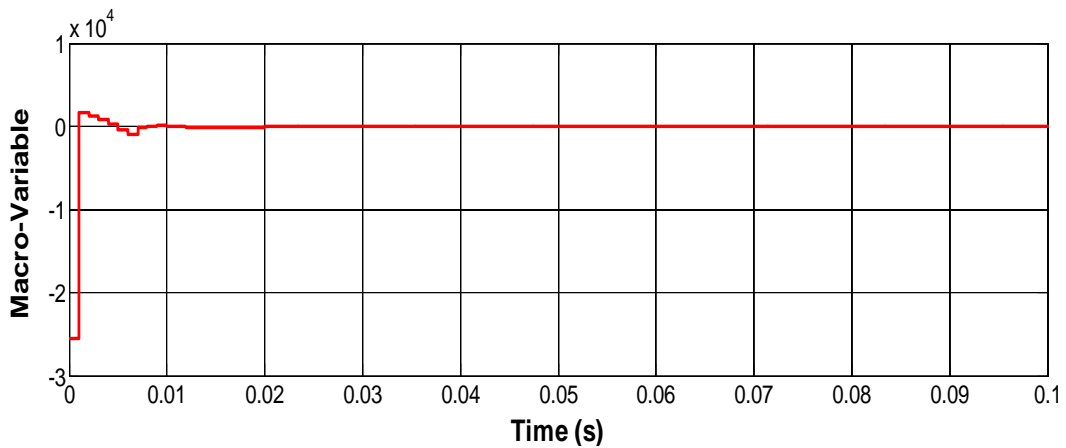
(a) PV Output power (P_{pv}), (b) Duty cycle (D).

Fig. 4.3. Convergence of the MV (Ψ) of the FTSC at STC (S=1000 W/m², T = 298 K)

In what follow, we will evaluate the strength of the proposed MPPT controller under a step change of irradiance and temperature.

As a first step, at a constant temperature equal to 298 K we applied irradiance equal to 500 W/m². Then, it is stepped up smoothly to 1000 W/m² after 0.2 s and finally it is stepped down to 650 W/m² at 0.35 s. The tracking results of this step change of the PV output power (P_{pv}), the output voltage (V_{out}), the PV voltage (V_{pv}) and the PV current (I_{pv}) are shown in figure 4.4. We can observe at different stages the fast convergence in the right direction to the maximum power without any disturbances of the developed controller under irradiance changes.
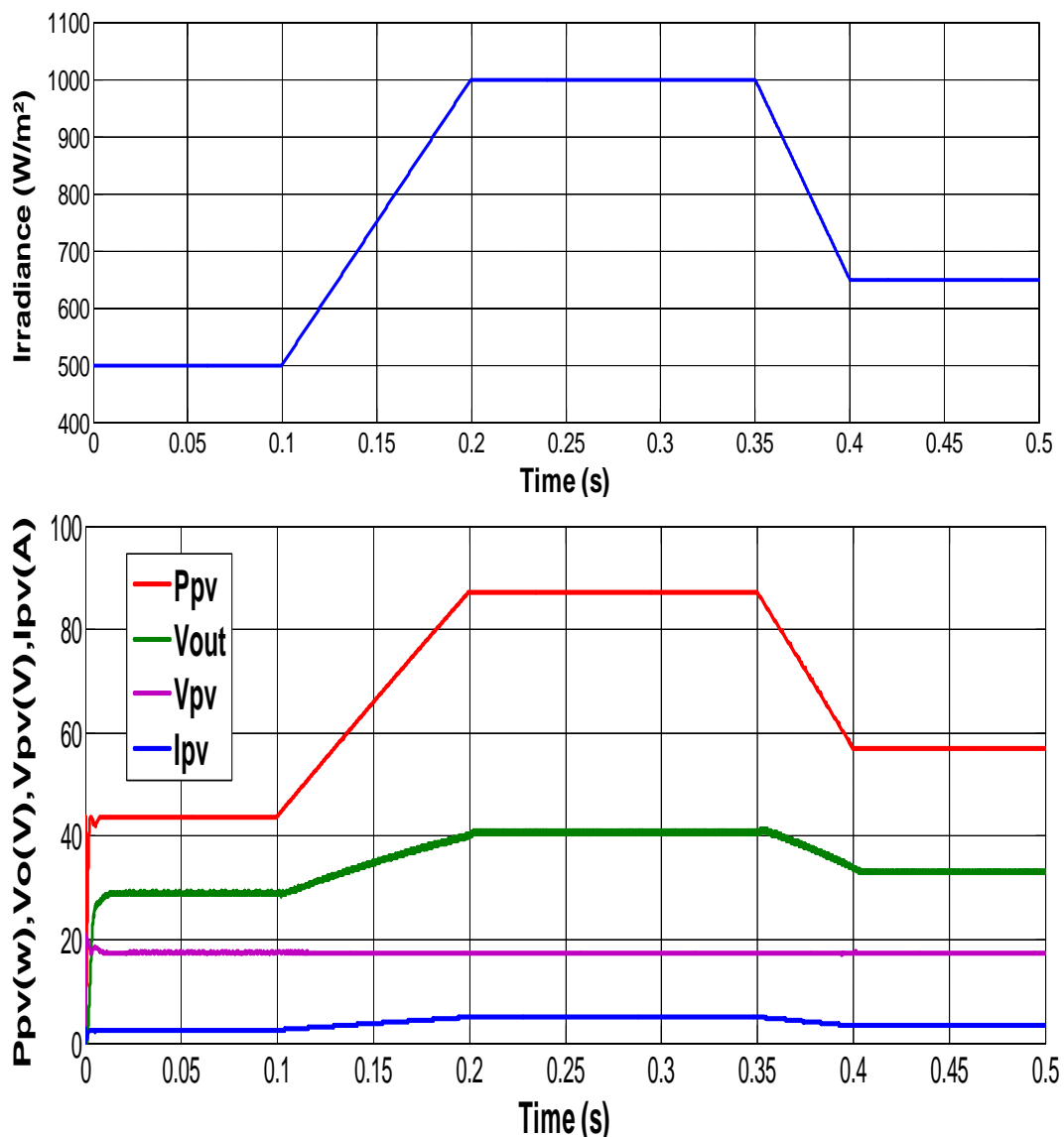

Fig. 4.4. Simulation results of FTS based MPPT controller during a trapezoidal irradiance profile at constant temperature (T=298 K).

95

Figure 4.5 shows simulation results of the PV output power (P_{pv}), the output voltage (V_{out}), the PV voltage (V_{pv}) and the PV current (I_{pv}) during a trapezoidal temperature profile using the proposed FTS controller. In this test, the temperature is suddenly decreased from 298 K to 288 K, and then increased from 288 K to 323 K at a constant irradiance equal to 1000 W/m².

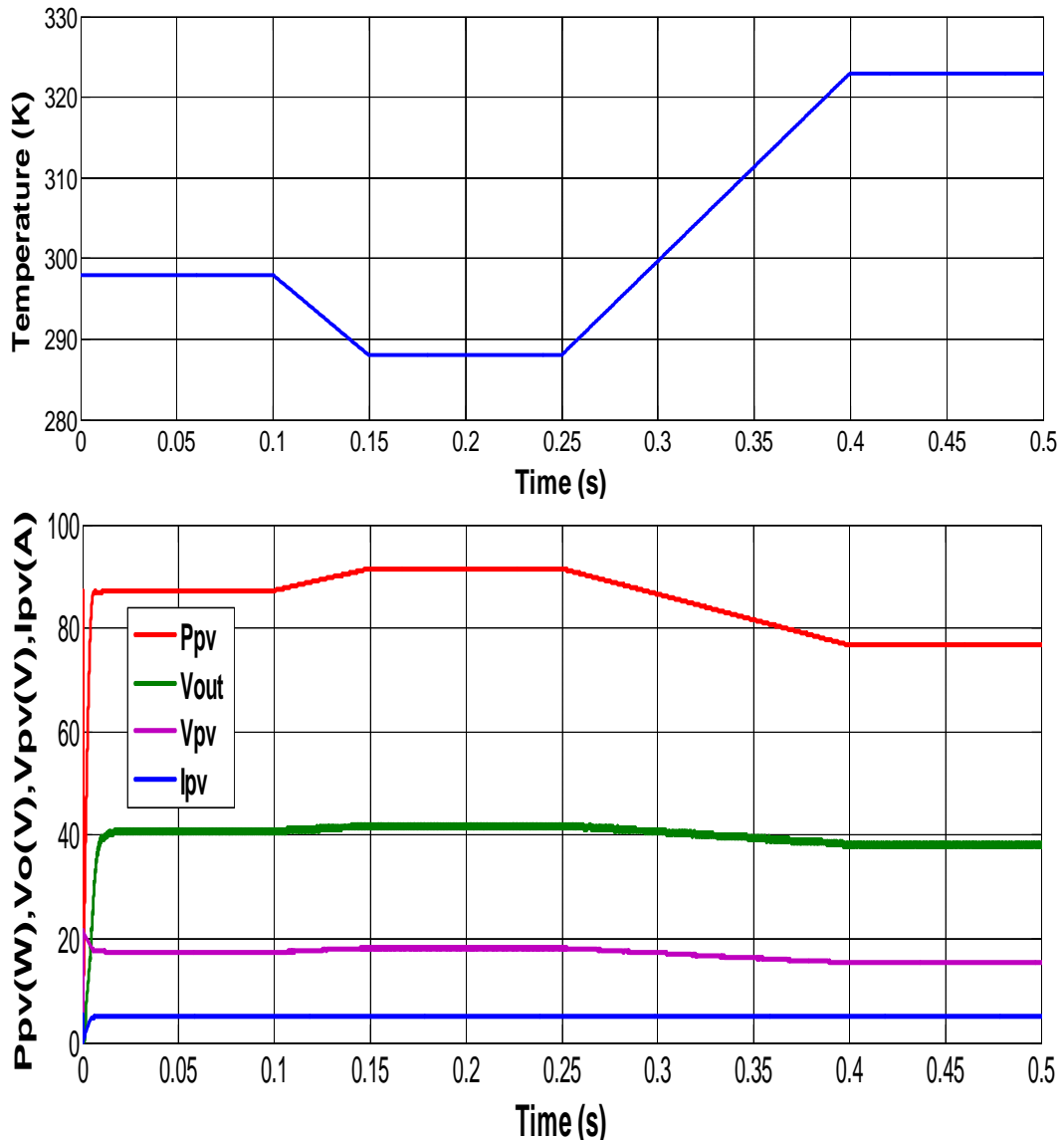**Fig. 4.5.** Simulation results during a trapezoidal temperature profile at constant irradiance (G=1000 W/m²).

All these results prove that the system's stability is successfully achieved after a very short transient and with no oscillations around the MPP what indicate the good robustness and the excellent efficiency of the FTS controller under atmospheric changes.

MPPT trajectory

In order to evaluate the tracking result, we plot the (P_{pv}-V_{pv}) curve obtained by the proposed FTS controller against that obtained by P&O algorithm on one side and synergetic controller on the other side under fast irradiance changing from 700 W/m² to 1000 W/m² then go back to 700 W/m² at a constant temperature equal to 298 K. From figure 4.6, we can see distinctly that the proposed technique follows the exact position of the MPP and therefore showcases a good performance by reducing the time convergence and eliminating the power perturbation compared to synergetic controller which takes relatively longer time before reaching the equilibrium point. Whereas the P&O technique tracks the MPP in the wrong direction before adjusting it and this results in important fluctuations.
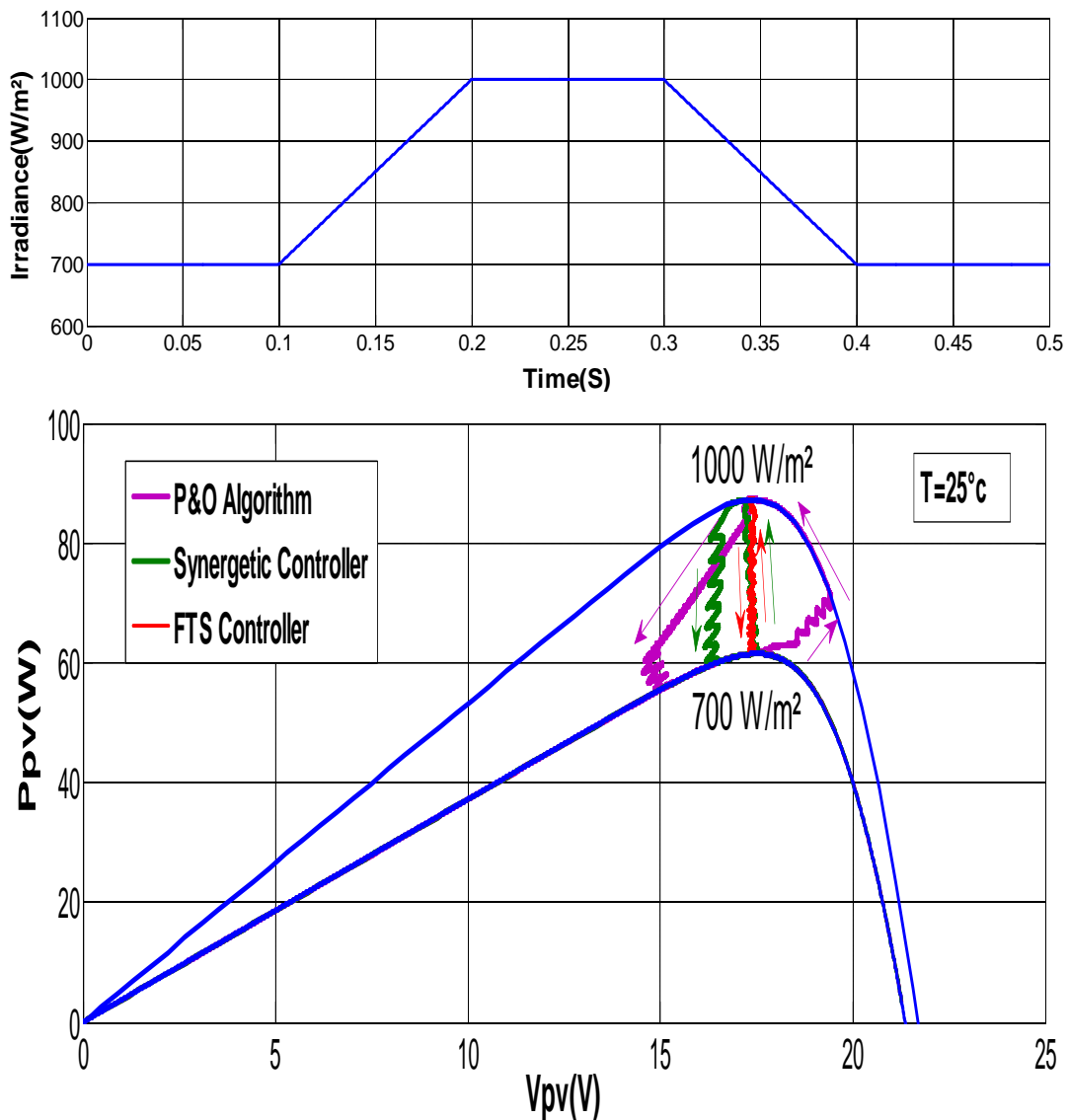

Fig. 4.6. MPPT trajectory under fast irradiance changing.

4.3.2. Influence of electric parameter

To further emphasize the good effectiveness of the proposed FTS controller we study the influence of the load variations on the PV output power at STC (1000W/m², 298 K). Figure 4.7 shows the simulation results of the PV output power and the duty cycle respectively under sudden resistance change from 25 Ω to 50 Ω, while figure 4.8 presents the same curves but under resistance change from 40 Ω to 20 Ω.

According to these results, we can say without slight doubt that the developed strategy based on the fast terminal synergetic theory is not very affected by the load variation. Indeed, we can see clearly that the controller is able to keep the PV output power at the optimum point despite the load variation, while the duty cycle convergence to the optimum value in record time.
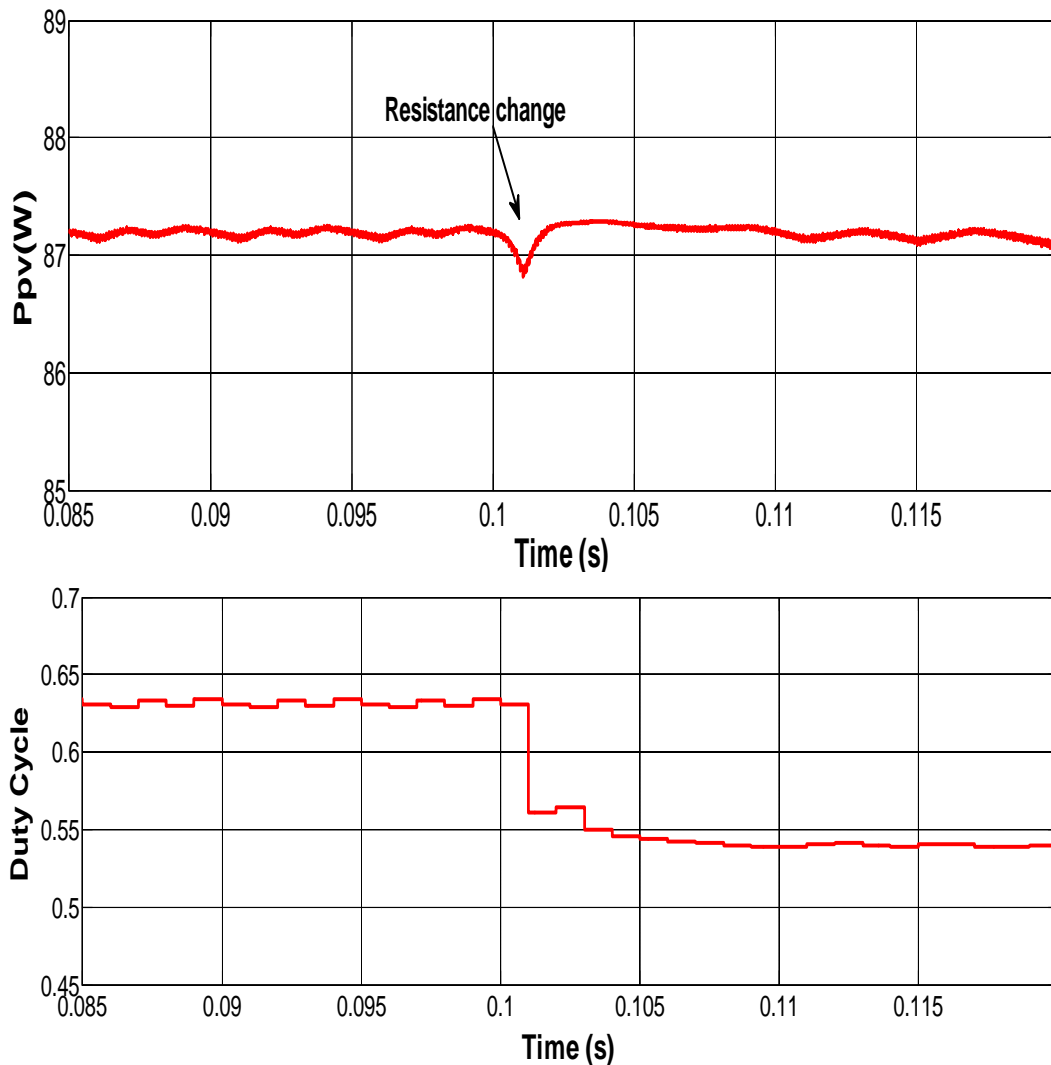

Fig. 4.7. Simulation results during a step increasing of resistance load from 25 Ω to 50 Ω.
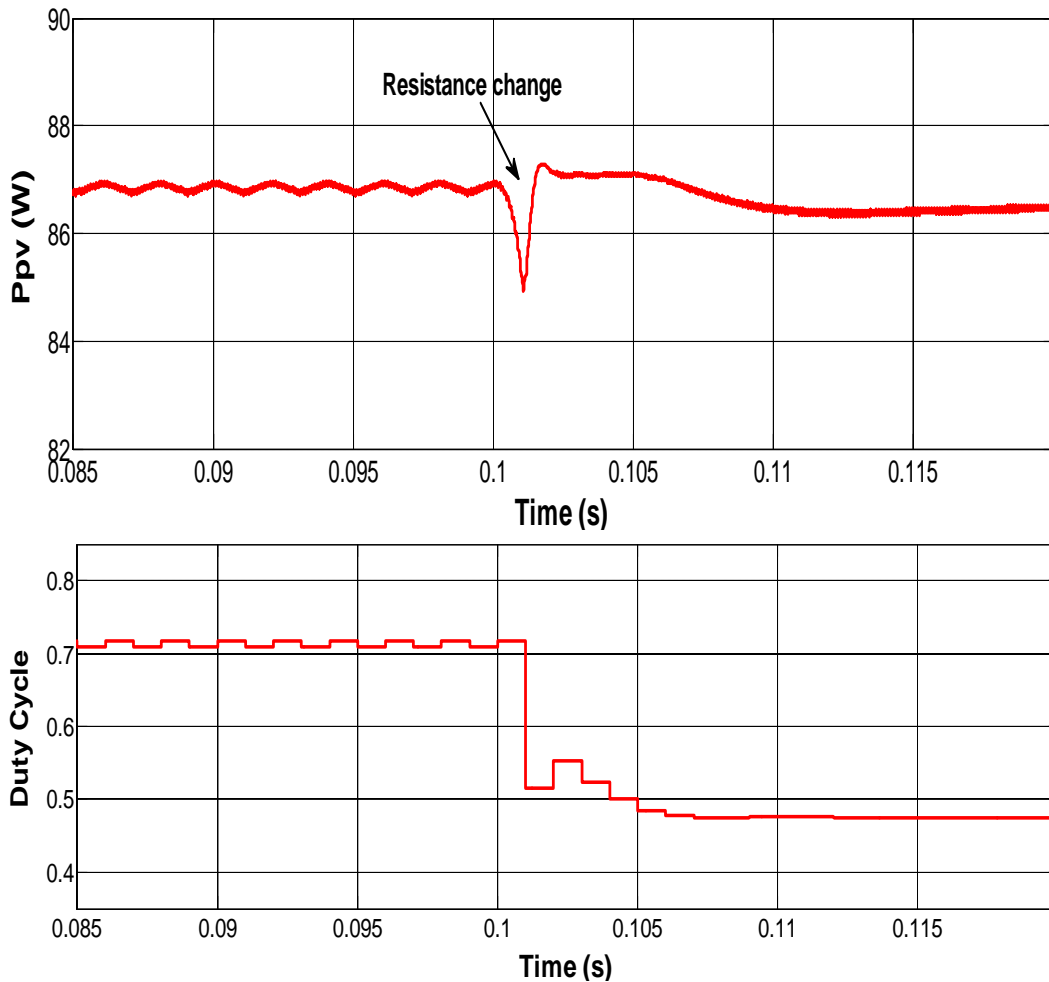
Fig. 4.8. Simulation results during a step decresing of resistance load from 40 Ω to 20 Ω.

4.3.3. Effect of errors on the control performance

The fast terminal synergetic-based MPPT control law of equation (4.23) depends on the selected values of parameters C_{in} and L of the circuit. In order to examine the effect of error in the value of both parameters, on the robustness and the performance of the proposed MPPT controller, simulation tests under standard conditions (Irradiance = 1000W/m², Temperature = 298 K) have proved that the developed MPPT controller keeps the same control performance in steady state even in case of error of ±10% (for C_{in}) and ±20% (for L).

As a first applied, the proposed strategy still maintaining strength and keep her performance until the estimation error on the input Capacity C_{in} reach to (+10%) and (-10%). Starting from this interval, we note that the FTSC technique features beginning to retreat which is mainly represented in moving away little bit on the MPP, which causes a loss of energy as shown in Fig. 4.9.

99
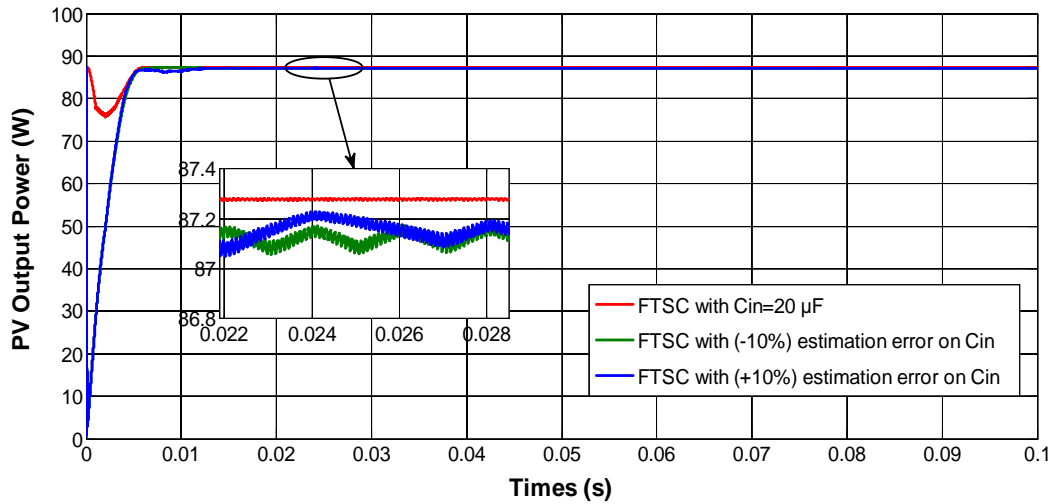
Fig. 4.9. Effect of input capacitance error C_{in} on the control performance.
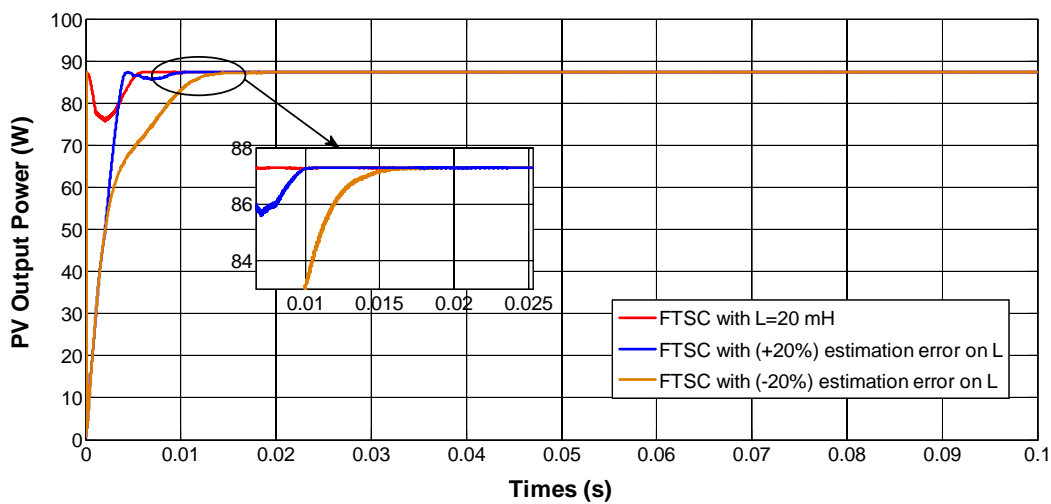
Fig. 4.10. Effect of Inductance error L on the control performance.

In the second application, we applied an estimation error reach to ($\pm 20\%$) on the inductance L. The simulation results obtained using Matlab/Simulink^{MT} confirm the good performance and the high robustness until this rang. From (20%), loss of energy appeared in transient state with delay in response time but the FTSC strategy was able to maintain the maximum power in steady state as shown in Fig. 4.10.

4.4. Summary

This work presents a new controller to track the MPP based on fast terminal synergetic theory for a standalone PV system which includes PV generator, DC–DC boost converter and a resistive load. The effectiveness and the robustness of the proposed MPPT controller were confirmed by simulation using Matlab/Simulink ^{MT} tools not only under atmospheric

100

conditions change but also under load resistance change. The good performance is proved in both transient and steady states. The proposed controller has successfully guaranteed the finite time convergence to reach the MPP in the right direction and almost with no oscillations compared to the conventional P&O algorithm that caused a significant energy loss. At the same time, the synergetic controller succeeded in recovering a part of the energy lost but not as the same quality and power provided by the FTS controller. Moreover, the developed controller has confirmed the high efficiency and the strong robustness under non uniform weather conditions or under resistance change as illustrated by simulation results obtained.

References

[4.1].   Zerroug, N., Harmas, M.N., Benaggoune, S., Bouchama, Z., Zehar, K., 2018. "DSP-based implementation of fast terminal synergetic control for a DC–DC Buck converter". Journal of the Franklin Institute 355, pp. 2329–2343.

[4.2].   Bouchama Z., Harmas M. N., Zehar K., 2019. Finite time nonlinear control for DC-DC converters. Soft computing and electrical engineering, vol.1, pp. 36-45.

[4.3].   Santi, E., Monti, A., Donghong, L., Proddutur, K., Dougal, A. 2003. Synergetic control for DC–DC boost converter: implementation options. IEEE Transaction on industry applications. Vol.39, pp. 1803–1813.

[4.4].   Jiang, Z., Dougal, R.A., 2004. Synergetic control of power converters for pulse current charging of advanced batteries from a fuel cell power source. IEEE Transaction in Power Electron. VOL. 19, pp. 1140–1150.

[4.5].   Hachana, A., Harmas, M.N., 2018. Synergetic and Higher Order Sliding Mode Control of Blood Glucose Regulation in Diabetes Patients. Vol. 140.

[4.6].   Attoui, H., Khaber, F., Melhaoui, M., Kassmi, K., Essounbouli, N., 2016. Development and experimentation of a new MPPT synergetic control for photovoltaic systems. Journal of Optoelectronics and Advanced Materials. Vol. 18, pp.165-173.

[4.7].   Mars, N., Grouz1, F., Essounbouli, N., Sbita, L., 2017. Synergetic MPPT Controller for Photovoltaic System. Journal of Electrical & Electronic Systems. Vol. 6.

General conclusion

Among different renewable energy resources, photovoltaic energy has found increased attention and wide attraction from researchers in many applications, for its capabilities of direct electric energy conversion without any environmental damage, ease of implementation, flexibility in size and low operation cost.

However, the non-linear behavior of the PV arrays and their dependency on weather changes show the importance of using an adaptation stage to ensuring the transfer of the power available delivered by the PV generator to the load. Generating the converter duty ratio directly considered the simplest and the cheapest control scheme however the PVG in this case is badly exploited, the power extracted from PVG is often very far from the maximum power that the PVG can delivered. In order to control the operating point and minimize the difference between the maximum available power and the power actually recovered under atmospheric conditions changes or load variation, PV maximum power point tracking (MPPT) is mandatory to enhance PV system efficiency. The MPPT technique's performance and implementation complexity differs from one to another.

The aim of this thesis is to design a high efficiency PV system configuration. This configuration includes PV generator, DC–DC boost converter controlled by a maximum power point tracking technique (MPPT) and a resistive load. To achieve this objective, two new robust control strategies have been developed.

In the first strategy, a nonlinear tracking technique based on Synergetic Control theory to track the maximum power point (MPP) of a stand-alone PV system under different atmospheric conditions is proposed and implemented in order to eliminate the effect of the chattering drawback provided by sliding mode controller, The developed MPPT controller was tested both in simulations using Matlab/Simulink^{MT} tool, and experimentally, using a dSPACE based experimental test bench. The obtained simulation results prove the good performance and the high robustness in transient and steady state of the proposed controller under different temperature and solar irradiance, not only regarding to the fast and accurate tracking but also regarding to the oscillations around the MPP. These features are confirmed by experimental results obtained using dSPACE RTI 1104 real-time platform. In fact, various atmospheric conditions are tested to prove the high efficiency of the proposed synergetic

MPPT controller. The EN 50530 standard test was used with different ramp gradients values from the slow to the very fast to calculate the MPPT efficiency under irradiance changes. The simulation results ensure the system stability at the maximum power.

In the second strategy, a new non-linear controller to track the MPP based on Fast Terminal Synergetic (FTS) approach for a standalone PV system is proposed. The effectiveness and the robustness of the proposed MPPT controller were confirmed by simulation using Matlab/Simulink^{MT} tools not only under atmospheric conditions changes but also under load resistance changes. The good performance is proved in both transient and steady states, the proposed controller has successfully guaranteed the finite time convergence to reach the MPP in the right direction and reduce the steady state error as much as possible. Moreover, the developed controller has confirmed the high efficiency and the strong robustness under non uniform weather conditions or under resistance change.

The work performed in this thesis addresses some challenges related to maximum power point tracking for stand-alone PV system under atmospheric conditions changes. Regarding the continuation of this work, Suggestions for future research as follows:

- ✓ The MPPT technique based on Fast Terminal Synergetic theory was confirmed only by simulation using Matlab/Simulink^{MT} tools, we seek in future to the practical validation on an experimental test bench.

- ✓ The proposed system was tested as a stand-alone connection. Therefore, there is a possibility to investigate the configuration for a grid-connected system.

- ✓ Applied the proposed MPPT techniques to the wind power system or hybrid system.

- ✓ During partial shading case, there is possibility to have multiple local maxima, but overall there is still only one global MPP. The suggested MPPT techniques should be tested under these conditions.

Scientific production

Journal papers:

1. **AYAT Rahma**, BOUAFI Abdelouahab and Gaubert Jean-Paul: '' Experimental validation of synergetic approach based MPPT controller for an autonomous PV system'', **IET Renewable Power Generation**. Vol. 15, I. 07, pp. 1515-1527. https://doi.org/10.1049/rpg2.12130.

2. **AYAT Rahma**, BOUAFI Abdelouahab and Gaubert Jean-Paul: '' Fast Terminal Synergetic Control for Maximum Power Point Tracking of Stand-Alone Photovoltaic System'', under reviewing.

International conferences papers:

1. **AYAT Rahma** and BOUAFI Abdelouahab: ''Design of Robust Synergetic MPPT Controller For PV Systems Using SimPower '', **International Conference on Nanomaterials and Renewable Energies (ICNRE 2018)**, 15th -17th October 2018. Skikda, Algeria.

2. **AYAT Rahma** and BOUAFI Abdelouahab: ''Novel Synergetic MPPT Controller For Stand-alone Photovoltaic Systems'', **International Conference on Electronics and Electrical Engineering (IC3E'18)**, 12th-13th November 2018, University of Bouira, Algeria.

The Institution of Engineering and Technology WILEY

ORIGINAL RESEARCH PAPER

Experimental validation of synergetic approach based MPPT controller for an autonomous PV system

Rahma Ayat[1,2] | **Abdelouahab Bouafia**[1] | **Jean-Paul Gaubert**[2]

[1] Laboratoire Qualité d'Energie dans les Réseaux Electriques (QUERE), Université de Ferhat Abbas, Setif, Algeria

[2] Laboratoire d'Informatique et d'Automatique pour les Systèmes, LIAS-ENSIP, Université de Poitiers, Bat B25, Poitiers Cedex 9, France

Correspondence

Jean-Paul Gaubert, Laboratoire d'Informatique et d'Automatique pour les Systèmes, LIAS-ENSIP, Université de Poitiers, Bat B25, Poitiers Cedex 9, France.
Email: jean.paul.gaubert@univ-poitiers.fr

Abstract

A novel nonlinear maximum power point tracking (MPPT) controller for autonomous photovoltaic systems based on synergetic control theory is presented in this paper as a solution to eliminate the chattering drawback provided by sliding mode controller, where the proposed strategy allows to generate continuous control law instead of a switching term. A DC/DC boost converter is introduced in the content of this work as an interface between a photovoltaic array and a resistive load. The developed MPPT controller was tested both in simulations using Matlab/Simulink tool and experimentally using dSPACE RTI 1104 real-time platform and compared with the sliding mode-based MPPT controller. Furthermore, the EN 50530 standard test with different ramp gradients values is used to calculate the MPPT efficiency under irradiance changes from the slow to the very fast. Illustrative results that prove the effectiveness and the robustness of the proposed MPPT controller even the non-uniform conditions (temperatures and solar irradiances) are presented here. The fast response and the accurate tracking to the maximum power point (MPP) with considerable reduction in the oscillations are successfully reached with the developed controller which is much better than sliding mode controller.

1 | INTRODUCTION

The huge restriction of fossil fuels on human development and the ever-increasing energy demand in every sphere have resulted to its depletion without forgetting the serious problems on the environment. To break these drawbacks, research and development of new energy has sparked wide interest worldwide.

Over the past few decades, renewable energy sources are considered to be a perfect choice to generating sustainable, abundant, inexhaustible energy and even more environmentally friendly. Among the various types of renewable energy sources is solar energy, or more popularly known as photovoltaic (PV) energy which has attracted a lot of interest with many important applications expanding continuously from lighting systems [1] to pumping systems [2].

Many people probably wonder: if solar energy is so beneficial, why do not we consume it more? The answer to this question is the unbalance between the high installation cost and the low energy conversion of PV array which varies according to irradiation and temperature during its operation. Thus, because of

these limitations, we should extract the maximum power and enhance the PV system's efficiency despite all these climatic variations. This challenge can be achieved by the wise choice of maximum power point tracker (MPPT) which determines the optimal functioning of the PV systems.

A large number of MPPT control algorithms have been developed for several years which drive the PV array to the peak of the power against environment changes. Each MPPT technique has its own advantages and disadvantages. These control techniques could be classified into two categories namely the conventional methods and intelligent methods.

Among conventional MPPT mentioned in the literature, perturbation and observation (P&O), incremental conductance (IC) and the hill climbing (HC), are the most widely used since they are simple and easy to implement. The P&O algorithm consists of disturbing the PV output voltage and observing the PV output power to determine the peak power direction [3–5]. The IC method compares between the instantaneous conductance (I/V) of PV array and the incremental conductance (dI/dV) to track MPP [4,6,7]. The HC technique locates

the MPP by relating changes in the power output to changes in duty ratio of the converter. Mathematically, the MPP is achieved when dP/dD is forced to be zero, where D represent the duty ratio [6,8].

However, these techniques have some disadvantages. The major of them is the power oscillation around MPP and the confusion in the direction of tracking caused by rapidly changing in atmospheric conditions [3,9]. Moreover, these commands vary in speed of convergence, cost and efficiency.

In order to overcome the above-mentioned drawbacks, a large number of intelligent control techniques have attracted a lot of interest over the past years such as fuzzy logic controller [10], artificial neural-network [11] and meta-heuristic techniques which are used for the global search under partial shading conditions like genetic algorithm (GA) [12], particle swarm optimization (PSO) [13], artificial bee colony (ABC) [14] and ant colony optimization (ACO) [15]. Despite of their effectiveness, these techniques are more complex and require huge knowledge in the design of the control system.

Recently, sliding mode control (SMC) is considered to be a powerful technique because of its fast convergence and high robustness [16,17]. On the other hand, its major flaw is a chattering phenomenon which induces many undesirable oscillations in control signal which may lead the system into instability [18–20].

All these difficulties inspired from the above study in particular, oscillation behaviour, robustness and speed of the MPPT in tracking the optimal power, have guided to move to improve the performance of the PV system. To achieve this objective, one of the most promising robust control strategy named synergetic control (SC) is suggested [21,22]. The synergetic control depends on the same invariance property of systems found in SMC, but without its chattering drawback because it provides a continuous control law unlike the conventional SMC which combines two terms, one ensures the attractiveness of the system states to the sliding surface while the other one maintains the operating point on sliding surface and displace it to the origin, this sudden change leads to the chattering phenomena. This theory has initially been successfully applied in power electronics control [23,24], in battery charging system [25], then recently in control of the epidemic system [26,27] and in the control of wind turbine system [28].

This paper proposes a new strategy based on synergetic control theory to track the MPP for stand-alone photovoltaic system under different atmospheric conditions. The main goal of the proposed MPPT controller is to ensure the system stability at the maximum power, good robustness and fast dynamic response simultaneously. The design of the synergetic MPPT controller is explained and mathematically described in the paper. The developed MPPT controller was tested both in simulations using Matlab/Simulink tool and experimentally using a dSPACE based experimental test bench, the MPPT efficiency is calculated using the EN 50530 standard test and illustrative results are presented here. It is shown via simulation and experimental results that the developed MPPT controller ensures an excellent transient and steady state performance without oscillations around the MPP, reduces greatly the tracking time in the
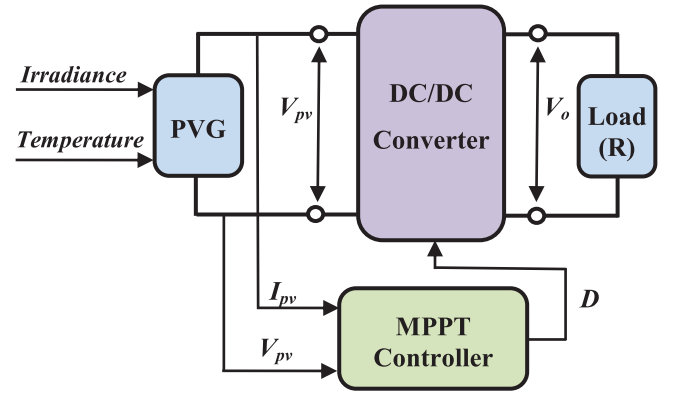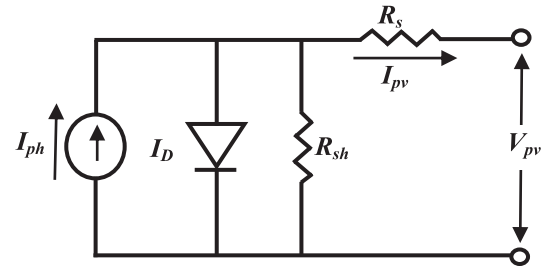

FIGURE 1   Block diagram of the photovoltaic system

FIGURE 2   Equivalent circuit of solar cell

right direction and moreover the high efficiency under atmospheric changes unlike other techniques.

2 | PHOTOVOLTAIC SYSTEM DESCRIPTION

The configuration of the proposed system consists of PV array, a DC–DC boost converter, a resistive load and a nonlinear MPPT controller as shown in Figure 1.

In order to extract the maximum power from the PV module regardless weather changes, a MPPT algorithm is used to adjust the duty cycle of the boost converter by continuously opening and closing the switch. This topology can be extended to a grid connected system through an inverter.

2.1 | Photovoltaic panel modelling

When the surface of the PV cell (the basic units in the structure of a PV module) is exposed to light it absorbs light energy and converts it into electrical energy [29]. Since the power generated by a solar cell is very small, they have to be compiled in series or parallel to produce enough amount of electrical power whether for industry or domestic use [30].

In this paper we use the single diode model proposed in references [30,31]. Its equivalent circuit consists of a current source in parallel with one diode, and two resistances, one in series and other in parallel as shown in Figure 2. According to this scheme,

FIGURE 3 Influence of irradiation on P–V curves
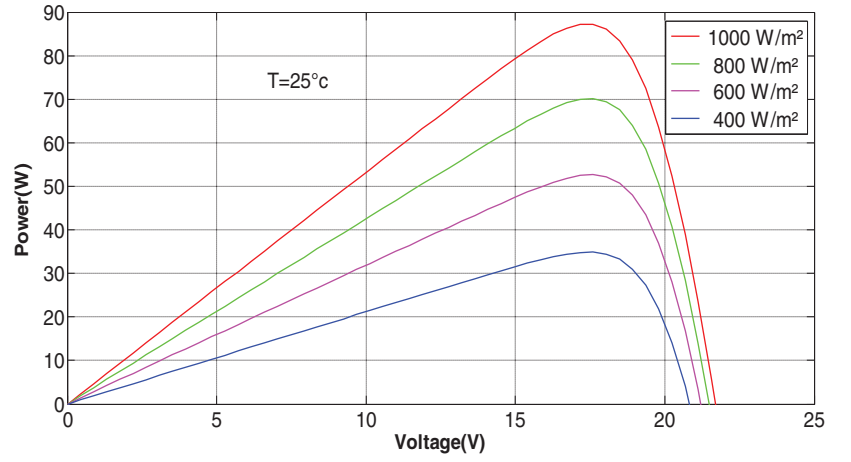
FIGURE 4 Influence of temperature on P–V curves
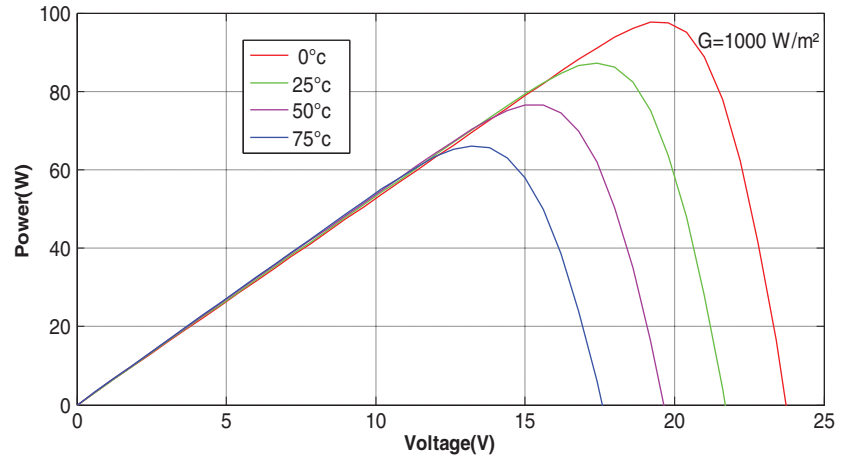
the mathematical model for the I-V characteristic is given by:

$$I_{pv} = I_{ph} - I_0 \underbrace{\left[\exp\left(\frac{q\left(V_{pv} + I_{pv}R_S\right)}{AKT} \right) - 1 \right]}_{I_d} - \frac{V_{pv} + I_{pv}R_S}{R_{sh}}$$

(1)

where I_{pv} is the PV output current, V_{pv} is the PV output voltage, R_{sh} is the shunt resistance and R_s is the series resistance. I_0 is the saturation current of the diode which depends on temperature T (in Kelvin) given as follows:

$$I_0 = I_{0r} \left(\frac{T}{T_r} \right)^3 \exp\left(\left[\frac{qE_g}{K_b A} \right] * \left[\left(\frac{1}{T_r} \right) - \left(\frac{1}{T} \right) \right] \right)$$

(2)

A is the diode ideality factor, k_b is Boltzmann's constant, E_g is the band gap energy, I_{or} is the saturation current at the reference temperature (T_r), I_{scr} is the short-circuit current of PV cell under standard conditions and I_{ph} is the photogenerated current, depends on solar irradiance E (W/m²), often given by:

$$I_{ph} = \frac{E}{E_r} \left[I_{scr} + K_i \left(T - T_r \right) \right]$$

(3)

This equation show clearly that the generated power of the PV module is strongly influenced by irradiance and temperature. So, it is necessary to study how these two climatic parameters will affect at the characteristics of the cell by drawing the curve of power (P) versus voltage (V) for various irradiations at constant temperature (Figure 3), and for different temperatures at constant irradiance (Figure 4). It is obvious that the maximum power increases with irradiance increasing or temperature decreasing.

The PV panel used for simulations is Kyocera KC85T consists of 36 solar cells connected in series to give a maximum output power of 87 W. Its electrical characteristics at standard test conditions (1000 W/m² and $T = 25°C$) are given in Table 1.

TABLE 1 Electrical characteristics of Kyocera KC85T PV module

Description	Kyocera KC85T
Maximum power (P_{max})	87 W
Open-circuit voltage (V_{oc})	21.7 V
Short-circuit current (I_{sc})	5.34 A
Optimum operating voltage (V_{mpp})	17.4 V
Optimum operating current (I_{mpp})	5.02 A

FIGURE 5 DC–DC boost converter circuit

FIGURE 6 Simulink block diagram of sliding mode controller
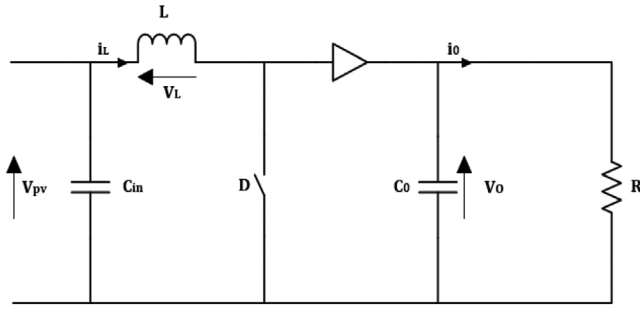
2.2 | DC–DC boost converter modelling

The most usual technique to extract the maximum power at any time is to use an adaptation stage between the PV array and the load. The use of DC–DC boost converter as an interface between the two elements enables the step up of the input voltage V_{pv} to the desired output voltage V_o [32]. The circuit of the DC–DC boost converter is shown in Figure 5.

The dynamic model of the DC–DC boost converter used in this paper can be described by the Equations (4). Where $D \in [0 \ 1]$ is the duty ratio, which is also the control law.

$$\frac{di_L}{dt} = -(1-D)\frac{V_o}{L} + \frac{V_{pv}}{L} \tag{4a}$$

$$\frac{dV_o}{dt} = (1-D)\frac{i_L}{C} - \frac{V_o}{RC} \tag{4b}$$

3 | SLIDING MODE BASED MPPT CONTROLLER

SMC is considered as one of the most well-known nonlinear control techniques where its design involves two basic steps. Firstly, determine the sliding surface that ensures the convergence property towards the desired values. Secondly, establish the control law that forces the system trajectory to reach and stay within the chosen sliding surface [33].

The MPP of the PV system is achieved when the following equality is satisfied:

$$\frac{dP_{pv}}{dI_{pv}} = \frac{dI_{pv}V_{pv}}{dI_{pv}} = V_{pv} + I_{pv}\frac{dV_{pv}}{dI_{pv}} = 0 \tag{5}$$

Accordingly, the sliding surface can be chosen as:

$$S = V_{pv} + I_{pv}\frac{dV_{pv}}{dI_{pv}} \tag{6}$$

If $S > 0$, so $(dP_{pv}/dI_{pv}) > 0$ which means that the operating point is to the right of the MPP.

If $S < 0$, so $(dP_{pv}/dI_{pv}) < 0$ which means that the operating point is to the left of the MPP.
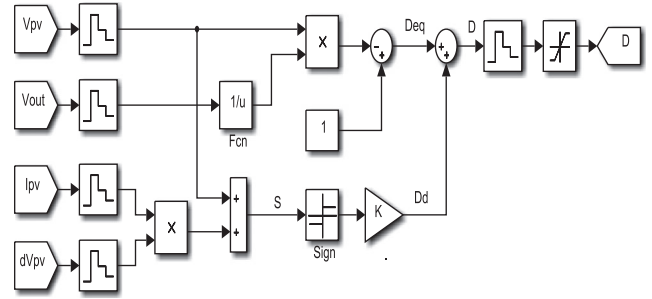
Let be the positive definite quadratic Lyapunov function $V_L = \frac{1}{2}S^2$. In order to ensure the attractiveness of the surface $S = 0$ over the entire operating range; it is enough that the time derivative of V_L must be negative.

$$\dot{V}_L = S * \dot{S} < 0 \tag{7}$$

Where the surface derivative is given by:

$$\dot{S} = \frac{dS}{dt} = \left[\frac{dS}{dx}\right]^T \dot{x} \tag{8}$$

The general control law D consists of two parts, the discrete control D_d and the equivalent control D_{eq}.

$$D = D_d + D_{eq} \tag{9}$$

The discrete control D_d, is determined to ensure the attractiveness to the sliding surface and is defined as follows:

$$D_d = K * \text{sgn}(S) \tag{10}$$

where K is a positive constant.

The equivalent control D_{eq}, serves to maintain the operation point on the sliding surface and displace it towards the origin, it is defined as follows:

$$D_{eq} = 1 - \frac{V_{pv}}{V_o} \tag{11}$$

So, the overall control law D has the expression mentioned in the following Equation ((12), where the corresponding block diagram is shown in Figure 6.

$$D = K * \text{sgn}(S) + 1 - \frac{V_{pv}}{V_o} \tag{12}$$

As the control law generated by the SMC combines two terms, it is not continuous. This sudden change or switching in the control law leads to the chattering phenomena [34–37]. To break this drawback, we propose in the next section the adoption of a new strategy to track the MPP depends on the same invariance property of systems found in SMC but provides

a continuous control law instead of a switching term in order to either reduce or eliminate the chattering phenomenon.

4 | SYNERGETIC BASED MPPT CONTROLLER

Synergetic control theory was first developed and introduced in general terms by Prof. Anatoly Klesnikov and his team [21]. The design of SC is very similar to that of the SMC; the main advantage of this command is the elimination of chattering problem.

4.1 | Synergetic control theory

Let us consider the system to be controlled is described by a non-linear differential equation of this form:

$$\frac{dx}{dt} = f(x, D, t) \tag{13}$$

where x represents the system state vector, D the control input vector and f a continuous differentiable nonlinear function.

Synergetic controller design starts by selecting a macro-variable (MV): $\Psi(x, t)$ as function of the system state variables according to performance and control specifications [19, 21]. This controller will force the system trajectory approaching exponentially to the manifold.

$$\Psi = 0 \tag{14}$$

Once the trajectory reaches the desired manifold, the synergetic controller will keep it there. The desired dynamic evolution of the MV is chosen such as Equation (15):

$$T_S \left(\frac{d\Psi}{dt} \right) + \Psi = 0; \ T_S > 0 \tag{15}$$

where T_s is a positive value which will affect smoothly at the convergence speed of the system to the desired equilibrium point. Differentiating the macro-variable along Equation (13) leads to Equation (16):

$$\frac{d\Psi}{dt} = \left(\frac{d\Psi}{dx} \right) \left(\frac{dx}{dt} \right) \tag{16}$$

By combining Equations (13), (15), and (16) we get:

$$T_S \left(\frac{d\Psi}{dx} \right) f(x, D, t) + \Psi = 0 \tag{17}$$

Finally, when solving Equation (17), we can describe the control law as follows:

$$D = g(x, t, \Psi(x, t), T_S) \tag{18}$$

It is obvious from Equation ((18), that the control output depends not only on the system state variables (x, t), but also on the adequate selection of the MV and time constant T_s to ensure the system stability and the good transient and steady state performances.

4.2 | Synergetic MPPT controller design

In what follows, we applied the concept of the SC explained above for the MPPT controller design. To apply this strategy we start by selecting a MV. This selection is based on the output power of the cell as follows:

$$\Psi(x, t) = \frac{dP_{pv}}{dI_{pv}} \tag{19}$$

Hence, the manifold is defined as:

$$\Psi = \frac{dP_{pv}}{dI_{pv}} = \frac{dI_{pv} V_{pv}}{dI_{pv}} = V_{pv} + I_{pv} \frac{dV_{pv}}{dI_{pv}} = 0 \tag{20}$$

By applying Equation (16) we find:

$$\frac{d\Psi}{dt} = \left(\frac{d\Psi}{dI_{pv}} \right) \left(\frac{dI_{pv}}{dt} \right) \tag{21}$$

Compensating Equation (21) in Equation (15) give us:

$$T_S \left[\left(\frac{d\Psi}{dI_{pv}} \right) \left(\frac{dI_{pv}}{dt} \right) \right] + \Psi = 0 \tag{22}$$

Where:

$$\frac{d\Psi}{dI_{pv}} = 2 \frac{dV_{pv}}{dI_{pv}} + I_{pv} \frac{d^2 V_{pv}}{dI_{pv}^2} \tag{23}$$

$$\frac{dI_{pv}}{dt} = -(1 - D) \frac{V_o}{L} + \frac{V_{pv}}{L} \tag{24}$$

The substitution of Equations (23) and (24) into the Equation (22) gives the control law equation described in (25):

$$D(t) = 1 - \frac{\Psi L}{V_o T_S \left(2 \frac{dV_{pv}}{dI_{pv}} + I_{pv} \frac{d^2 V_{pv}}{dI_{pv}^2} \right)} - \frac{V_{pv}}{V_o} \tag{25}$$

From Equation (25), we see that the control law generated by the synergetic approach is continuous instead of a switching term by thus the chattering phenomenon can be either reduced or eliminated.

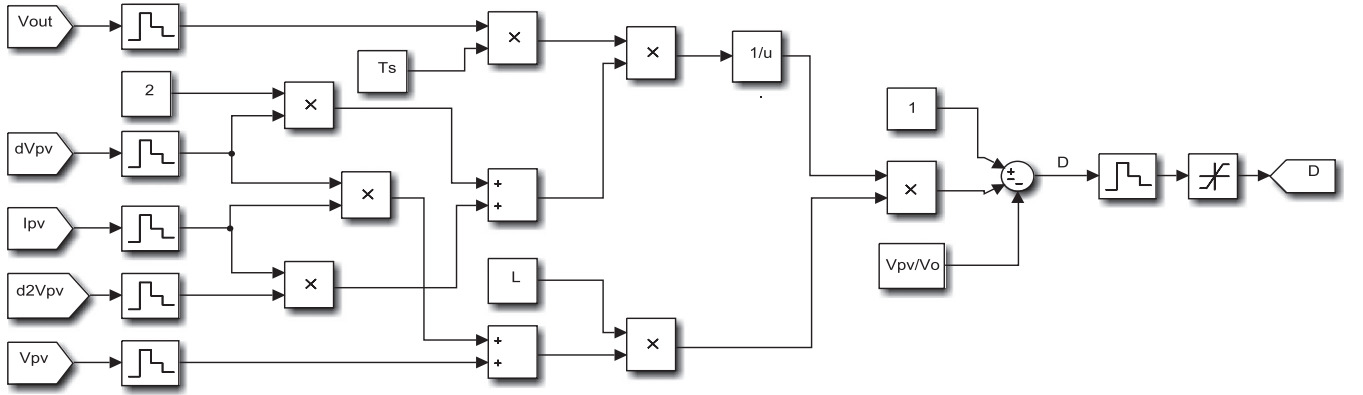The block diagram of the proposed synergetic strategy is given in Figure 7.

FIGURE 7 Simulink block diagram of synergetic controller

4.3 | Stability proof

The system stability is ensured using the Lyapunov's theory. Let the Lyapunov's function be defined positive as follows:

$$V_L = \frac{1}{2}\, \Psi^2 \; > 0 \tag{26}$$

We say that the system is stable if the derivative of the Lyapunov's function is less than zero. The derivative of V_L is given by:

$$\frac{dV_L}{dt} = \; \Psi\left(\frac{d\Psi}{dt}\right) = \; \Psi\left[\left(-\frac{1}{T_s}\right)\Psi\right] = \; \left(-\frac{1}{T_s}\right)\Psi^2 \le 0 \tag{27}$$

According to Equation (27), the derivative of the Lyapunov's function is always negative, which ensures system stability.

5 | RESULTS AND DISCUSSION

In order to evaluate the effectiveness of the proposed synergetic controller, the model of the PV system, shown in Figure 1, has been first implemented in Matlab/Simulink environment for simulation. Next, the proposed MPPT controller is implemented in dSPACE RTI 1104 real-time platform and several tests were performed on an experimental test bench to confirm the simulation results obtained.

5.1 | Simulation results

To verify the performance of the proposed MPPT controller, the PV model system has been designed in Matlab/Simulink as shown in Figure 8. It includes the PV array, the DC–DC boost converter controlled by the proposed MPPT controller and a resistive load. The PV modules specifications and the system specifications used in the simulation are shown in Table 1 and Table 2 respectively.

TABLE 2 System specifications

Description	DC–DC boost converter
Capacity C_{in}	200 μF
Capacity C_o	20 μF
Inductance L	15e-3 mH
Resistive load R	25 Ω
Switching frequency	10 kHz

The simulation results obtained by the developed controller are compared to that obtained by sliding mode controller at Standard Climatic Conditions SCC (irradiance = 1000W/m² and temperature = 298 K).

Figure 9(a) shows the output power of all above mentioned methods, these results have confirmed the good performance and the high effectiveness of the proposed controller in transient and steady state. We can note clearly, in a transient state, that the synergetic approach ensures the convergence to the MPP more rapidly compared to sliding mode controller and in the right direction. At the same time, the duty cycle of the proposed technique converges to the optimal value in limited time as shown in Figure 9(b) and the macro-variable is maintained very close to zero as shown in Figure 9(c), by this we guarantee the ability to reach the optimum point ($dP_{pv}/dI_{pv} = 0$). Moreover, in a steady state, once the output power of the PV system is maintained at the maximum, a significant reduce of the oscillation around the MPP is appeared and as result, the power extracted using synergetic approach is much larger compared to the power extracted using SMC technique as shown obviously in attached zoom in Figure 9(a).

In order to evaluate the robustness of the proposed MPPT controller under variable atmospheric conditions, the sun insolation 700 W/m² is applied to the PV system. Then, it is stepped up to 1000 W/m² and finally it is stepped down to 500 W/m² as shown in Figure 10(a). The tracking result of this step change of both techniques is shown in Figure 10(b). While Figure 10(c) and (d) illustrate the duty cycle, the output voltage
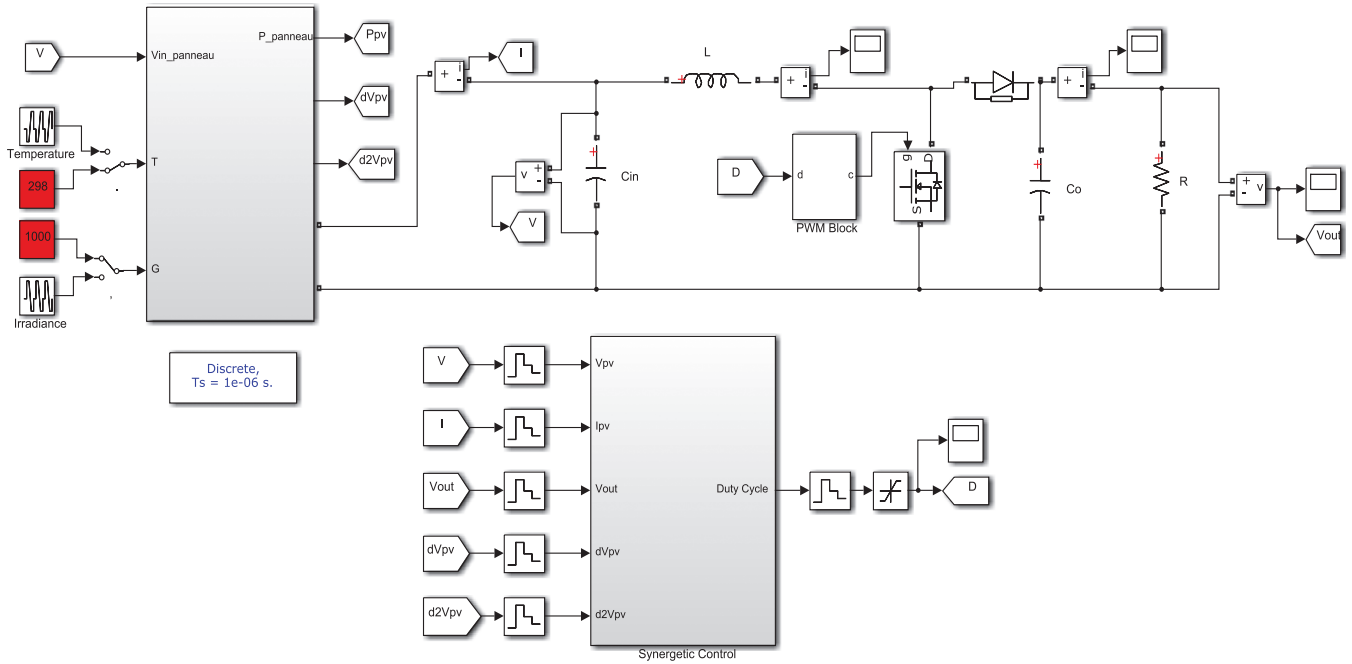
FIGURE 8 Implementation of PV system in Matlab/Simulink

(V_{out}), the PV voltage (V_{pv}) and the PV current (I_{pv}) of the proposed synergetic controller at the same step change.

In the first step change introduced at 0.1 s we stepped up the irradiance from 700 to 1000 W/m² in short time equal to 0.05 s. On the obtained results we can make a detailed analysis. In transient state, the SMC takes a relatively long time to reach the MPP without an overshoot. The settling time in this case is equal to 0.08 s. While the SC reaches the MPP at the same time that the irradiance settled at 1000 W/m² as it is shown in zoom 1 of Figure 10(b). In steady state, once the power extracted by SMC will be stable, the oscillations around the MPP introduce a power with an average value equal to 86.95 W which creates a static error equal to 0.33 W. On the other hand, the average value of the power extracted by SC is estimated to 87.28 W which provides almost neglected static error. The second step change is distinguished by a stepped down of irradiance at 0.25 s from 1000 to 500 W/m² in relatively long time, compared to the time of the first step change which equals 0.15 s. In this case, SMC shows a fast tracking where the settling time is estimated by 0.003 s (Zoom 3 of Figure 10(b)) and this is caused by the slow change in the irradiance but it is still not able to extract the maximum power estimated by 43.8 W under 500 W/m² which creates a static error equal to 0.2 W. On the other hand, the proposed strategy managed to reach the MPP at 0.4 s, which is the same time that the irradiance is stable at 500 W/m². The average value of the power extracted in steady state is 43.79 W which creates a static error around 0.01W.

To examine the performance of the proposed MPPT controller under temperature variations, we suddenly change the temperature from 303 to 288 K, then to 323 K as shown in Figure 11(a). The tracking result of these changes is shown in Figure 11(b). While Figure 11(c) and (d) illustrate the duty cycle, the output voltage (V_{out}), the PV voltage (V_{pv}) and the PV current (I_{pv}) of the proposed controller at the same step change.

In both cases of temperature change, the SMC shows a fast tracking to the MPP but not with the same accuracy given by Synergetic controller as it is shown in attached zoom of Figure 11(b). In steady state and by using SMC, sizeable oscillations were appeared around the MPP to give a power with an average value equal to 90.75 W, in the first step change, which provides a static error equal to 0.75 W. A power with an average value equal to 75.78 W is obtained in the second step change which provides a static error equal to 0.92 W. On the other hand, the use of the proposed MPPT controller based on synergetic approach makes the extraction of the maximum power possible and with highly reduced oscillations, which achieves almost neglected static error, where the average power value equals 91.5 W in the first step change and 76.7 W in the second step change.

Thus, all the obtained simulation results have confirmed the strong robustness, in transient and steady state conditions, of the proposed synergetic MPPT controller against the SMC technique. The synergetic control ensures the convergence to the MPP quickly under different tests and towards the environment changes without affecting inversely at the output power.
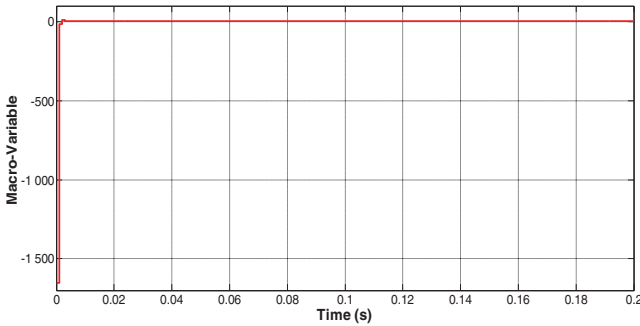
5.2 | Experimental results

An experimental test bench, Figure 12, has been developed in LIAS-ENSIP-laboratory, France, to confirm the validity of the proposed synergetic-based MPPT controller. It consists of the following equipment's: a programmable DC power supply with
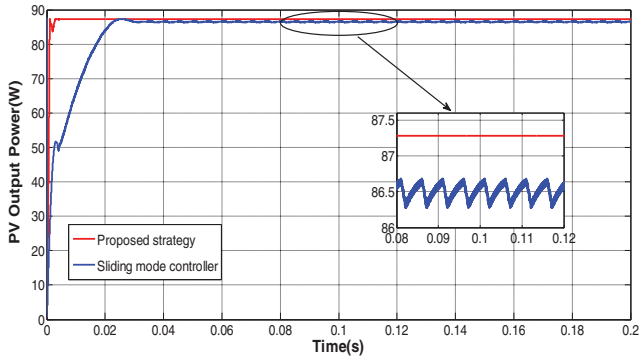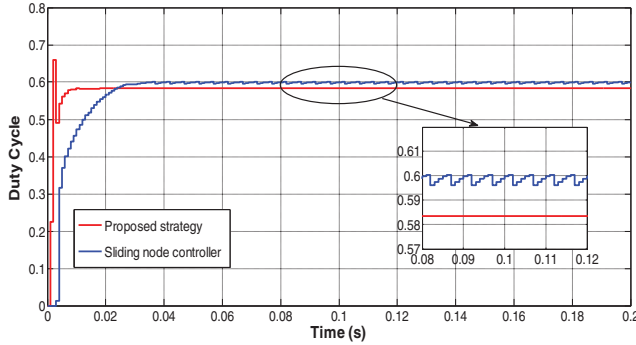
FIGURE 9 Simulation results of the studied methods at SCC ($S = 1000$ W/m², $T = 298$ K, (a) output power (P_{pv}), (b) duty cycle (D), (c) macro-variable (Ψ)

solar array simulation: 62020H-150S manufactured by the company Chroma to simulate two Kyocera KC85T panels (whose specifications are illustrated in Table 1) connected in series to generate 177W at PV peak power, a DC–DC boost converter with a switching frequency of 10 kHz (whose specifications are illustrated in Table 2) and a linear resistive load. The synergetic-based MPPT algorithm is digitally implemented on a dSPACE RTI 1104 system real-time platform through a Matlab/Simulink environment.

The experimental results under standard test conditions (Irradiance = 1000 W/m² and Temperature = 298 K) are presented in Figure 13(b). The proposed synergetic MPPT controller is able to maintain the output power P_{pv}, current I_{pv}, voltage V_{pv} and the output voltage V_{out} constant. Figures 13(c) and (d) show the experimental results of the duty cycle and the macro-variable respectively.
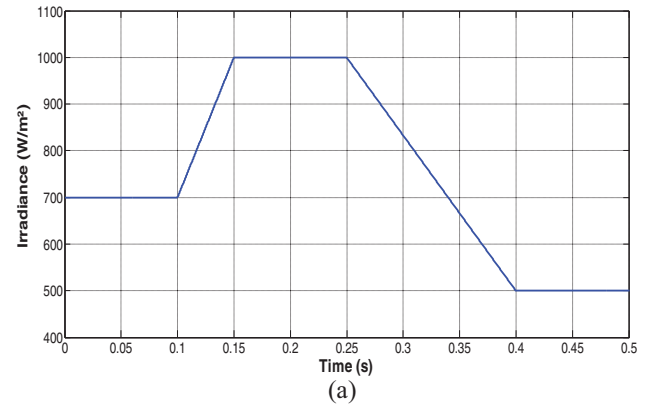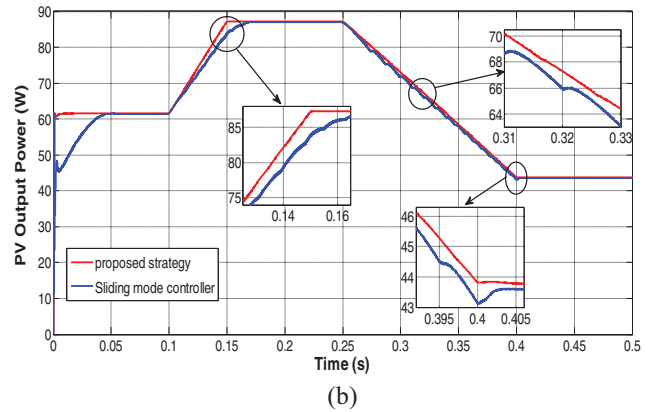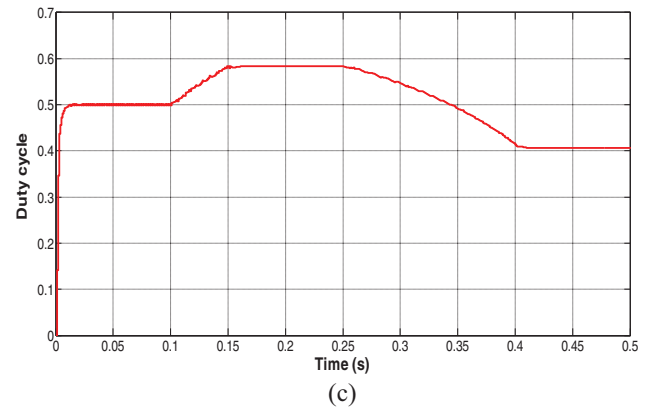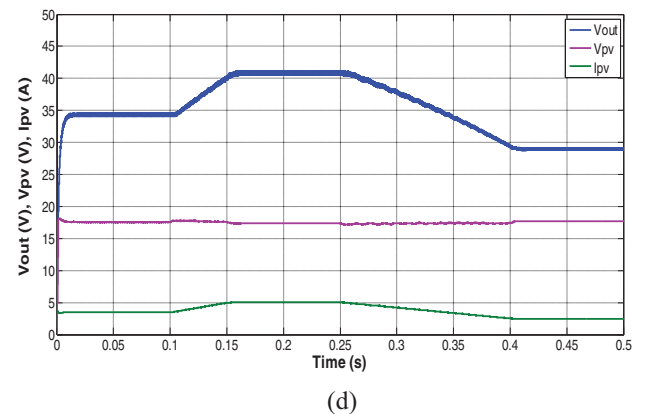

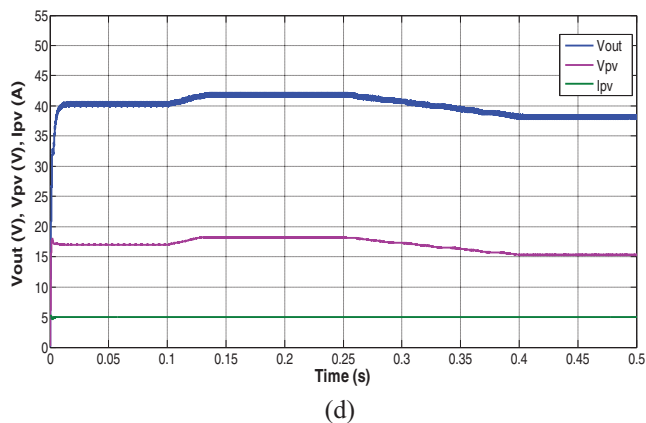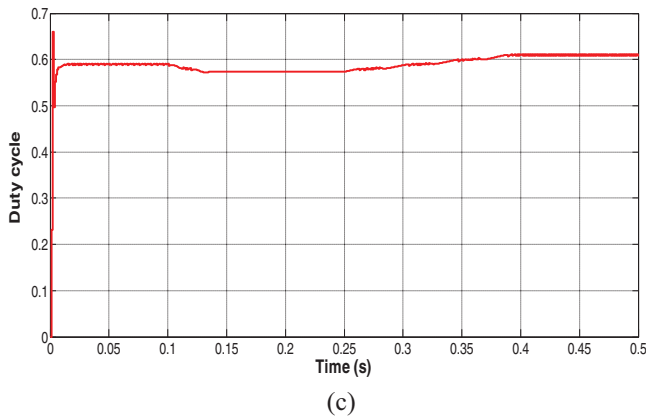**FIGURE 10** Simulation with step irradiance change ($T = 298$ K)
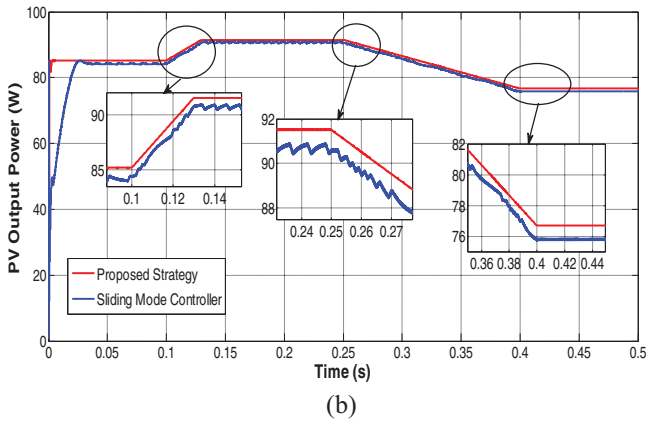
(a)

(b)

(c)

(d)

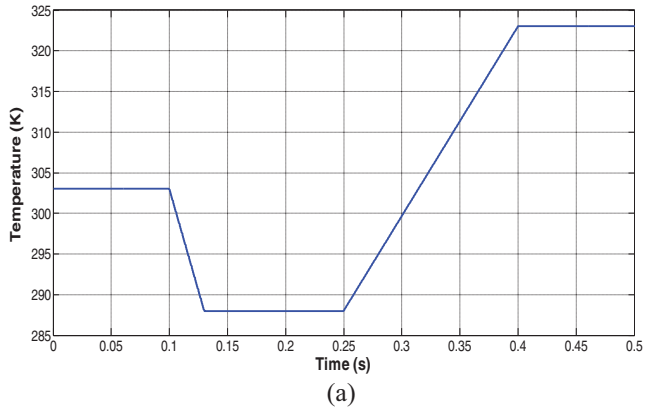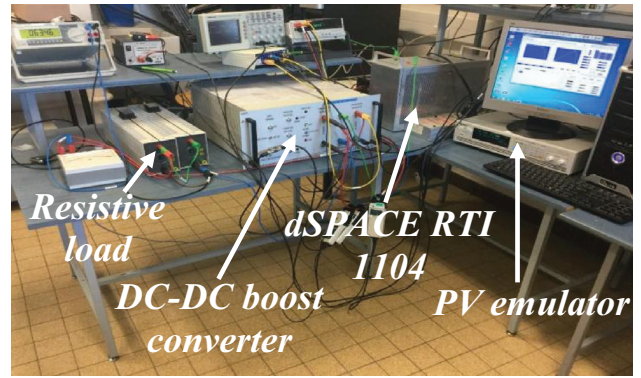**FIGURE 11**   Simulation with step temperature change ($S = 1000$W/m²)

FIGURE 12   Experimental test bench of PV system with the developed MPPT controller

In order to examine the performance of the proposed MPPT controller, the dynamic behaviour under a step change of irradiance and temperature, in the experimental test, is presented in Figures 14 and 15 respectively.

In Figure 14, the irradiance is increased from 200 to 500 W/m² at 3.5 s and increased from 500 to 1000 W/m² at 7 s. After a very short transient, the output power P_{pv}, current I_{pv}, voltage V_{pv} and the output voltage V_{out} are maintained constant with good stability.

Figure 15 shows experimental results under a step change of temperature using the proposed synergetic MPPT controller. In this experimental test, the temperature is increased from 298 to 313 K and decreased from 313 to 283 K at constant irradiance of 1000 W/m². From this figure, it can be observed that the stability of the system is successfully achieved by maintaining the output power P_{pv}, current I_{pv}, voltage V_{pv} and the output voltage V_{out} constant after a very short transient.

All experimental results are in concordance and very close to the previous simulation results. Thus, confirm the validity and the feasibility of the proposed synergetic-based MPPT controller. This approach provides high efficiency 99.97% at standard test conditions, as shown in Figure 13(a), with correct and fast tracking as shown in Figure 13b). Oscillations around the MPP are approximately eliminated and the variable is maintained very close to zero (see Figure 13(d)). At the same time, the duty cycle converges to the optimal value to reach the MPP as shown in Figure 13(c). Moreover, the experimental results show the effectiveness and the good robustness of the PV system with the proposed MPPT against the variation of external conditions, irradiance (Figure 14) and temperature (Figure 15).

5.3 │ The EN 50530 MPPT efficiency test

To further evaluate the developed strategy, the EN 50530 standard test of dynamic MPPT efficiency is used [38]. It is implemented by providing triangular irradiance waveforms sequentially but with different ramp gradients values from 0.5 W/m²/s to 100W/m²/s, so thus covered a comprehensive set of irradiance changes from the slow to the very fast.
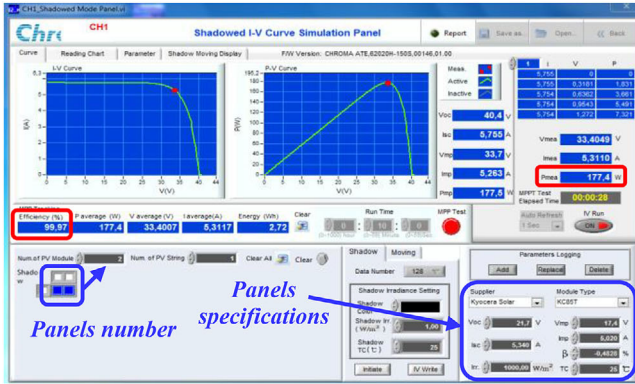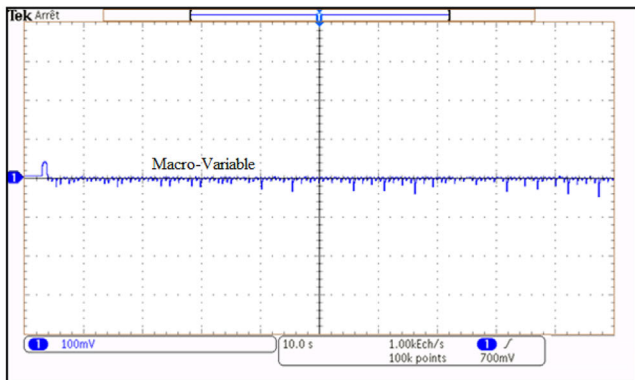
(a)
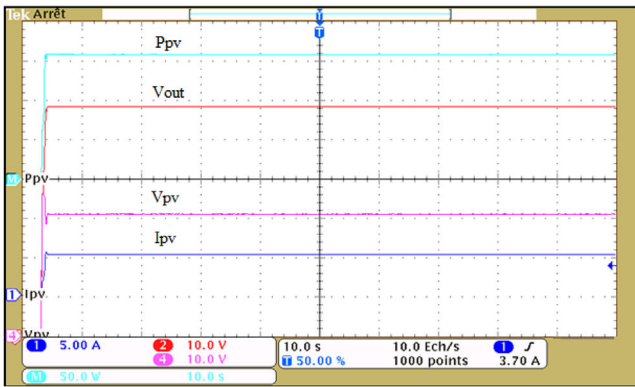
(b)
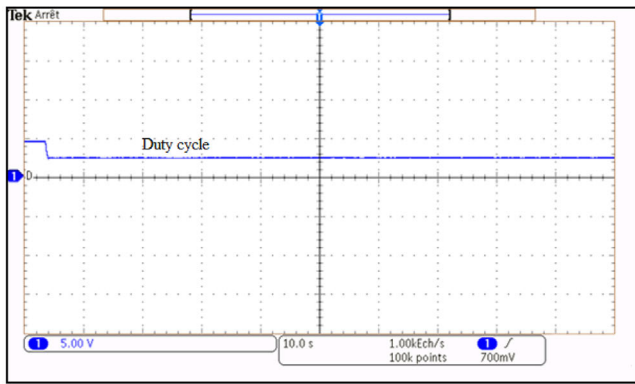
(c)

(d)

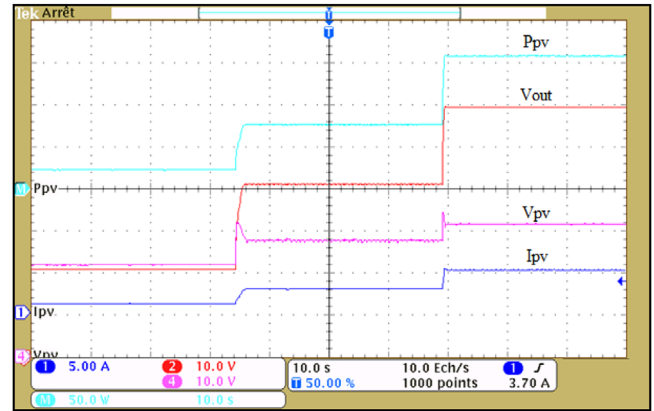**FIGURE 13** Experimental results at standard test condition (irradiance = 1000 W/m² and temperature = 298 K)

FIGURE 14 Experimental results under a step change of irradiation (T = 298 K)

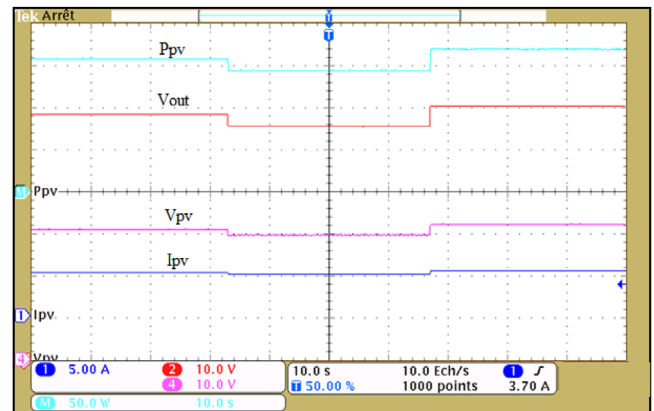**FIGURE 15** Experimental results under a step change of temperature (S = 1000 W/m²)

In this work, we use the EN50530 standard test with two different irradiance levels from 300 to 1000 W/m² (medium to high irradiance), but without repeating the same triangular waveforms as mentioned in the original document [38], because MPPT techniques as agreed keep the same responds during the same ramp (up and down). We applied three sequences with different ramp gradients: 10, 35 and 70 W/m²/s (slow, fast, and very fast) respectively, the irradiation remains constant for a certain period of time at the high level as well as the low as shown in Figure 16. The power tracking result of the proposed strategy and the sliding mode controller is presented in Figure 17, certain parts are zoomed in to be clearer.

During a slow solar irradiance change (10 W/m²/s); the tracking power obtained by the proposed strategy is almost perfect and the ability to extract the maximum power is very high compared to sliding mode controller as shown in Zoom 1. The SMC also provides a good performance when the irradiance changes slowly as shown in zoom 2, it is true that the tracking power deviate from the right direction compared to synergetic controller but after each relatively large period which makes the disturbances along the tracking smaller. In the second sequence, the solar irradiance changes faster: 35
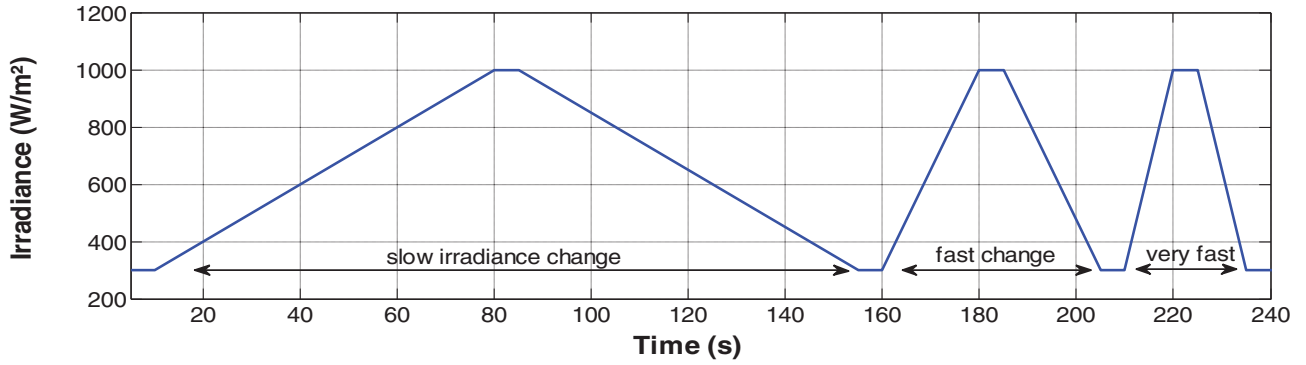
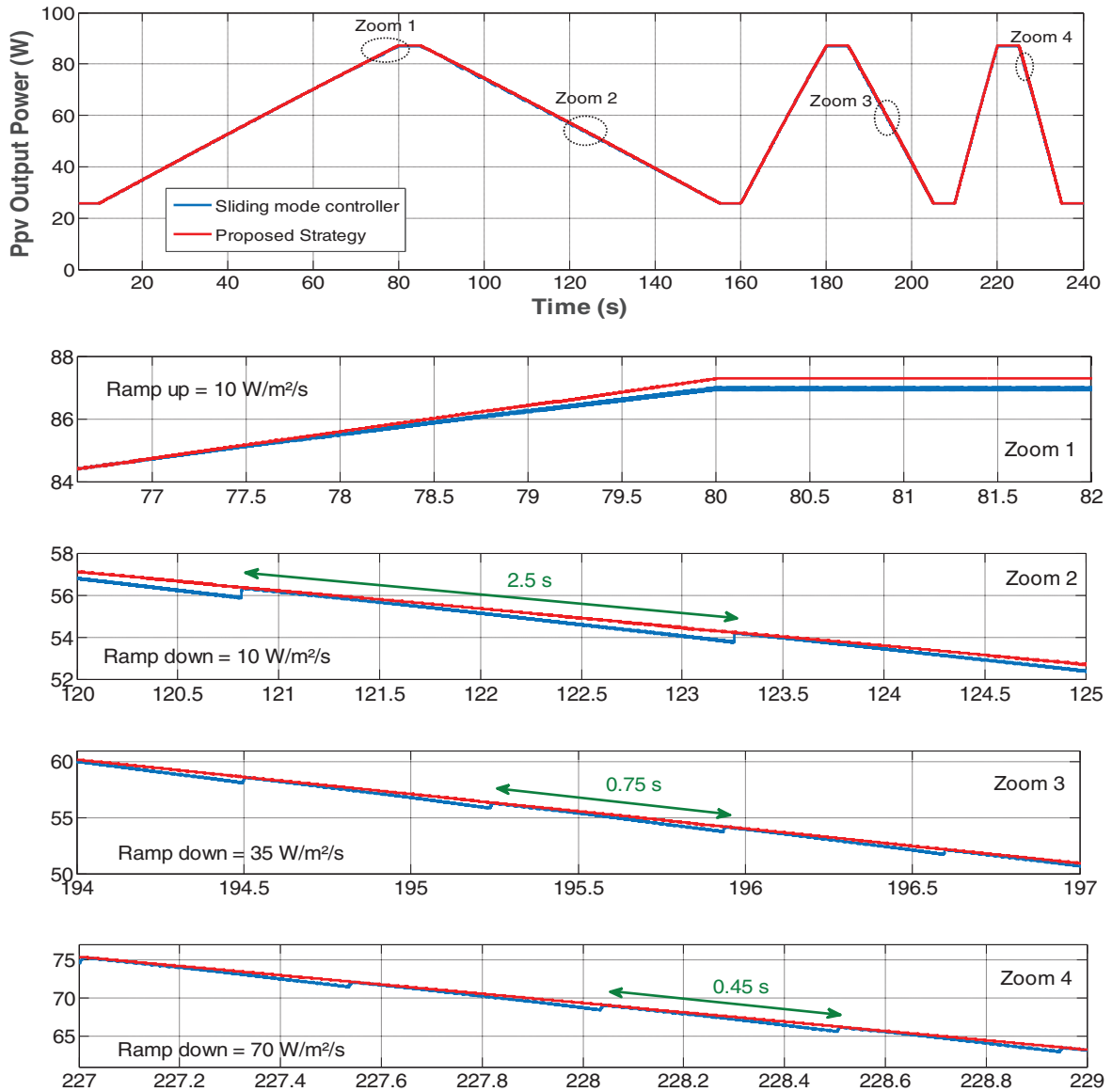**FIGURE 16** Triangular irradiance waveforms for the EN 50530 standard test of dynamic MPPT efficiency

FIGURE 17 Power tracking result of the synergetic controller and the sliding mode controller
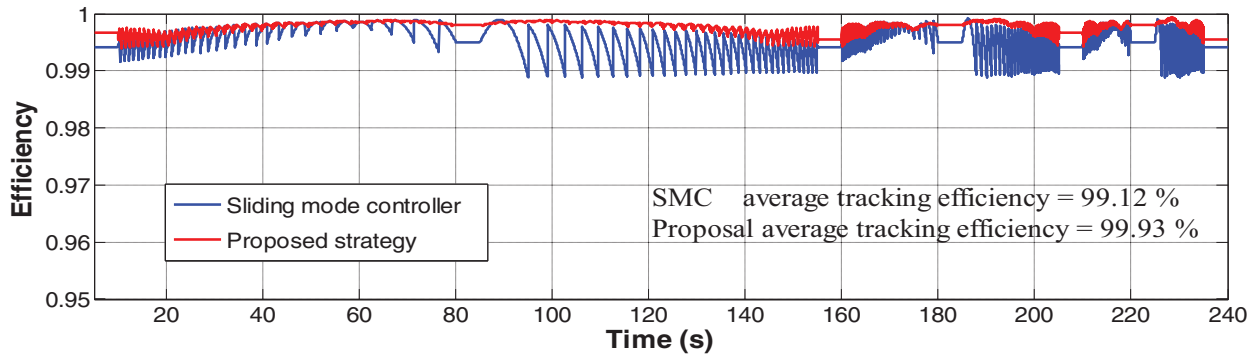
FIGURE 18   The efficiency of the synergetic controller and the sliding mode controller under the EN50530 standard test

W/m²/s (increase and decrease), the synergetic controller is still able to maintain the good and the accurate tracking while the deviations of the tracking power from the correct direction provided by SMC become more (each 0.75 s) as illustrated in Zoom 3, which make more oscillations. During the third sequence, the increasing and the decreasing of irradiance is very fast (70 W/m²/s), the deviations of SMC become much more than the previous sequence (each 0.45 s) and as a result the oscillations along the tracking increase more and more while the proposed controller still copes with the very fast change with high performance as shown in Zoom 4.

The MPPT efficiency is measured using the following formula [39]:

$$\eta_{\text{MPPT}} = \frac{P_{\text{out}}(t)}{P_{\text{max}}(t)} \tag{28}$$

So the average efficiency is calculated according to equation (29):

$$\eta_{\text{MPPT,avg}} = \frac{\int P_{\text{out}}(t)\,dt}{\int P_{\text{max}}(t)\,dt} \tag{29}$$

where P_{out} is the output power extracted from the PV array and P_{max} is the theoretical maximum power. Although the efficiency is volatile in certain parts of the approved profile in the EN 50530 standard test especially in low irradiance and fast changes, the proposed strategy achieves an average tracking efficiency of 99.93 % under all stages of changing weather whereas the SMC achieves 99.12 % as shown in Figure 18.

6 | CONCLUSION

This paper presents a new nonlinear MPPT controller based on the synergetic control theory applied to a stand-alone PV system. A DC–DC boost converter is used as an interface between the PV array and the load. The proposed controller was tested both in simulation and experimentally. The EN 50530 standard test was used with different gradients values to calculate the MPPT efficiency under irradiance changes.

The simulation results, obtained using Matlab/Simulink tools, prove the good performance in transient and steady state of the proposed synergetic-based MPPT controller, under different temperature and solar irradiance. Moreover, it is much better than sliding mode-based MPPT controller. The synergetic MPPT controller overcomes the problems that exist in the conventional and intelligent algorithms, not only regarding to the fast and accurate tracking but also regarding to the oscillations around the MPP. These features are confirmed by experimental results obtained using dSPACE RTI 1104 real-time platform. In fact, various atmospheric conditions are tested to prove the high efficiency of the proposed synergetic MPPT controller.

ORCID
Rahma Ayat https://orcid.org/0000-0002-4295-7076

REFERENCES
1. Roche, O.M., Blanchard, R.E.: Design of a solar energy centre for providing lighting and income-generating activities for off-grid rural communities in Kenya. Renewable Energy 118, 685–694 (2018)
2. Talbi, B., et al.: A high-performance control scheme for photovoltaic pumping system under sudden irradiance and load changes. Sol. Energy 159, 353–368 (2018)
3. Femia, N., et al.: Optimization of perturb and observe maximum power point tracking method. IEEE Trans. Power Electron. 20, 963–973 (2005)
4. Zegaoui, A., et al.: Comparison of two common maximum power point trackers by simulating of PV generators. Energy Procedia 6, 678–687 (2011)
5. Noppadol, K., Theerayod, W., Phaophak, S.: FPGA implementation of MPPT using variable step-size P&O algorithm for PV applications. In:IEEE Int. Symp. on Communication and Information Technologies, pp. 212–215. IEEE, Piscataway, NJ (2006)
6. Esram, T., Chapman, P.L.: Comparison of Photovoltaic Array Maximum Power Point Tracking Techniques. IEEE Trans. Energy Convers. 22, 439–449 (2007)

7. Elgendy, M.A., Zahawi, B., Atkinson, D.J.: Assessment of the incremental conductance maximum power point tracking algorithm. IEEE Trans. Sustainable Energy 4, 108–117 (2013)

8. Shiqiong, Z., et al.: A novel maximum power point tracking algorithms for stand-alone photovoltaic system. Int. J. Control, Autom. Syst. 8, 1364–1371 (2011)

9. Gomes de Brito, M.A., et al.: Evaluation of the main MPPT techniques for photovoltaic applications. IEEE Trans. Ind. Electron. 60, 1156–1167 (2013)

10. Li, X., et al.: A novel beta parameter based fuzzy-logic controller for photovoltaic MPPT application. Renewable Energy 130, 416–427 (2019)

11. Attia, H.A.: High performance PV system based on artificial neural network MPPT with PI controller for direct current water pump applications. Int. J. Power Electron. Drive Syst. 10, 1329–1338 (2019)

12. Hadji, S., Gaubert, J.P., Fateh, K.: Theoretical and experimental analysis of genetic algorithms based MPPT for PV systems. Energy Procedia 74, 772–787 (2015)

13. Li, H., et al.: An overall distribution particle swarm optimization MPPT algorithm for photovoltaic system under partial Shading. IEEE Trans. Ind. Electron. 66, 265–275 (2019)

14. Salmi, H., et al.: An advanced MPPT based on artificial bee colony algorithm for MPPT photovoltaic system under partial shading condition. Int. J. Power Electron. Drive Syst. 8(2), 647–653 (2017)

15. Titri, S., et al.: A new MPPT controller based on the Ant colony optimization algorithm for Photovoltaic systems under partial shading conditions. Appl. Soft Comput. 58, 465–479 (2017)

16. Mojallizadeh, M.R., et al.: Designing a new robust sliding mode controller for maximum power point tracking of photovoltaic cells. Sol. Energy 132, 538–546 (2016)

17. Belkaid, A., Gaubert, J.P., Gherbi, A.: An improved sliding mode control for maximum power point tracking in photovoltaic systems. Control Eng. Appl. Informatics 18, 84–96 (2016)

18. Sahraoui, H., et al.: Second order sliding mode control of DC-DC converter used in the photovoltaic system according an adaptive MPPT. Int. J. Renewable Energy Res. 6(2), 375–383 (2016)

19. Zerroug, N., et al.: DSP-based implementation of fast terminal synergetic control for a DC–DC Buck converter. J. Franklin Inst. 355, 2329–2343 (2018)

20. M. Rezkallah, et al.: Lyapunov function and sliding mode control approach for the solar-PV grid interface system. IEEE Trans. Ind. Electron. 64, 785 (2017)

21. Kolesnikov, A., Veselov, G.: Modern Applied Control Theory: Synergetic Approach in Control Theory, vol. 2. TSURE Press, (in Russian) Moscow-Taganrog (2000)

22. Kolesnikov, A.: Introduction of synergetic control. In: American Control Conference, pp. 3013–3016. IEEE, Piscataway, NJ (2014)

23. Santi, E., et al.: Synergetic control for DC–DC boost converter: Implementation options. IEEE Trans. Ind. Appl. 39, 1803–1813 (2003)

24. Bouchama, Z., Harmas, M.N., Zehar, K.: Finite time nonlinear control for DC-DC converters. Soft Computing Electr. Eng. 1, 36–45 (2019)

25. Jiang, Z., Dougal, R.A.: Synergetic control of power converters for pulse current charging of advanced batteries from a fuel cell power source. IEEE Trans. Power Electron. 19, 1140–1150 (2004)

26. Boonyaprapasorn, A., et al.: An application of finite time synergetic control for vaccination in epidemic systems. In: Proc. of IEEE Conf. on Systems, Process and Control, pp. 30–35. IEEE, Piscataway, NJ (2017)

27. Hachana, A., Harmas, M.N.: Synergetic and Higher Order Sliding Mode Control of Blood Glucose Regulation in Diabetes Patients. J. Dynamic Syst. Meas. Control 140(10), 100801 (2018)

28. Ettouil, R., Chabir, K., Abdelkrim, M.N.: Optimal synergetic control for wind turbine system. Int. J. Eng. Sci. 7, 44–48 (2018)

29. Sarkar, M.N.I.: Effect of various model parameters on solar photovoltaic cell simulation: A SPICE analyses. Renewables: Wind, Water, Solar 3, 13 (2016).

30. Tian, H., et al.: A cell-to-module-to-array detailed model for photovoltaic panels. Sol. Energy 86, 2695–2706 (2012)

31. Boukezata, B., et al.: An improved fuzzy logic control MPPT based P&O method to solve fast irradiation change problem. J. Renewable Sustainable Energy 8, 043505 (2016)

32. Selva Kumar, R., et al.: Design and comparison of quadratic boost converter with boost converter. Int. J. Eng. Res. Technol. 5, 877–881 (2016)

33. Irfan, Y., Ersagun, K.Y.: Fast and robust voltage control of DC–DC boost converter by using fast terminal sliding mode controller. IET Power Electron. 9(1), 120–125 (2015)

34. Chi-Hua, L., Ming-Ying, H.: Design of Fuzzy Synergetic Controller. In: IEEE Int. Conf. on Fuzzy Systems, pp. 2477–2481. IEEE, Piscataway, NJ (2014)

35. Zehar, D., et al.: Fast terminal synergetic control of underactuated system. In: Int. Multi-Conf. on Systems, Signals & Devices, pp. 1184–1189. IEEE, Piscataway, NJ (2018)

36. Zerroug, N.: Contribution au contrôle robuste des convertisseurs DC-DC. Ph.D. Thesis, Batna University (2018)

37. Bregeault, V.: Quelques contributions à la théorie de la commande par modes glissants. Ph.D. Thesis, Ecole Centrale de Nantes (2010)

38. Brundlinger, R., et al.: prEN 50530 - The new European standard for performance characterisation of PV inverters. In: Proc. 24th European Photovoltaic Solar Energy Conf., pp. 3105–3109, WIP Wirtschaft and Infrastruktur GmbH, Munich (2009)

39. Jubaer, A., Zainal, S.: A modified P&O maximum power point tracking method with reduced steady state oscillation and improved tracking efficiency. IEEE Trans. Sustainable Energy 7, 1506–1515 (2016)

ملخص

من بين مصادر الطاقة المتجددة المتنوعة ، حظيت الطاقة الكهروضوئية باهتمام متزايد واستقطاب كبير من الباحثين في العديد من التطبيقات ، لقدرتها على التحويل المباشر للطاقة الكهربائية دون أي ضرر بيئي ، وسهولة تنفيذها ، ومرونة الحجم ، وانخفاض تكلفة التشغيل. يعتمد أداء النظام الكهروضوئي بشكل أساسي على درجة حرارة، الإشعاع، الأوساخ والظلال أثناء تشغيلها. وبالتالي ، نحتاج إلى استخراج أقصى طاقة متوفرة بواسطة المولد الكهروضوئي ونقلها إلى الحمل لتحسين كفاءة النظام الكهروضوئي في جميع الأوقات ، حتى لو تعرضت الوحدات الكهروضوئية لتغيرات مناخية غير موحدة. من الضروري إستعمال تقنية فعالة لتتبع نقطة الطاقة القصوى والحفاظ على نقطة تشغيل النظام الكهوضوئي في نقطة الطاقة القصوى في جميع الحالات. الهدف الرئيسي من عمل الأطروحة هو تطوير وتنفيذ استراتيجيات تتبع غير خطية جديدة تعتمد على التحكم التآزري والتحكم التآزري النهائي و السريع القادر على تتبع نقطة الطاقة القصوى لنظام كهروضوئي مستقل في ظل ظروف مختلفة وبالتالي زيادة كفاءة النظام الكهروضوئي. النتائج التي تم الحصول عليها في ظل ظروف مختلفة أثبتت فعالية الاستراتيجيات التي تم تطويرها وأظهرت أدائها الجيد وقوتها الكبيرة بالمقارنة مع تقنيات أخرى.

الكلمـــات :الأنظمـة الكهروضـــــوئية ,محول Boost DC-DC ، MPPT ، التحكـــم فـي الوضـع الانـــزلاقي ,التحكـــم التـــآزري، التحكـــم التـــآزري الســـريع

Abstract

Among the different renewable energy resources, photovoltaic energy has found increased attention and wide attraction from researchers in many applications, for its capabilities of direct electric energy conversion without any environmental damage, ease of implementation, flexibility in size and low operation cost. The performance of the PV system is mainly depended to temperature, irradiation, dirt and shadows during its operation. Thus, we should extract the maximum power available by the photovoltaic generator (PVG) and transfer it to the load to enhance the PV system's efficiency at any moment although PV units are exposed to non-uniform climate changes. Competent maximum power point tracking (MPPT) technique is needed to track the MPP and maintain the operating point of the PV system at the MPP under any cases. The main purpose of this thesis work is to develop and implement new nonlinear MPPT strategies based on Synergetic Control (SC) and Fast Terminal Synergetic Control (FTSC) able to track the MPP for stand-alone PV system under different conditions and therefore increase the PV system efficiency. The obtained results under different conditions have validated the developed strategies and highlighted their good performance and high robustness compared to other MPPT controllers.

Key words: PV system, DC-DC boost converter, MPPT, Sliding mode control, Synergetic control, Fast Terminal Synergetic control.

Résumé

Parmi les différentes ressources d'énergie renouvelable, l'énergie photovoltaïque a suscité une attention accrue et une grande attraction de la part des chercheurs dans de nombreuses applications, pour ses capacités de conversion directe d'énergie électrique sans aucun risque environnemental, sa facilité de mise en œuvre, sa flexibilité et son faible coût d'exploitation. Les performances du système PV dépendent principalement de la température, irradiation, de la saleté et des ombres pendant son fonctionnement. Ainsi, nous devons extraire la puissance maximale disponible par le générateur photovoltaïque (GPV) et la transférer à la charge pour améliorer l'efficacité du système PV à tout moment, même si les unités PV sont exposées à des changements climatiques non uniformes. Une technique compétente de suivi du point de puissance maximale (MPPT) est nécessaire pour suivre le MPP et maintenir le point de fonctionnement du système PV au MPP dans tous les cas. L'objectif principal de ce travail de thèse est de développer et de mettre en œuvre de nouvelles stratégies MPPT non linéaires basées sur la commande Synergétique et la commande Synergétique Terminale Rapide capables de suivre le MPP pour un système PV autonome dans différentes conditions et donc d'augmenter l'efficacité du système PV. Les résultats obtenus sous différentes conditions ont validé les stratégies développées et mis en évidence leurs bonnes performances et leur grande robustesse par rapport à d'autres techniques MPPT.

Mots clés : Systèmes PV, convertisseur DC-DC Boost, MPPT, Commande par mode glissant, Commande synergétique, Commande synergétique terminale rapide.